

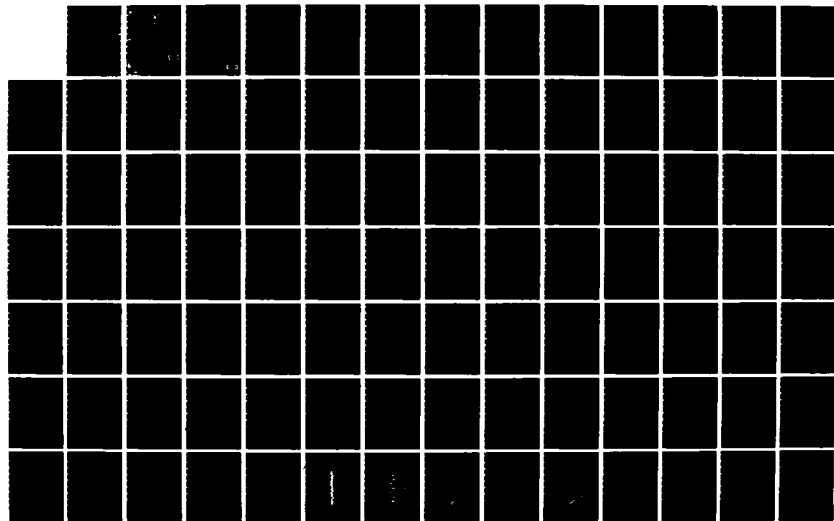
AD-A138 545

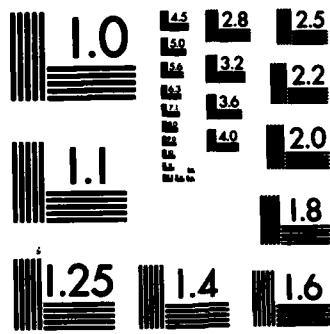
TARGET SUPER-RESOLUTION COMPENSATION FOR COHERENT
AIRBORNE RADAR UTILIZIN. (U) AIR FORCE INST OF TECH
WRIGHT-PATTERSON AFB OH SCHOOL OF ENGI. K W ALBERT
DEC 83 AFIT/GE/EE/83D-5 F/G 17/9

1/2

UNCLASSIFIED

NL





MICROCOPY RESOLUTION TEST CHART
NATIONAL BUREAU OF STANDARDS-1963-A

AD A138545



TARGET SUPER-RESOLUTION COMPENSATION
FOR COHERENT AIRBORNE RADAR
UTILIZING SPREAD SPECTRUM WAVEFORMS

Thesis

AFIT/GE/EE/83D-5 Kennenth W. Albert
2Lt USAF

DISTRIBUTION STATEMENT A

Approved for public release
Distribution Unlimited

DTIC
ELECTE
S MAR 5 1984 **D**
B

DEPARTMENT OF THE AIR FORCE
AIR UNIVERSITY

AIR FORCE INSTITUTE OF TECHNOLOGY

Wright-Patterson Air Force Base, Ohio

DTIC FILE COPY

84 02 21 192

AFIT/GE/EE/83D-5

TARGET SUPER-RESOLUTION COMPENSATION
FOR COHERENT AIRBORNE RADAR
UTILIZING SPREAD SPECTRUM WAVEFORMS

Thesis
AFIT/GE/EE/83D-5 Kennenth W. Albert
2Lt USAF

Approved for public release; distribution unlimited

DTIC
ELECTE
MAR 5 1984
S B D

TARGET SUPER-RESOLUTION COMPENSATION
FOR COHERENT AIRBORNE RADAR
UTILIZING SPREAD SPECTRUM WAVEFORMS

THESIS

Presented to the Faculty of the School of Engineering
of the Air Force Institute of Technology
Air University
in Partial Fulfillment of the
Requirements for the Degree of
Master of Science

by

Kenneth W. Albert, BSEE
2Lt USAF

Graduate Electrical Engineering
December 1983

Approved for public release; distribution unlimited.

Acknowledgements

I would like to express my appreciation and gratitude to Maj Ken Castor, my thesis advisor, for his patience and guidance throughout the entire thesis work. I would also like to thank Dr. Vic Syed, the solo member of my thesis committee, for his assistance.

Kenneth W. Albert

Accession For	
NTIS GRA&I	<input checked="checked" type="checkbox"/>
DTIC TAB	<input type="checkbox"/>
Unannounced	<input type="checkbox"/>
Justification	
By _____	
Distribution/	
Availability Codes	
Dist	Avail and/or Special
A-1	

DTIC COPY NTIS 2

Contents

	<u>Page</u>
Acknowledgements	ii
List of Figures	v
List of Tables	vii
Abstract	viii
I. Introduction	1
Problem Statement	1
Scope	2
Problem Solving Approach	3
Presentation	3
II. Background	5
III. Theoretical Considerations	31
Complex Signal Notation	31
Matched Filter Theory	37
Optimum Receiver in White Gaussian Noise	40
Received Signal Representation	43
Ambiguity Function	47
Sampled Signal Theory	54
IV. Computer Simulation Development	58
Approach	58
Calculating the Magnitude of the	
Ambiguity Function	58
Signal Spectrum Calculations	62
Matched Filter and Target Filter Calculations ..	64
Coherent and Incoherent Target Filtering	66
V. Software Application and Results	69
Simulation Test Waveform	69
Phase Coded Signal	70
Interpulse Frequency Hopping Waveform	72
Interpulse Frequency Hopping with	
Subpulse Chirp	72
Summary	72
VI. Conclusions and Recommendations	102
Conclusions	102
Recommendations	103

Bibliography	<u>Page</u> 105
Appendix A: Simulation Flow Chart	106
Appendix B: Program Listings	109

List of Figures

<u>Figure</u>		<u>Page</u>
1	Interpulse vs. Intrapulse Modulation	8
2	Interpulse Frequency Hopping Waveform Characteristics	11
3	Interpulse Frequency Hopping Implementation	12
4	Intrapulse Biphase Coding Waveform Characteristics	14
5	Intrapulse Biphase Coding Scheme	16
6	Waveform Characteristics of Intrapulse Frequency Hopping	17
7	Matched Filter Techniques for Intrapulse Frequency Coding	18
8	Stretch Processor Concept and Implementation for Intrapulse Frequency Coding	19
9	Typical Modern Airborne Radar Achitecture	24
10	Graphical Representation of Complex Signal Spectrum	37
11	Coherent Pulse Train	47
12	Spectra of Continous and Sampled Signals	55
13	Signal Spectrum fo 13-Element Barker Code	76
14	Ambiuity Cut for 13-Element Barker Code	77
15	Intrapulse Phase Coded Spectrum	78
16	Ambiguity Cut, Phase Coded Signal	79
17	Received Spectrum, Non-Fluctuating Case	80
18	Matched Filter Output, Non-Fluctuating Case	81
19	Target Filter, Alpha=0.1	82
20	Coheren' Target Filter Output, Non-Fluctuating Case	83
21	Received Signal Spectrum, Swerling I	84
22	Matched Filter Output, Swerling I	85

<u>Figure</u>		<u>Page</u>
23	Received Signal Spectrum, Swerling II, Alpha =0.01	86
24	Matched Filter Output, Swerling II, Alpha=0.01 ..	87
25	Target Filter, Swerling II, Alpha=0.01	88
26	Target Filter Output, Swerling II, Alpha=0.01 ...	89
27	Received Signal Spectrum, Swerling II, Alpha=0.01	90
28	Matched Filter Output, Swerling II, Alpha=0.01 ..	91
29	Target Filter, Swerling II, Alpha=0.01	92
30	Target Filter Output, Swerling II, Alpha=0.01 ...	93
31	Received Signal Spectrum, Swerling II, Alpha=0.01	94
32	Matched Filter Output, Swerling II, Alpha=0.01 ..	95
33	Target Filter, Swerling II, Alpha=0.1	96
34	Target Filter Output, Swerling II, Alpha=0.1	97
35	Received Signal Spectrum, Swerling II, Alpha=0.001	98
36	Matched Filter Output, Swerling II, Alpha=0.001	99
37	Target Filter, Swerling II, Alpha=0.2	100
38	Target Filter Output, Swerling II, Alpha=0.2	101

List of Tables

<u>Table</u>		<u>Page</u>
I	Spread Spectrum Modulation Techniques	10
II	Coherent vs. Incoherent Target Filter Output Signal Power for Phase Coded Waveforms	73
III	Coherent vs. Incoherent Target Filter Output Signal Power for Interpulse FM Waveform	74
IV	Coherent vs. Incoherent Target Filter Output Signal Power for Interpulse FM with Subpulse Chirp	74

Abstract

Both a coherent and incoherent target filter are compared on an output signal-to-noise power ratio basis. Three spread spectrum waveforms are tested: intrapulse biphase coded, interpulse frequency hopped, and interpulse frequency hopped with subpulse chirp. In all three cases, the incoherent target filter provided superior output power. Typical incoherent/coherent signal power ratios were 1-3 dB, 0.75 dB, and 0.18 dB for the phase coded, FM, and FM with subpulse chirp respectively.

I. Introduction

Problem Statment

The application of spread spectrum technology in military radar systems may provide several desirable characteristics normally associated with spread spectrum communication system techniques. Spread spectrum communication systems are well known and provide the following benefits to the communicator: 1) high resistance to jammers, 2) low probability of signal interception, 3) simultaneous use of signal spectrum by multiple users, 4) multipath suppression, and 5) high resolution ranging. The feasibility of applying spread spectrum to radar has been studied by Salzman (Ref11) with the emphasis on exploiting the low probability of intercept and jammer resistance characteristics of such wideband signal formats. The general conclusion of the study asserts that spread spectrum is applicable to airborne radar (utilizing coherent pulse trains) within a decade or two. The major obstacle is the high sampling rates required to process the signal. The sampling rate must, in general, be on the order of the signal bandwidth: approximately 100-500MHz for a typical spread spectrum scenario. The utilization of such bandwidth extent yields high range resolution properties. It is possible that a 30 meter target could be resolved to 1 meter, resulting in the appearance of 30 distinct returns. This target spatial break-up or super-resolved return can appear in several different range bins. Further, each individual return may be

too weak for detection. Therefore, simply integrating the adjacent range bins (non-coherent filtering) would lead to incomplete range collapse losses. In an effort to put the distributed target back together, a target filter has been suggested by Salzman (Ref11). This is a narrowband, matched-filter designed to collapse the doppler-filtered return signal into a centriodal peak at the proper time-delay value. The objective of this study is to determine if the target filter is feasible. More specifically, is a narrowband filter more effective in target range collapse than a non-coherent filter. The criterion for comparison is the resultant signal-to-noise ratio.

Scope

The study will cover radars using several different waveforms with extents on the order of 100 MHz. Various modulations will be computationally simulated and include: bi-phase coding, pseudo-random intrapulse and interpulse frequency hopping with subpulse chirp applied to the frequency hopping signals. Pseudo-random codes will be generated to control the phase and the frequency variations and thereby spread the spectrum. Other waveforms are not considered for reasons developed in chapter II. Return signal formats will be constrained to be a superposition of time-delayed versions of the transmitted signal. This is applicable to the noise-type waveforms simulated under the assumption of negligible doppler shift between scatterers (Ref4:52).

Problem Solving Approach

In order to determine the feasibility of the narrowband target filter, a computer simulation will be implemented. Signal parameters are specified by the user and the program generates a pseudo-random code sequence of length 63 which spreads the signal (via frequency or phase modulation as previously stated). Next, the user specifies one of three types of calculations: 1) produce ambiguity diagram plot and signal spectrum plot, 2) produce received signal spectrum plot and matched-filter response plot, or 3) produce received signal spectrum and target filter response plots. The received signal is generated assuming Swerling I or II type target cross-section fluctuations(RCS). Also, the target filter spectral characteristics are assumed to be the product of the signal spectrum and the range extended scattering function. According to Salzman(Ref11), the range extended scattering function has a Gaussian frequency spectrum. Various computer runs will be made, testing the waveforms developed in Chapter II and the coherent target filter response compared to the incoherent target filter response. The results will be compiled and tabulated for each waveform and type of RCS fluctuation. The basic scenario consists of ten scatterer target occupying ten range bins.

Presentation

This study begins with an extensive review of the study done by Salzman(Ref11), with emphasis on waveform selection. The various type of modulation techniques are presented along

with fundamental definitions and elaboration on the problem of target super-resolution. The next chapter, chapter III, develops the necessary theoretical tools to understand and implement the computer simulation. In this section are: complex signal notation, matched filter theory, optimum receiver in white Gaussian noise, received signal characteristics, development of the radar ambiguity function, and a sampling theory review. Chapter IV describes the rudiments of the simulation software and in this aspect, certain signal parameters such as pulse width, number of subpulses, and time-bandwidth product are presented. Chapter V presents the results of the simulation with tables and graphs. Finally, Chapter VI states the conclusions and recommendations.

II Background

The successful operation of an airborne radar in any hostile electronic warfare scenario will depend on: 1) the radars ability to operate without being detected; 2) the capability to resist electronic counter counter measures(ECM) (Ref11:11). ECM consists of any electronic technique which disrupts the operation of the radar system. Examples include noise or spot jammers, repeater transponders, chaff, and decoys. The ability to resist detection is generally termed low probability of intercept(LPI), while ECM resistance is termed electronic counter-counter measures(ECCM). Salzman (Ref11:34) has concluded that coherent airborne radar systems can optimize both LPI and ECCM capabilities via spread spectrum techniques. The report also indicates that the most significant advantages of a spread spectrum radar system can best be utilized by the fighter/attack mission(Ref11:34).

The term spread spectrum is frequently used to describe systems or signals which possess one of the following: 1) signal modulation schemes with an RF bandwidth considerably wider than required for normal operations or 2) waveforms with time-bandwidth products on the order of 100 to 1000. Spread spectrum communication most often means the transmit bandwidth is several orders of magnitude greater than the data bandwidth. Spread spectrum radar implies that the transmit bandwidth is several orders of magnitude greater than the reciprocal of the desired range resolution. Regardless of

whether the spectral extent is much greater than required for either data transmission or range resolution, the critical feature of any spread spectrum system is the broad transmitted bandwidth. These bandwidths may range from tens to hundreds of mega-hertz. It is useful to note that the second definition above is also referred to as pulse-compression. Historically, pulse-compression was a result of energy conservation efforts by radar engineers. For clarity, spread spectrum will mean that the transmit bandwidth is much larger than the data bandwidth (ie definition 1 above) (Ref 11:9-10). These large bandwidths will dictate special system hardware requirements and prudent radar waveform selection.

The design of a spread spectrum radar system begins with the selection of a signal waveform and it is this selection which the system design must accommodate. The paramount criterion for selection of a waveform will be the maximum LPI/ECCM benefit given acceptable ease of system implementation, complexity, and cost. The spread spectrum waveforms discussed are categorized according to their respective modulation techniques.

A RF carrier may be modulated via amplitude or angle (or frequency) and is represented in complex form as

$$s(t) = u(t) \exp j [2\pi (f_c + f_m(t)) + \phi(t)] \quad (1)$$

where $u(t)$ is the signal envelope, f_c is the carrier frequency,

$\phi(t)$ the phase modulation, and $f_n(t)$ is the frequency modulation. The real part of $s(t)$ constitutes the physical signal. Typical of coherent airborne radar are pulse-doppler systems which can be grouped as either intrapulse(internal to the pulse) or interpulse(pulse-to-pulse) modulation. Further modulation classification would be discrete verses continuous changes in phase, frequency, or amplitude. For a series of pulses the complex signal is

$$s(t) = \sum u_n(t_n - T) \exp[j2\pi(f_0 t + f_n(t_n - T)) + \phi_n] \quad (2)$$

where the summation is not a mathematical one, but rather a description of a series of pulses. The subscript n above indicates discrete coding by either frequency(f_n) or phase(ϕ_n). Imbedded in $u_n(t)$ is any continuous modulation internal to a given pulse and can further be expressed as

$$u_n(t) = A_n(t) \exp[j\theta(t)] p_n(t) \quad (3)$$

where $\theta(t)$ is continuous angle modulation, $A_n(t)$ amplitude modulation, and $p_n(t)$ is the pulse function defined by

$$p_n(t) = \text{rect}\left(\frac{t - T_p/2}{T_p}\right) = u(t) - u(t - T_p); \text{interpulse}$$

$$\text{rect}\left(\frac{t - T/2}{T}\right) = u(t) - u(t - T) \quad ; \text{intrapulse}$$

where $u(*)$ is the unit step function. The difference between interpulse and intrapulse schemes is illustrated in figure 1.

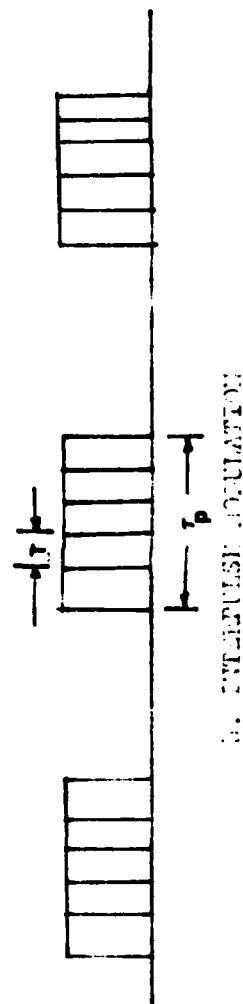
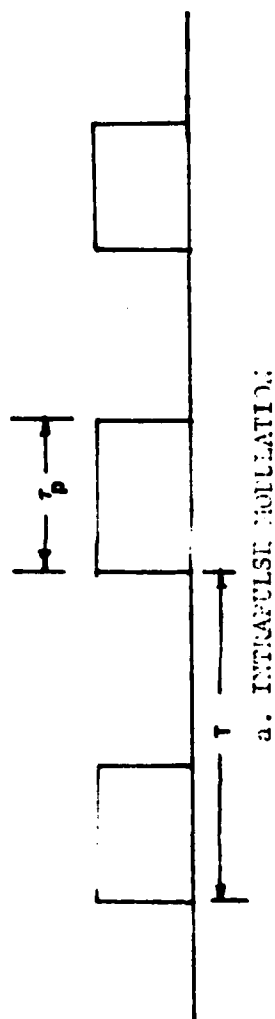


Figure 1. INTRAPULSE AND INTERPULSE MODULATION

Salzman(Ref11:80) has designated the waveforms(modulation techniques) shown in table I as candidate for the coherent airborne mission. In order to select one of the signal formats of table I, system implementations must be reviewed to insure the feasibility of any given selection. This has been done by Salzman(Ref11:82-109) with the following modulations selected for further consideration: random FH, bi-phase intrapulse coding with dwell-to-dwell PRF stagger. The rudiments of the above implementations will be discussed next. The system configurations are offered for completeness and should not be viewed as the only realization.

Varying the frequency from pulse to pulse ,as shown in figure 2, constitutes interpulse, random frequency hopping. The transmitted signal will be wideband but the processing can be either wideband or narrowband. Wideband processing will yield high range resolution and at the same time require the frequency hop to be commensurate with the pulse bandwidth. This will help to reduce clutter and range ambiguous targets. A particular system is shown in figure 3. This implementation has as its main advantage an A/D converter which requires sampling rates that are currently realizable. In other words, the bandwidth at the output of the phase detectors is on the order of the pulse envelope bandwidth; thus requiring conventional sampling rates of the A/D circuitry. Phase shifting and combining samples of the pulse train will restore the spread spectrum resolution. Physically, this is accomplished in the range bins which correspond to a given

Spread Spectrum Modulation Techniques

Interpulse	Interapulse	Hybrid
linear frequency hopping (FH)	linear FM(LFM) or chirp	random interpulse FH with LFM-**
random FH-*	FM variates VFM parabolic FM	random interpulse FH with intra-pulse phase coding-**
phase coding-** biphase polyphase	phase coding-** biphase polyphase	random intrapulse FH with subpulse chirp-**
pulse jitter-*	stepwise chirp random FH-** simultaneous multi freq. pulse-**	any of the above with pulse jitter simultaneous multi freq. with pulse jitter-**

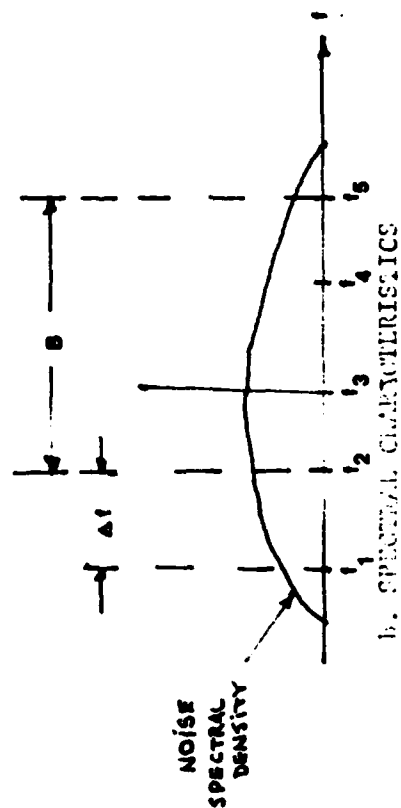
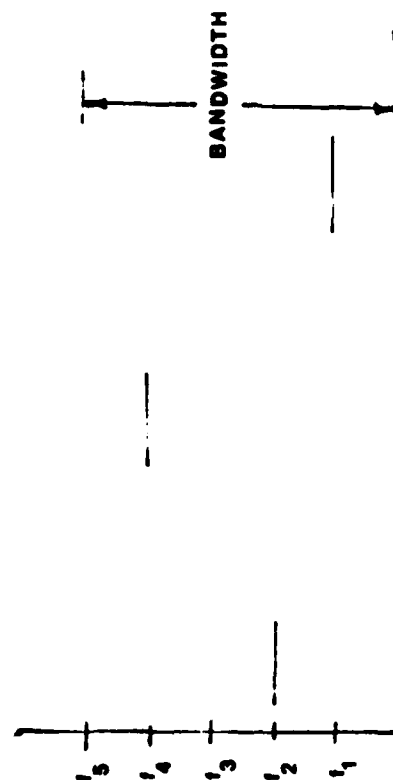
* ECCM/LPI at narrow per pulse bandwidth

** ECCM/LPI at wide per pulse bandwidth

Table I. (Ref11:81)



a. PULSE TRAIN CHARACTERISTICS



Copy available to DTIC does not permit fully legible reproduction

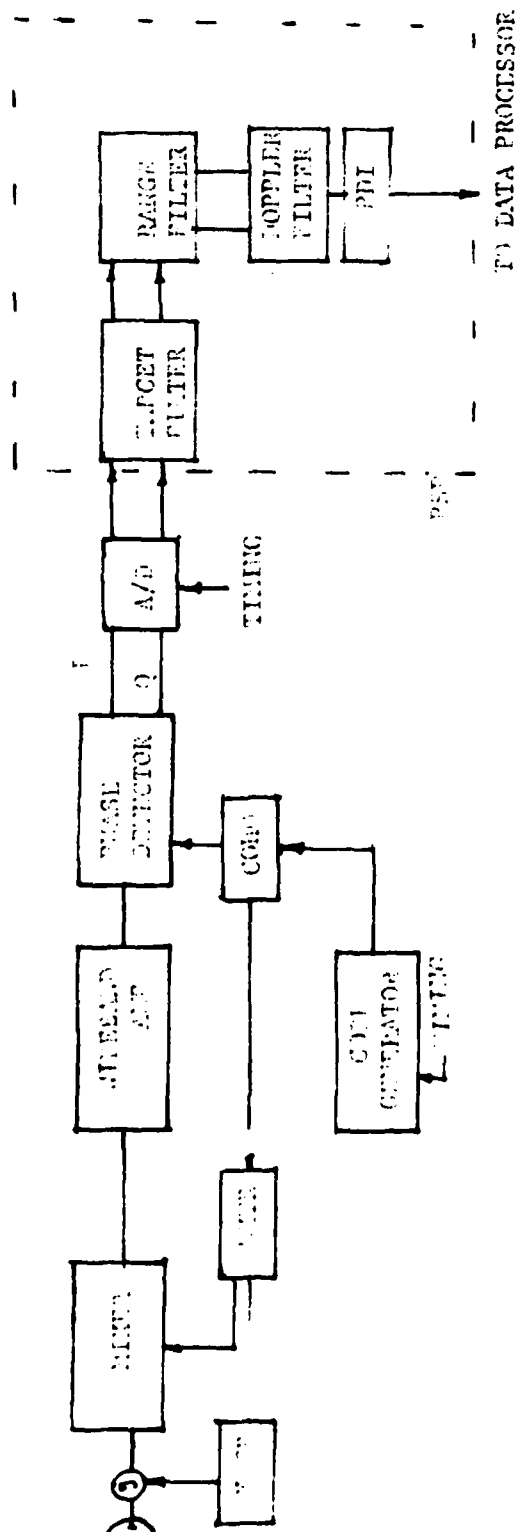


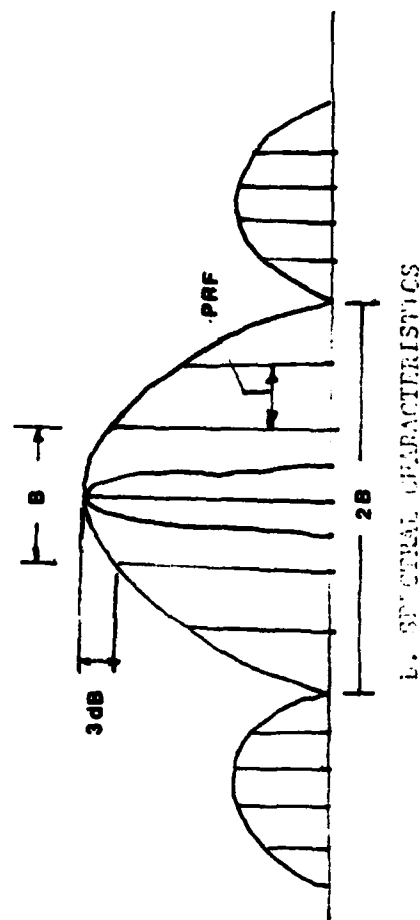
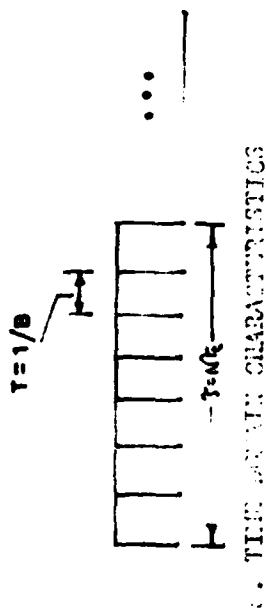
FIGURE 3. SIGNAL PATH IN A TARGET TRACKING SYSTEM

Copy available to DTIC does not permit fully legible reproduction

doppler shift. The process is repeated for each sample and once the range bins have been processed for all samples, the entire range process is repeated for each doppler bin. Doppler bins are separated in frequency by the reciprocal of the code length produced by the code generator.

Intrapulse modulation consists of a pulse train where each individual pulse is modulated discretely. This modulation can be viewed as a series of subpulses whose phase or frequency content is dictated by a pseudo-random code. The utilization of bi-phase coding or frequency hopping for the subpulse modulation yields a maximum ECCM capability at a minimum in target degradation and clutter rejection.

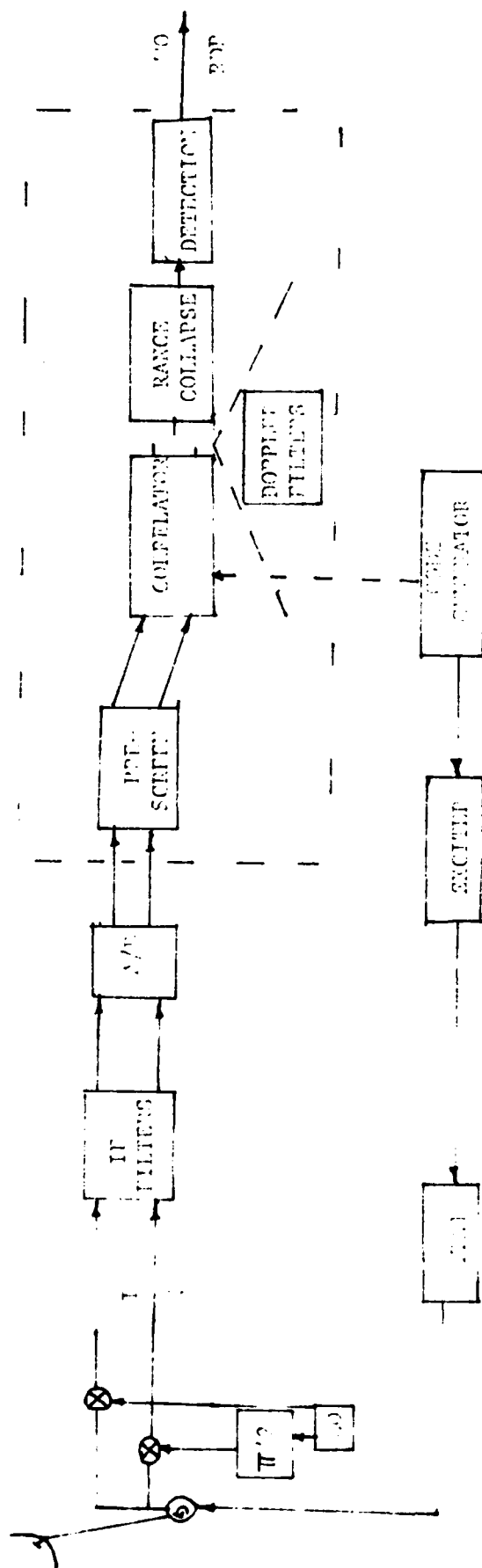
Biphase coding consists of a transmitted pulse with subpulse shifted Π radians in phase from the center frequency. The phases of each subpulse are determined by a known code. The frequency and temporal characteristics are illustrated in figure 4. The generating code is N bits long and is determined based on its affect on the waveform ambiguity function. The ambiguity function is reviewed in Chapter III. Each subpulse represents one code bit and requires $B=1/T$ Hz. The critical feature is that the bandwidth and hence the range resolution is determined by the fine structure of the temporal signal. Comparatively, an uncoded pulse would require B/N Hz, thus biphase coding results in spreading the spectrum by a factor of N . The corresponding range resolution is $r= 1/2 cT$, where c is the speed of light, r the range, and T the time extent of each subpulse. An



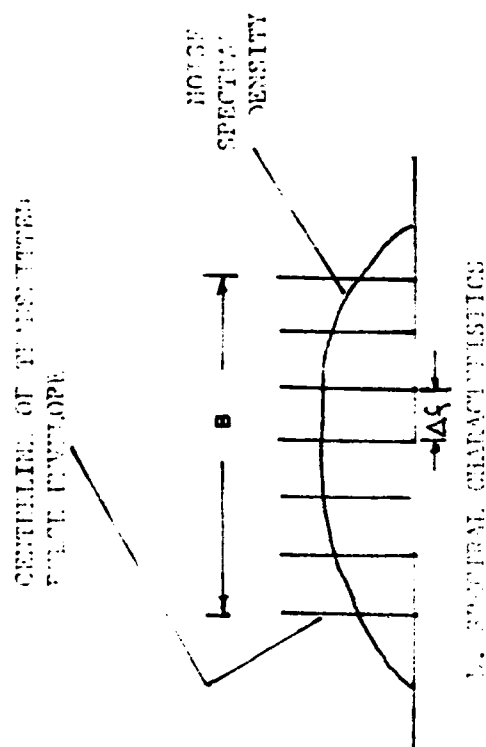
Copy available to DTIC does not
 permit fully legible reproduction

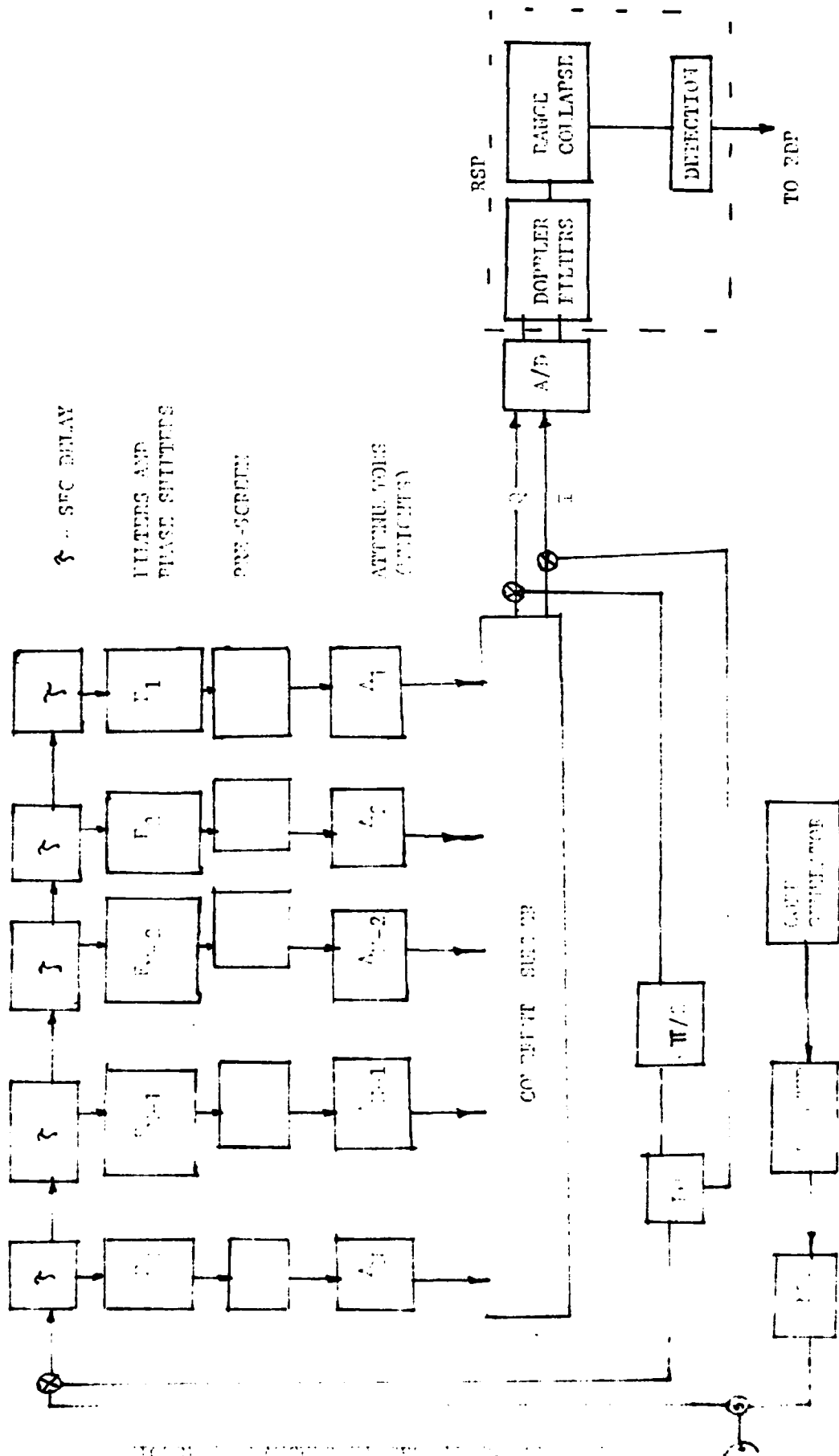
example of one particular processing scheme is shown in figure 5. Since each transmitted pulse contains the full frequency spread, the entire bandwidth must be processed upon return of the signal in order to insure complete correlation. This in turn requires the A/D circuitry to sample at a rate as high as the signal bandwidth. Therefore, biphas-coded spread spectrum is currently limited to approximately 100 MHz or less by the A/D. The most effective solution, in general, would be to relieve the programable signal processor (PSP) from processing the entire bandwidth. One such method might be a "target filter" placed before the PSP, which would coherently narrowband the return (pre-detection range collapse). The target filter will be the focus of this paper and explained more fully in later chapters.

Pseudo-random intrapulse frequency hopping is similar to intrapulse phase coding as previously discussed. The only difference is that now each subpulse is frequency shifted according to the pseudo-random code. Figure 6 reveals the waveform modulation characteristics. Figures 7 and 8 depict two processing techniques, the first is essentially a matched filter receiver and the second is termed "stretch" processing. The matched filter receiver uses tapped delay lines, filters, phase shifters, attenuators, and a coherent summer to correlate the return. The stretch receiver mixes the return with a local oscillator that is stepped in frequency according to the transmitted code. The result is that the processed signal will have a frequency shift that corresponds to the



Copy available to DTIC does not permit fully legible reproduction





\uparrow - SEC DELAY

FILTERS AND
PHASE SHIFTERS

ATTENUATORS

ATTENUATORS
(GAINERS)

RSP

DOPPLER
FILTERS

A/D

I

Q

COEFFICIENT SUMMING

$\pi/2$

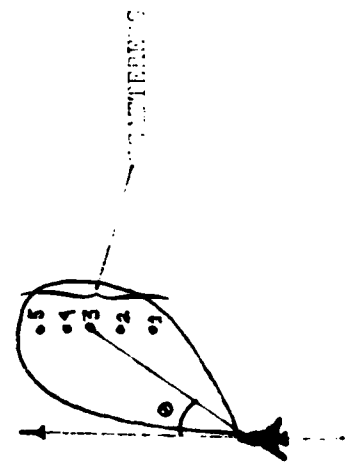
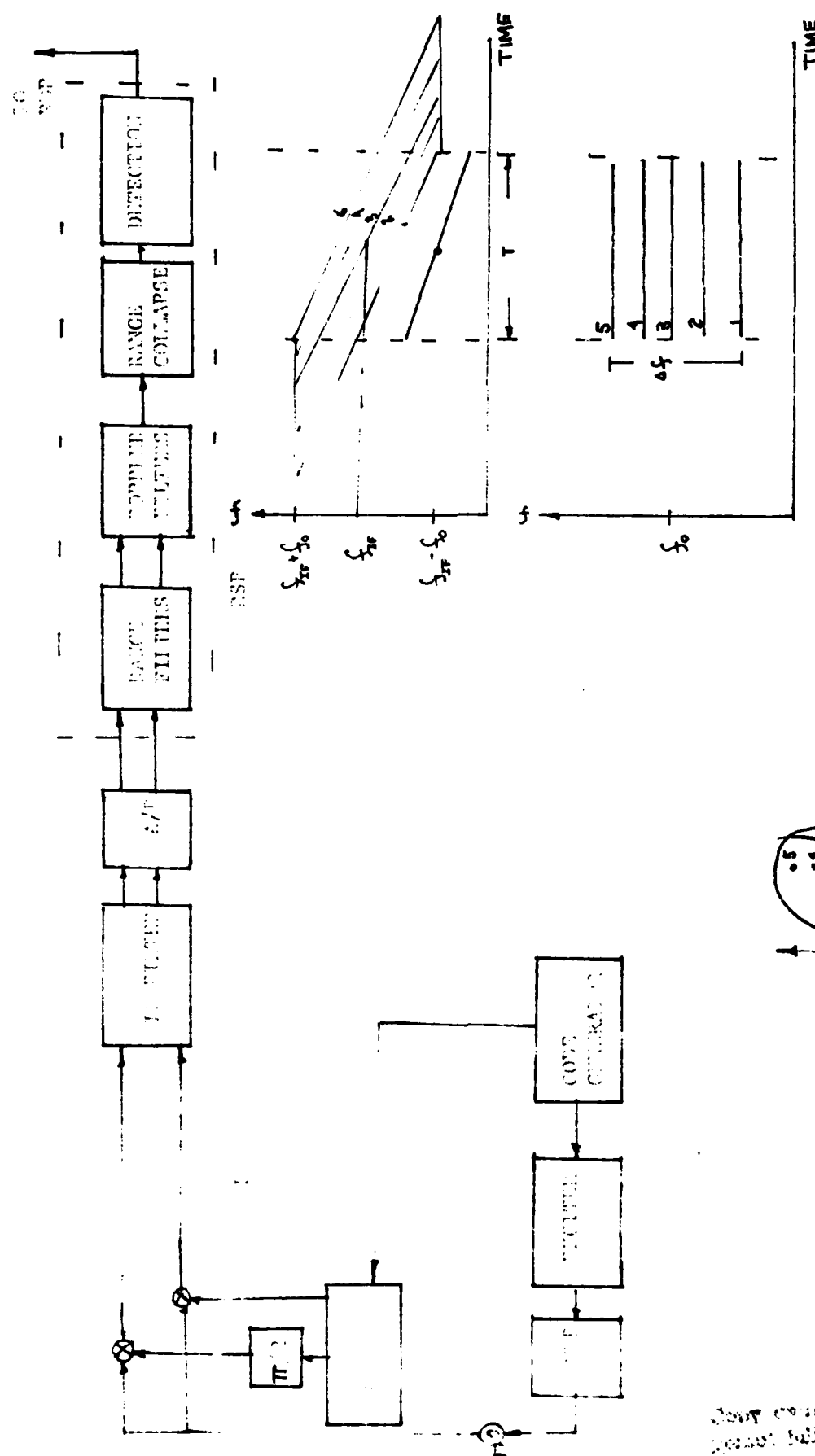
$\pi/2$

COEFFICIENT SUMMING

DEFLECTION

TO RDP

Copy available to RDP for not
perfect fully legible reproduction



DO NOT CORRELATE WITH THE COST CORRELATOR

target range. The signal is sampled by the A/D, Fast Fourier transformed to form range filters, and finally doppler processed and range collapsed prior to detection. The stretch techniques primary is that it removes the A/D limitations on bandwidth. The sampling rate of the A/D needs only to be twice the frequency content of the stretched signal over the frequency span of interest (ie Δf in figure 8). There is an additional load placed on the programable signal processor in that it is required to perform a range FFT.

The actual design implementation of any of the previously stated spread spectrum systems presents several challenges and limitations. These problem areas generally consist of hardware limitations and difficulties associated with spread spectrum waveforms.

State of the art hardware limits the possible operation of a spread spectrum system in several areas. Current RF equipment restricts the bandwidth to a few hundred MHz with available signal processors and A/D circuitry limiting the receiver bandwidth to less than 100 MHz. Wideband antenna design becomes difficult when constrained by such parameters as narrow beamwidth, high gain, and low sidelobes; all of which are important from both an ECCM standpoint and for optimum target detection/clutter suppression in a fighter/attack mission. The use of phased-array antenna systems, although costly, provide the desired bandwidth response necessary for a spread spectrum radar.

Another area of concern is in the proper use and/or

design of wideband elements. The important figures of merit include: phase and amplitude distortion, RF power levels, dynamic range and noise figure. Most of the phase and amplitude distortion is encountered in the transmission lines which may be coaxial cable or waveguide. The frequency response for long coaxial lines is generally non-uniform resulting in amplitude distortion. Properly matched lengths of up to 100 feet can achieve bandwidths of approximately 25%. Radars operating at or above S-band utilize waveguide in order to avoid propagation losses of the higher modes. However, wideband operations create dispersive losses resulting from the propagation of the TM modes. The delays are not constant with frequency. These distortions can be corrected via waveguide filters, proper selection of waveguide size, and digital correction in the radar signal processor. As far as power amplifiers are concerned, the traveling wave tube can achieve bandwidths of 10-30% and is generally the transmitter type found in coherent airborne radar. Also, the use of solid state devices such as GaAs FET amplifiers provide low noise (noise figure 3dB), high dynamic range, wideband, and low distortion, RF receivers.

Spread spectrum modulation can be classified as intrapulse, interpulse, or hybrid as was previously illustrated in table I. The technological limitations of using these modulations is the subject of this section. The pseudo-random polyphase intrapulse codes are common in both radar and communications applications. The technology is well

developed. The hardware is readily available, low cost, standard, and broadband. Polyphase code generators operating at or above 500 MHz are currently available.

On the receiving side, despreading processors or pulse compressors (PC) can be either correlation or convolutional matched filter processing. A matched filter convolves the return with the filters impulse response (a time inverted and shifted form of the transmitted signal). The output of the filter is a narrow, time compressed pulse. State of the art technology available to perform the operation include:

- 1) digital: bipolar, CMOS/SOS, charged-coupled devices (CCD)
- 2) discrete time analog CCDS
- 3) surface acoustic wave devices (SAWD):
fixed-code and programable, coherent
memory, convolvers, MOS-hybrid.

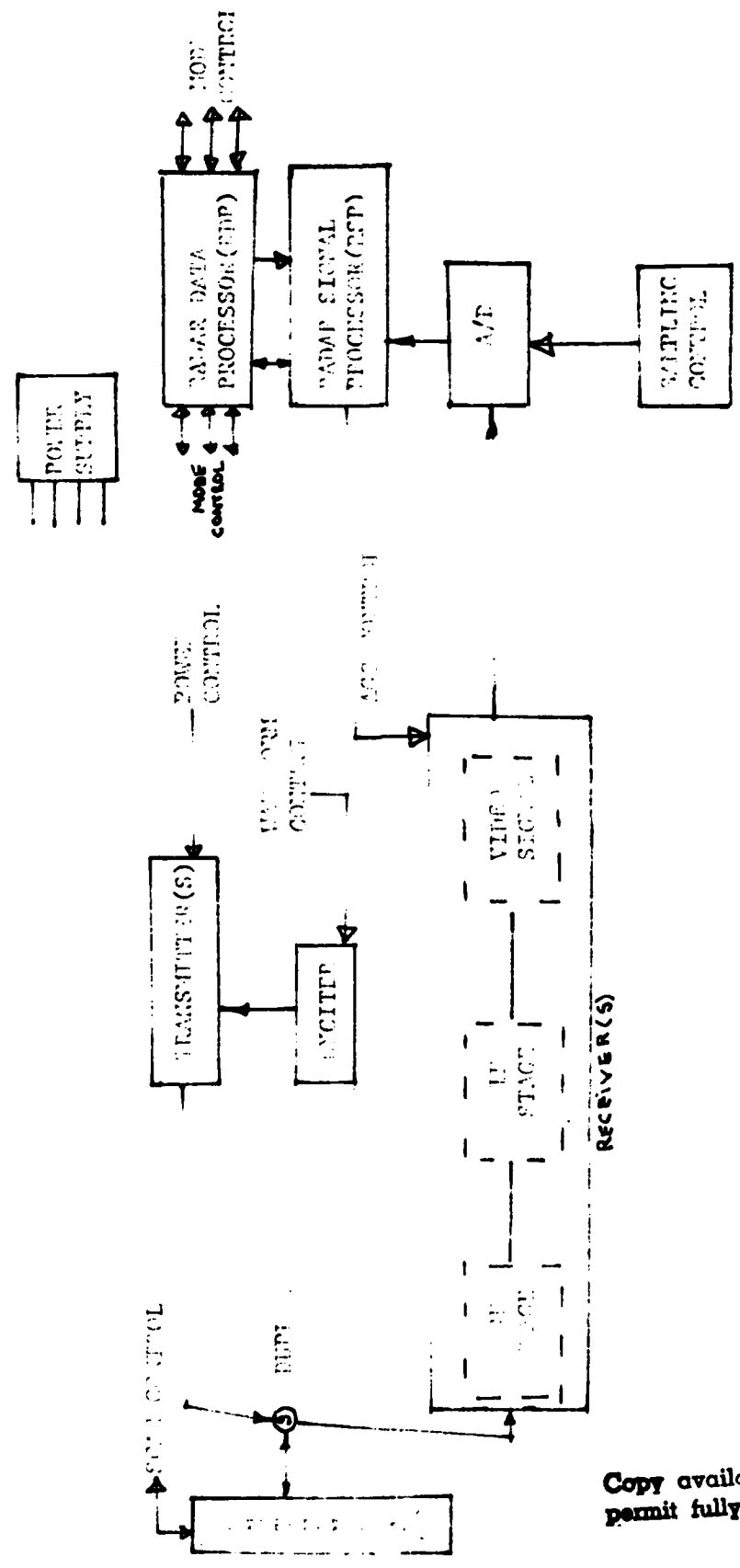
Thus, current technology exceeds present or near term system requirements, capabilities, and frequency allocation restrictions for matched filters.

The generation of either interpulse or intrapulse frequency hopped (FH) signals requires a fast, coherent switching frequency synthesizer. Two methods exist for generating a FH waveform: direct and indirect synthesis. Direct synthesis produces the output frequency from one precise frequency source and uses mathematical multipliers, dividers, adders, and/or subtractors. This allows faster switching times and fine frequency resolution assuming the time delay through the bandpass filters is negligible compared to the switching transient. Indirect synthesis yields the

output frequency by mixing one or more voltage controlled oscillators which are often phase locked to a frequency reference. In either of the above cases, the ability to produce the frequency translations of FH systems is presently available.

Another hardware limitation involves the radar digital signal processor. Its function is to condense the sensor data several orders of magnitude so that the radar data processor (RDP) can make decisions concerning the radars current tasking. Figure 9 is a generalized diagram of a typical coherent airborne radar. Typical values for a conventional radar would include a 3 MHz operating rate for the A/D converter at the signal processors front end. For a spread spectrum radar, the A/D may be required to operate at rates up to the signal bandwidth. This will depend on the particular system configuration as was reviewed previously. Present capabilities of A/D converters have been greatly enhanced by the integrated circuit chip. Current monolithic A/D converters are operating at several MHz with 12 to 14 bits of resolution. The tactical fighter/attack mission requires this level of resolution due to the environment in which it operates (ie ECM and clutter). Sampling rates for intrapulse phase codes require the A/D to operate on the order of the transmit bandwidth, which could be as much as 500 MHz. FH configurations, however, can be designed to require much lower, realizable sampling rates. Future predictions for A/D converters are promising in terms of their effect on spread

- - - - - SIGNAL/VIDEO/CONTROL FLOW
 - - - - - POWER FLOW



Copy available to DTIC does not
 permit fully legible reproduction

spectrum technology. GaAs FET devices are scheduled to deliver rates above 1 GHz with 12 to 14 bits of resolution by 1985 while Josephson Junction technology will provide 10 GHz by 1990.

The quantized data output of the A/D is delivered to the radar signal processor where algorithms perform various inner-products on large data sets. Such operations include: filtering, convolution, correlation, and spectrum analysis (discrete and Fast Fourier transforms). Generally, the processors are programmable due to the complexity (ie number of operational modes) of state of the art radar systems. The use of spread spectrum waveforms places considerable burden on the programmable signal processor (PSP), where a 500 MHz signal bandwidth may require the PSP to operate at 1 giga-operation per second (GOPS). This is currently unrealizable since present PSP capability is in the area of about 20 MOPS. Projected VLSI, GaAs technology should yield 1 GOPS within 10 years. The conclusion to draw from the above discussions of the various hardware limitations, design challenges, and future technology is that as far as device technology is concerned, spread spectrum is a viable concept for coherent airborne radar in the near future (10 years). The development and implementation of spread spectrum radar with current technology is feasible, but only if certain problems (such as A/D sampling rates) can be circumvented. Also, the transmit waveform must be carefully selected as it has direct bearing on the receiver configuration and thus feasibility of the design.

Certain problems unique to excessively broadband waveforms exist that are not encountered with low resolution waveforms. The following discussion presents the major design challenges of selecting a suitable spread spectrum waveform. These characteristics are dependent solely on the waveform modulation (FH, biphase coded) structure and its corresponding spectral characteristics.

Waveform self-clutter is a problem with any radar signal and can be thought of as any output from a matched filter due to non-matched targets (ie targets with doppler and delay which should not cause a response). The figure of merit which is used to describe the self-clutter of a waveform is the ambiguity function and its corresponding ambiguity diagram. The function is defined as:

$$\chi(\tau, \nu) = \int_{-\infty}^{\infty} s(t) s^*(t-\tau) \exp[j2\pi \nu t] dt \quad (4)$$

The function is the correlation of the signal with a doppler shifted, range delayed version of itself. By taking the square of the functions magnitude and plotting it against delay(τ) and doppler(ν), we obtain a visual representation of the output of a matched filter matched to the signal and whose input is any combination of delayed and/or doppler shifted versions of the signal. This can also be viewed as the output of a correlation followed by envelope detection. A cross-section of the ambiguity surface taken parallel to the doppler axis and at $\tau = \tau_0$ would represent the filter output

corresponding to a fixed range (γ) and doppler mismatched over all possible values. The radar receiver approximates the ambiguity function via a two-dimensional array of correlators (time delay .vs. doppler shift) or a single array of matched filters (doppler shifted). In order to resolve a target in both range and doppler, the majority of the filter response must be located at the center of the ambiguity diagram. This is where the γ, v combination for that target intersect. Therefore, the ideal ambiguity diagram would be a single spike at the origin and zero elsewhere. This is physically impossible. The reason for this is made clear in Chapter III, where a mathematical treatment of the ambiguity surface is presented.

A receiver response to interference (clutter, noise, non-matched targets) is largely a function of its ambiguity characteristics. Complicating the problem is the fact that there does not appear to be an analytic method to construct a signal from a particular ambiguity surface. Therefore, a particular signal(s) is selected and from this we can construct the ambiguity surface and predict the waveforms self-clutter properties.

The inherently high range resolution of a spread spectrum radar (assuming the entire bandwidth is effectively processed) presents a problem termed "target super-resolution". This super resolution is a direct consequence of the Fourier integral property: large spectral extent transforms to short time extent. For a target whose spatial

extent is greater than the radar resolution (waveform bandwidth), it appears to the receiver as several targets each resulting from the targets individual scatterers. Assuming a transmit bandwidth of several MHz, the resolution is approximately one foot. Thus, a forty foot target is "broken up" into forty separate returns. If the radar receiver bandwidth were matched to the largest target extent, the individual returns could simply be non-coherently integrated and the complete RCS recovered. The individual scatterers of the super-resolved target may be too weak to be detected. This is the essence of the super-resolution problem and the focal point of this paper. In order to compensate for the over resolution properties of wideband radar signals, a "target filter" is required. This filter will perform an integration on the individual returns in one of two ways: post-detection, non-coherent range collapse or pre-detection, coherent integration.

The non-coherent target filter consists of post-detection integration or equivalently range collapsing the range data to match the target dimension. This is done after envelope detection and requires the entire signal bandwidth to be processed. If the majority of the target scatterers occupied a single range cell, then the optimum processing would be single cell observation. Target scatterers which have low RCS and occur in several range cells require cell-to-cell integration for detection enhancement. Processing the entire signal bandwidth places a burden on current programmable

signal processor capabilities. In certain instances, 500 MHz bandwidths with phase coding for example, this makes the system unrealizable. Other disadvantages of post-detection integration include those normally associated with this type of processing: collapsing loss and post-detection integration loss. In an effort to reduce the bandwidth restrictions and PSP loading, a coherent, pre-detection filter is considered.

A coherent target filter is a matched filter (ie correlator) which may depend on the return signal being narrowband. Assuming the signal spectrum is represented as $S(j\omega)$, and the spectral characteristics of the scattering function (range-extended target) as $H(j\omega)$, a matched filter would have a spectrum which is $S(-j\omega)H(-j\omega)$. The bandwidth of this filter may be narrowband (see Chapter III) with respect to the signal spectrum. If this conjecture holds, a considerable processing advantage (on the PSP) could be gained; the result being realization of a spread spectrum radar system.

The objective of this thesis will be to explore narrowbanding effects of the transmitted waveform. This will be accomplished via comparisons of signal-to-noise ratios for non-coherent filtering .vs. coherent narrowband filtering. Two waveforms are considered: FH and biphase coded. Also, target models will include Swerling I and II amplitude fluctuations. The thesis will, in the process of simulating the above filter, attempt to verify the results of Salzman (Ref11) that the coherent filter is advantageous (SNR) only 20% of the

time,(assuming intrapulse biphase coding ,length 63, Swerling
I and II fluctuations).

III Theoretical Considerations

Complex Signal Representation

Many radar signals, systems, and filters of practical interest satisfy the narrowband criterion. This means the frequency content (signal) or frequency response (filters) is confined to a frequency band which is a small percentage of the center or carrier frequency (Ref12:55). A generally accepted figure of 10% has been applied in most radar applications and will be adhered to through out this study (Ref2). Complex signal notation will now be presented assuming narrowband signals. This is not a necessary condition but serves to simplify interpretation of the results. A real, narrowband signal, $f(t)$, can be expressed as

$$f(t) = \text{Re}[u(t)\exp(jw_0 t)] \quad (5)$$

Since $u(t)$ is by definition a slowly varying function of time, its Fourier transform, $U(w)$, is band limited to $w > -w_0$. The exponential factor serves to shift the spectrum to the right by w_0 , resulting in a purely positive spectrum. The component, $u(t)$, is referred to as the complex envelope of the real signal, $f(t)$, and contains the angle and amplitude modulation of the real signal (Ref3:58). The product $u(t)\exp(jw_0 t)$ represents the analytic signal and is further developed:

$$f(t) = \text{Re}[u(t)\exp(jw_0 t)] \quad (6)$$

$$= \text{Re}[f_s(t)] \quad (7)$$

$$\text{where } f_s(t) = f(t) + j\hat{f}(t) \quad (8)$$

$\hat{f}(t)$ is the Hilbert transform of $f(t)$ and is defined by

$$\hat{f}(t) = \frac{1}{\pi} \int_{-\infty}^{+\infty} \frac{s(\tau)}{t-\tau} d\tau$$

where the integration calculates the Cauchy principle value. The analytic signal spectrum has only positive frequencies and is related to the real signal spectrum via

$$U(w) = \begin{cases} 2F(w) & , w > 0 \\ F(w) & , w = 0 \\ 0 & , w < 0 \end{cases}$$

$u(t)$ is a complex, lowpass function which can further be written as

$$u(t) = x(t) + j y(t)$$

where $x(t)$ and $y(t)$ are the quadrature components of $f(t)$. In this manner we can mathematically describe signals in the complex domain and derive the physical process via the above transforms. Further, any bandpass signal can be mathematically processed in complex signal notation and physically interpreted as manipulations of the quadrature components (Ref2). To illustrate this we start with equation 7 and a

bandpass, real signal $Z(t)$:

$$\begin{aligned} Z(t) &= \text{Re}[Z_c(t)] \\ &= \text{Re}[u(t)\exp(j\omega_0 t)] \\ &= \text{Re}[|u(t)| \exp(j\omega_0 t) \exp(j\phi(t))] \end{aligned}$$

where $\phi(t)$ is the angle of $u(t)$,

$$\begin{aligned} Z(t) &= \text{Re}[\sqrt{X^2(t)+Y^2(t)} \exp[j\omega_0 t + \phi(t)]] \\ &= \sqrt{X^2(t)+Y^2(t)} \cos[\omega_0 t + \phi(t)] \end{aligned} \quad (9)$$

$$\begin{aligned} \text{using} \quad Z(t) &= X(t)\cos(\omega_0 t) - Y(t)\sin(\omega_0 t) \\ &= M(t)\cos(\omega_0 t + \theta(t)) \end{aligned} \quad (10)$$

$$\begin{aligned} \text{where} \quad M(t) &= \sqrt{X^2(t)+Y^2(t)} \\ \theta(t) &= \tan^{-1}\left[\frac{Y(t)}{X(t)}\right] \end{aligned}$$

and comparing this to equation 9 we see that $Z(t)$ can be represented as

$$\begin{aligned} Z(t) &= \text{Re}[u(t) \exp(j\omega_0 t) \exp(j\phi(t))] \\ &= \text{Re}[a(t) \exp(j\phi(t)) \exp(j\omega_0 t)] \end{aligned}$$

where $a(t) = M(t) = |u(t)|$
and $\theta(t) = \phi(t)$ above.

Thus, $u(t)$ contains all the angle and amplitude information of the real bandpass signal. Suppression of the $\exp(j\omega_0 t)$ factor causes no loss of information; therefore the complex envelope $u(t)$ will be used to represent the signals simulated in this

study. The above has assumed the narrowband criterion so that $a(t)$ (the signal amplitude modulation) can be directly associated with $|u(t)|$ and $\phi(t)$ associated with any angle modulation ($\theta(t)$).

In an analogous manner, complex notation can be extended to the definition of filter transfer functions. The real impulse response of a linear, time invariant filter may be expressed as

$$h(t) = \text{Re}[2 \tilde{h}(t) \exp(j\Omega t)] \quad (11)$$

where $\tilde{h}(t)$ is the complex impulse response function and the factor of 2 is for convenience in later expressions. Let $x(t)$ and $y(t)$ be the real input and output expressions respectively and express their analytic counterparts as

$$x_s(t) = x(t) + j\hat{x}(t) = \tilde{x}(t)\exp j\Omega t \quad (12)$$

$$y_s(t) = y(t) + j\hat{y}(t) = \tilde{y}(t)\exp j\Omega t \quad (13)$$

Further,

$$y(t) = h(t) * s(t) \quad (14)$$

where $*$ denotes convolution and

$$\begin{aligned} y_s(t) &= h(t) * x(t) + jH[h(t) * x(t)] \\ &= h(t) * x(t) + jh(t) * \hat{x}(t) \end{aligned} \quad (15)$$

where H represents the Hilbert transform, and we have used the property of Hilbert transform theory: if $y(t) = v(t) * x(t)$, then

$\hat{y}(t) = v(t) * \hat{x}(t)$. Proceeding further,

$$\begin{aligned} y_s(t) &= h(t) * [x(t) + j\hat{x}(t)] \\ &= h(t) * x_s(t) \end{aligned} \quad (16)$$

Equation 16 can be written in integral form as

$$\begin{aligned} y_s(t) &= \int h(\tau) x(t-\tau) d\tau \\ \text{or} \quad \tilde{y}(t) \exp j\Omega t &= \int h(\tau) \tilde{x}(t-\tau) \exp j(t-\tau) d\tau \\ \text{also,} \quad \hat{y}(t) &= \int h(\tau) \exp -j\Omega\tau \tilde{x}(t-\tau) d\tau \end{aligned} \quad (17)$$

using the property for any complex function, $z(t)$,

$\text{Re}[z(t)] = z(t)/2 + z^*(t)/2$ and applying this to $2\tilde{h}(\tau) \exp j\Omega t$ we obtain

$$h(\tau) = \tilde{h}(\tau) \exp j\Omega\tau + \tilde{h}^*(\tau) \exp -j\Omega\tau \quad (18)$$

and

$$h(\tau) \exp -j\Omega\tau = \tilde{h}(\tau) + \tilde{h}^*(\tau) \exp -j2\Omega\tau \quad (19)$$

Equation 18 is now substituted into equation 17 to obtain

$$\tilde{y}(t) = \int \tilde{h}(\tau) \tilde{x}(t-\tau) d\tau + \int \tilde{h}^*(\tau) \tilde{x}(t-\tau) \exp -j2\Omega\tau d\tau$$

For narrowband signals, the second integral becomes negligible (ie designates radian frequency) and

$$\tilde{y}(t) = \int \tilde{h}(\tau) x(t-\tau) d\tau \quad (20)$$

We see that the complex envelope of the output is the

convolution of the complex envelope of the input with the complex impulse response of the filter (Ref12:74). The real bandpass output is obtained via

$$\begin{aligned} y(t) &= \text{Re}[\tilde{y}(t)\exp j\omega_0 t] \\ &= \text{Re}[(\tilde{x}(t)*\tilde{h}(t))\exp j\omega_0 t] \end{aligned} \quad (21)$$

Given the transfer function of a narrowband filter, the complex impulse response is determined by the following:

$$H(j\omega) = \tilde{H}(\omega - \Omega) + \tilde{H}^*(-\omega - \Omega) \quad (\text{note equation 18 above}) \quad (22)$$

For a filter with lumped circuit elements, the poles are located near $\omega = \pm \Omega$. If the poles near $+\Omega$ are associated with $\tilde{H}(\omega - \Omega)$ and the poles near $-\Omega$ associated with $\tilde{H}(\omega + \Omega)$, then

$$h(t) = \text{Re}[2 \tilde{h}(t)\exp j\Omega t]$$

and

$$\tilde{h}(t) = 1/2\pi \int \tilde{H}(j\omega)\exp j\omega t d\omega$$

Therefore, the procedure is to take the positive frequency content of the real transfer function, shift it to the origin, and inverse Fourier transform to determine $\tilde{h}(t)$ (Ref12:74). This can be seen graphically through the following three spectral representations:

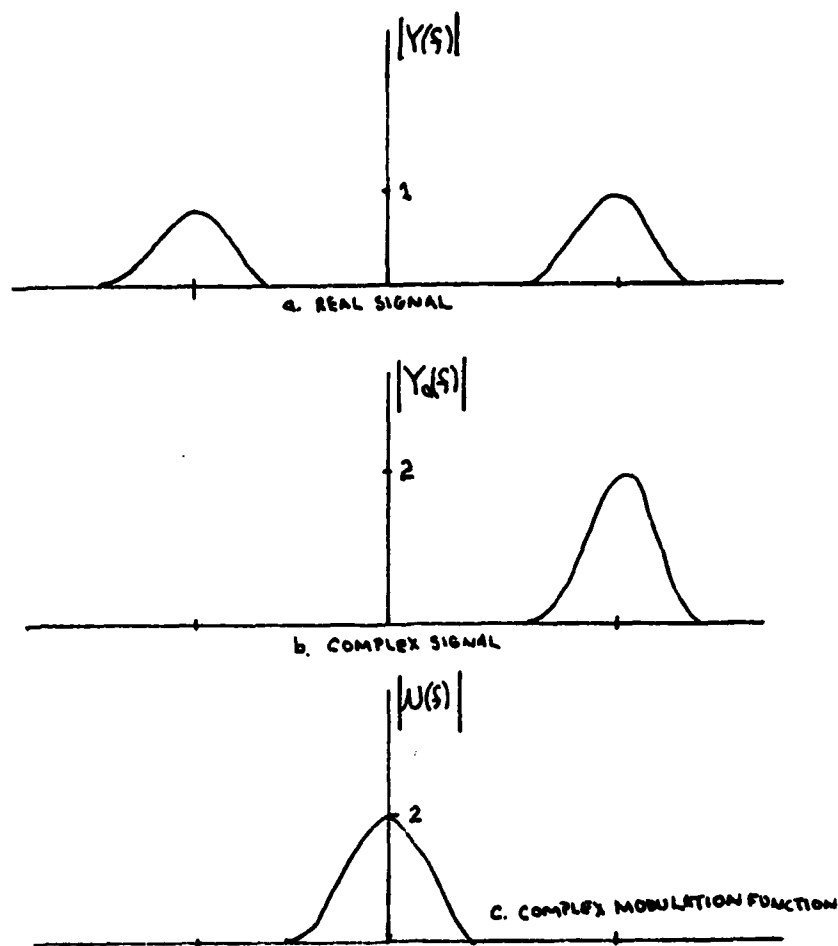


Figure 10. Graphical Representation of Complex Signal Spectrum

The above procedure will be used to develop complex representations for several radar signals and the simulated target filter.

Matched Filter Theory

A standard engineering parameter used to measure the effectiveness of a radar receiver is the signal-to-noise ratio. The ratio is defined as the peak signal power divided by the average noise power. The goal of any radar system is to maximize this ratio thus improving the ability to detect and track targets. Signal-to-noise also has an indirect affect on the range and doppler estimation. The maximization of the signal-to-noise ratio leads to the definition of the matched

filter. Identical results can be achieved via decision theory, specifically the optimum receiver in white Gaussian noise (Ref3:143,145-149).

Assume an input waveform $z(t)=s_i(t)+n_i(t)$ where: $s_i(t)$ = input signal, $n_i(t)$ = noise component; and an output waveform $y(t)=s_o(t)+n_o(t)$. The objective is to determine the linear filter, $h(t)$, which maximizes the output signal-to-noise ratio at some particular time $t=t_m$. The signal-to-noise ratio is defined as:

$$S/N = \frac{s_o^2(t_m)}{n_o^2(t_m)} \quad (23)$$

For white Gaussian noise, we know that the autocorrelation function is impulsive:

$$R_n(\tau) = \frac{N_o}{2} \delta(\tau) \quad (24)$$

where $N_o/2$ = amplitude of the noise spectral density, $\delta(\tau)$ = Dirac delta function. Thus,

$$S/N = \frac{\left| \int_{-\infty}^{t_m} s_i(\tau) h(t_m - \tau) d\tau \right|^2}{\int_{-\infty}^{t_m} \frac{N_o}{2} h^2(t_m - \tau) d\tau} \quad (25)$$

performing the Fourier transform of the above and applying the Schwarz inequality leads to

$$S/N = \frac{1}{2\pi} \frac{\left| \int_{N_0/2} H(\omega) S_i(\omega) \exp(j\omega t_m) d\omega \right|^2}{\int_{N_0/2} |H(\omega)|^2 d\omega} \leq \frac{1}{2\pi} \frac{\int_{N_0/2} |S_i(\omega)|^2 d\omega}{N_0/2} \quad (26)$$

If $H(\omega)$ is selected such that the equality is satisfied, then

$$H(\omega) = \frac{2k}{N_0} S_i^*(\omega) \exp(-j\omega t_m) \quad (27)$$

Therefore, the optimum filter in white Gaussian noise is

$$h(t) = \frac{2k}{N_0} S_i^*(t_m - t) \quad (28)$$

Next, we repeat the derivation using complex signal notation. Again we seek the filter, $h(t)$, which maximizes the signal-to-noise ratio at $t=t_m$. The input is $x(t) = \text{Re}[\tilde{x}(t)\exp(j\omega_0 t)]$, the filter $h(t) = \text{Re}[\tilde{h}(t)\exp(j\omega_0 t)]$, and the output signal is $y(t) = \text{Re}[\tilde{y}(t)\exp(j\omega_0 t)]$. White Gaussian noise is assumed to pass through the bandpass filter, thus $R_n(\tau) = \text{Re}[R_{\tilde{n}}(\tau)\exp(j\omega_0 \tau)]$ and $R_{\tilde{n}}(\tau) = N_0/2 \delta(\tau)$. Equation 28 is utilized to assert that

$$\begin{aligned} \tilde{y}(t) &= 1/2 \int \tilde{x}^*(t_m - t + \tau) \tilde{x}(\tau) d\tau \\ &= R_{\tilde{x}}(t - t_m) \end{aligned} \quad (29)$$

using the same definition of signal-to-noise ratio,

$$S/N = \frac{1/4 \left| \int \tilde{X}(f) \tilde{H}(f) \exp(2\pi f t_m) df \right|^2}{N_0/4 \int |H(f)|^2 df} \quad (30)$$

The Schwarz inequality produces

$$S/N \leq \frac{\int |H(f)|^2 df \int |X(f)|^2 df}{N_0 \int |H(f)|^2 df} \quad (31)$$

selecting the equality yields $\tilde{H}(f) = \tilde{X}^*(f) \exp(-j\omega t_m)$ and via the Fourier transform:

$$\tilde{h}(t) = \tilde{x}^*(t_m - t) \quad (32)$$

In the next section, the optimum receiver in white Gaussian noise is derived. The result is a matched filter and we see that Decision theory and the maximization of the signal-to-noise ratio lead to the same conclusion.

Optimum Receiver in White Gaussian Noise

The determination of the optimum receiver will assume that we receive a signal with known parameters, and apply Bayes detection criteria in the form of a likelihood ratio. Knowledge of the form of the likelihood ratio yields a test statistic which is used to interpret the structure of the optimum Bayes receiver(Ref8:18).

First, sampling theory is applied to a bandlimited

signal, $s(t)$, limited to $(-w_c, w_c)$. The signal is sampled in time every $1/2w_c$ seconds and is written as:

$$s(t) = \sum_{k=-\infty}^{+\infty} s(k/2f_c) \frac{\sin[2\pi f_c (t - k/2f_c)]}{2\pi f_c (t - k/2f_c)} \quad (33)$$

where $f_c = w_c / 2\pi$ (Ref3:51-53).

It can be shown that

$$E = \int_0^T s^2(t) dt \approx 1/2f_c \sum_{k=1}^{2f_c T} f^2(k/2f_c) \quad (34)$$

where T is the signal duration. Equation 34 simply states that by sampling at twice the bandwidth (Nyquist rate); we can represent the majority of the energy in the sampled domain.

Assuming a known signal bandlimited to $(-f_c, f_c)$, the noise is also bandlimited and the input waveform $z(t)$ becomes \underline{z} , where $\underline{z} = \underline{s} + \underline{n}$ ($z_i = s_i + n_i$) and each sample $z = z(i/2f_c)$, $s = s(i/2f_c)$, and $n = (i/2f_c)$, $i = 1, 2, 3, \dots, 2f_c T$. The hypothesis of the signal plus noise (H_1) is described by the conditional joint probability density function

$$p(\underline{z}/H_1) = \frac{1}{(2\pi)^{N/2} (N_0 f_c)^N} \exp(-1/2f_c N_0 \sum_{i=1}^N (z_i - s_i)^2) \quad (35)$$

Where $N = 2f_c T$ and the power spectral density of the noise is $N_0/2$. In a similar fashion, the noise alone hypothesis (H_0) is represented via

$$p(\underline{z}/H_0) = \frac{1}{(2\pi)^{N/2} (f_c N_0)^{N/2}} \exp(-1/2 f_c N_0 \sum_{i=1}^N z_i^2) \quad (36)$$

The likelihood ratio is

$$\Lambda(\underline{z}) = \frac{p(\underline{z}/H_1)}{p(\underline{z}/H_0)} = \frac{\exp[-1/2 f_c N_0 \sum_{i=1}^N (z_i - s_i)^2]}{\exp(-1/2 f_c N_0 \sum_{i=1}^N z_i^2)} \quad (37)$$

Applying equation 34 to the likelihood ratio we have

$$\Lambda(\underline{z}) = l(z(t)) = \exp[-1/N_0 \int_0^T s^2(t) dt + 2/N_0 \int_0^T z(t)s(t) dt] \quad (39)$$

Further,

$$\ln l(z(t)) = -E/N_0 + 2/N_0 \int_0^T z(t)s(t) dt \quad (40)$$

Thus, the Bayes likelihood ratio receiver is

$$2/N_0 \int_0^T z(t)s(t) dt \underset{H_0}{\overset{H_1}{>}} \text{Threshold} + E/N_0 \quad (40)$$

The left side of the inequality or test statistic is the cross-correlation of $z(t)$ and $s(t)$. A matched filter is used to perform the correlation and we note that the optimum detector in white Gaussian noise is the matched filter. Specifically, for a fixed probability of false alarm, the matched filter is the receiver that maximizes the probability

of detection (Ref2).

As a final note on matched filters, we observe that given a complex signal (analytic) $\psi(t)$, the response of the matched filter is

$$\rho(\tau) = \int_{-\infty}^{+\infty} \psi(t) \psi^*(t-\tau) dt$$

The above complex autocorrelation function can be equivalently represented as a convolution (designated by "*"):

$$\rho(\tau) = \psi(\tau) * \psi^*(-\tau) \quad (41)$$

Equation 41 will later be used to simulate the complex matched filter processing as convolutions (ie FFT algorithm).

Received Signal Representation

The basic radar signal examined in this study is a high-resolution, coherent pulse train with some form of frequency or phase modulation. The simulation will assume we are processing the video (baseband) signal which results from an environment (target model) of many point scatterers. Simulating the received signal from a single scatterer will permit the construction of the return from a conglomerate of scatterers via superposition. This will automatically simulate the phasor interference among several scatterers and is the only way to effectively simulate the environment of high-resolution radar (Ref4:10).

The general form of the received signal from a point scatterer, moving, fluctuating in amplitude or phase, and antenna scanned is

$$s_R(t) = s_T(t - \tau(t)) (\lambda^2 / (4\pi)^3 r^4) G(t) \gamma(t) \quad (42)$$

where $G(t)$ is the one-way antenna power gain, $\gamma(t)$ is the complex reflection coefficient (a voltage quantity related to radar cross-section ($\sigma = |\gamma|^2$)), and $\tau(t)$ is the round trip delay for the target (Ref4:6-10). Equation 42 is difficult to simulate and therefore several simplifications are necessary. If $G(t)$, $\tau(t)$, and $\gamma(t)$ are slow varying functions of time, equation 42 becomes a delayed and doppler-shifted replica of the transmitted signal:

$$s_R(t) = s_T(t - \tau) \exp(j2\pi v t) (\lambda^2 / (4\pi)^3 r^4) G \gamma \quad (43)$$

$$\text{where } \tau = 2r/c \quad (44)$$

$$v = -2\dot{r}/\lambda \quad (45)$$

with r = range
 v = doppler frequency shift
 \dot{r} = velocity
 λ = wavelength

The above specifications are generally termed constant-doppler theory (slowly moving target with respect to a radar look interval) and is valid if the following hold:

$$1. \tau \text{ is constant for } \dot{r} \ll c/2TB \quad (46)$$

where TB is the time-bandwidth product
and $c=3 \times 10^8$ m/s

$$2. v \text{ is constant for } \ddot{r} \ll \sqrt{2T^2} \quad (47)$$

A factor of four is usually sufficient to ensure the conditions are satisfied (Ref4:13). Continuing with equation 42 and setting

$$V_k = [\lambda / (4\pi)^{3/2}] [1/r_k^2] G_k Y_k \quad (48)$$

where the subscript k refers to the k^{th} scatterer, we now have a received signal of the form

$$s_R(t) = V_k s_T(t - \tau(t)) \quad (49)$$

where $\tau(t)$ is not approximated as constant. In terms of complex notation we can express

$$s_T(t) = u_T(t) \exp(j\omega_c t) \quad (50)$$

and

$$s_R(t) = V_k u_T[t - \tau(t)] \exp[j2\pi f_c(t - \tau(t))] \quad (51)$$

The delay is a function of time and depends on the target range at the instant of signal reflection:

$$\tau(t) = 2/c r[t - \tau(t)/2] \quad (52)$$

where $r(t)$ is the range function. Performing a Taylor series yields

$$\zeta(t) = \zeta_k - \frac{v_k(t-t_0)}{f_c} + \text{additional terms} \quad (53)$$

ζ_k , and v_k represent the time and doppler coefficients of the k^{th} scatterer, and t_0 is the time at which they are defined. If equations 46 and 47 are satisfied we can write

$$s_R(t) = V_k u_T(t - \zeta_k) \exp[j2\pi(f_c(t - \zeta_k) + v_k(t - t_0))] \quad (54)$$

Further, we assume multiple scatterers, thus

$$s_R(t) = \exp(j2\pi f_c t) \sum_K V_k u_T(t - \zeta_k) \exp(j2\pi v_k t) \quad (55)$$

The above equation will be simulated with the carrier term suppressed and a simplification made which applies to noise-type waveforms.

If the amplitude or phase modulation of a radar signal is noise-like, equation 55 cannot be simplified further unless we assume short pulses. For a pulse train as shown in figure 12, the bandwidth is approximately the inverse of the pulse width $B = 1/T_p$, and the time-bandwidth product is on the order of unity ($TB=1$).

Resolution in delay is given by $\Delta\zeta = 1/B$ and is also determined by the pulse width: $\Delta\zeta = T_p$. When T_p is short enough to achieve a given resolution in delay, it will be impossible

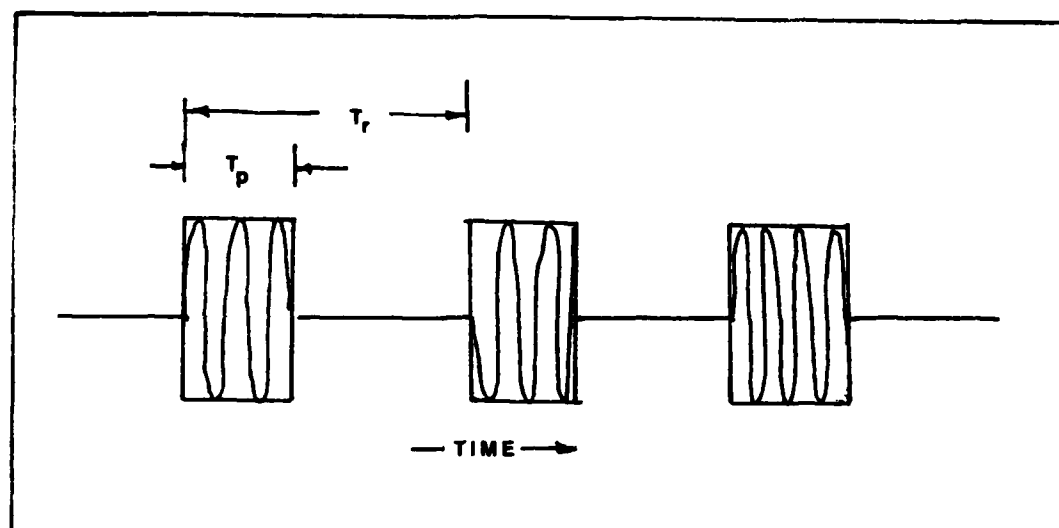


Figure 11. Coherent Pulse Train (Ref4:55)

to resolve scatterers in doppler due to the property $\Delta v = 1/T_p$, thus it is possible to assume all scatterers have the same doppler velocity (Ref4:51). Further, the doppler is assumed equal to zero for convenience. This yields a received signal:

$$s_R(t) = \exp[j2\pi f_c t] \sum_K V_K u_T(t - \tau_K) \quad (56)$$

Equation 56 (with $\exp[j2\pi f_c t]$ suppressed) will be directly simulated in this study. The assumption of short pulses ($T_B = 1$) is equivalent to assuming the doppler spread of all scatterers is small (Ref4:52). It is the later assumption which we are simulating. The actual waveform may or may not have a time-bandwidth product on the order of unity.

Ambiguity Function

In order to quantitatively assess the performance of a particular radar waveform and its processing filter(s), we

need a function which describes the signals performance in a multitarget enviroment. This function is the ambiguity function and is a measure of the signals range and doppler resolution (Ref1:127). Resolution is the ability of the radar to resolve (detect) two or more targets. For the purposes of this study, the multitarget enviroment consists of point targets located on the same target. Further, The ambiguity function can be though to represent the self-clutter of the waveform as well a measure of performance in a multitarget scenario. This will become evident as the properties of the function are stated.

Suppose we have two point scatterers with different ranges and we are using matched filter processing. Let $x(t) = a(t)\cos[w_0 t + \phi(t)]$ be the return from scatterer1 and $x(t-\tau) = a(t-\tau)\cos[w_0(t-\tau) + \phi(t-\tau)]$ be the return from scatterer2. The range separation between the two is $c\tau/2$, where c is the speed of light. We will next use complex signal representations:

$$\begin{aligned} x(t) &= \text{Re}\{u(t)\exp(jw_0 t)\} \\ x(t-\tau) &= \text{Re}\{u(t-\tau)\exp(jw_0 t)\exp(-jw_0 \tau)\} \end{aligned}$$

The two scatterers (point targets) are assumed resolvable if the average mean square difference between them exceeds a specified threshold. Therefore, our objective is to maximize

$$\frac{1}{E} \int_{-\infty}^{+\infty} |x(t) - x(t-\tau)|^2 dt \quad (57)$$

or

$$\frac{1}{E} \int_{-\infty}^{+\infty} [u(t) - u(t-\tau)\exp(-jw_0 \tau)][u^*(t) - u^*(t-\tau)\exp(jw_0 \tau)] dt$$

$$\begin{aligned}
&= 2 \int_{-\infty}^{+\infty} |u(t)|^2 - 2 \operatorname{Re}[\exp(-j\omega_0 \tau) u^*(t) u(t-\tau)] dt \\
&= 2[2E] - 2 \operatorname{Re}[B(\tau) \exp(-j\omega_0 \tau)]
\end{aligned} \tag{58}$$

$B(\tau) = \int_{-\infty}^{+\infty} u^*(t) u(t-\tau) dt$. Minimizing $B(\tau)$ will result in the maximum amount of resolution. Defining a delay resolution parameter:

$$T_R = \frac{\int |B(\tau)|^2 d\tau}{|B(0)|^2} \leftrightarrow \frac{\int |M(f)|^2 df}{(\int |M(f)|^2 df)^2} \tag{59}$$

Equation 59 utilizes Fourier transform properties. Further, a range resolution constant can be defined as $R = cT_R/2$ and an effective bandwidth constant as $B_e = 1/2T_R$. The point is that improving range resolution requires increased effective bandwidth.

By analogy, we can determine the velocity resolution of two point targets where $x(t)$ is the first target return and $x(t) \exp(j\omega_D t)$ is the doppler-shifted return of the second target. Again e^2 is formed and we proceed as before:

$$e = \int |x(t) - x(t) \exp(j\omega_D t)|^2 dt \tag{60}$$

$$= 2 \int |x(t)|^2 dt - \operatorname{Re} \left[\int x(t) x^*(t) \exp(j\omega_D t) dt \right] \tag{61}$$

using the transform

$\int x(t) x^*(t) \exp(j2\pi vt) dt \leftrightarrow \int X^*(v) X(v+w) dw = K_x(v)$ with $\omega_D = 2\pi v$ and $X(v)$ = Fourier transform of $x(t)$. Next, we define the frequency resolution constant T_r as

$$T_r = \frac{\int |u(t)|^4 dt}{[\int |u(t)|^2 dt]^2} \quad (62)$$

which leads to the effective time duration $\tau_e = 1/F_r$. Now for two scatterers at the same range, they can be resolved in doppler if

$$\Delta w_D / 2 > F_r$$

where Δw_D is the doppler-shift difference.

A similar consideration of target resolution for a single parameter (range or doppler) is related to the physical processing. Return signals are effectively filtered in bins of range and doppler. A bin width or interval is defined as the half-power width of the central lobe of the matched filter response. Restating $B(\tau) = \int u^*(t)u(t-\tau) dt = \int |M(f)|^2 \exp(j2\pi ft) df$ and defining the bin width as

$$|B(\tau_e)| = 1/\sqrt{2} = \left| \int |M(f)|^2 \exp(j2\pi \xi t) df \right| \quad (63)$$

A Taylor series expansion of $|B(\tau)|^2$ yields

$$|B(\tau)|^2 = 1/2 = |B(0)|^2 + 1/2 \frac{d^2 |B(\tau)|^2}{d\tau^2} \bigg|_{\tau=0} \cdot \tau^2 \quad (\text{Ref9:100-102}) \quad (64)$$

assuming $B(0)=1$, then $1/2 = 1 + 1/2(-2\xi^2)\tau^2$

where ξ is the rms bandwidth and

$$\xi^2 = \frac{\int w^2 |F(w)|^2 dw}{\int |F(w)|^2 dw} \quad (65)$$

This yields $\xi^2 \gamma^2 = 1/2$ and $\gamma = 1/\sqrt{2} \xi$. The response envelope spectrum is two-sided, therefore we use $\gamma' = 2\gamma = \sqrt{2}/\xi$ and define the range bin as $r_b = \gamma' c/2 = c/\sqrt{2} \xi$. For velocity resolution, we note that $|K_u(v)|^2 = \left| \int |u(t)|^2 \exp(j2\pi vt) dt \right|^2$. Again, performing a Taylor series expansion about $v=0$, we obtain

$$|K_u(v)|^2 = 1/2 = |K(0)|^2 + \frac{1/2 \gamma'^2 |K(v)|^2}{\int v^2} \cdot v^2 \quad (66)$$

Assuming normalized signal energy, $K_u(0)=1$, we define $v_b = \sqrt{2}/t_d$ where t_d is the rms time duration defined as

$$t_d^2 = \frac{\int t^2 |f(t)|^2 dt}{\int |f(t)|^2 dt} \quad (67)$$

The doppler bin width is $\dot{r}_b = \lambda v_b/2 = \lambda/\sqrt{2} t_d$ (68)

The above can be extended to the more general case of two scatterers which differ in both range and doppler. In similar fashion the integral square error is maximized:

$$\begin{aligned} \bar{e}^2 &= \int_{-\infty}^{\infty} |x(t) \exp(jw_0 t) - x(t-\gamma)|^2 dt \\ &= 2 \int_{-\infty}^{\infty} |x(t)|^2 dt - \text{Re} \left[\int_{-\infty}^{\infty} x(t) x^*(t-\gamma) \exp(jw_0 t) dt \right] \end{aligned} \quad (69)$$

Maximizing \bar{e}^2 requires the minimization of

$$\int x(t)x^*(t-\tau)\exp(jw_0t) dt$$

Applying complex envelope notation results in

$$\chi(\tau, w_0) = \int u(t)u^*(t-\tau)\exp(jw_0t) dt \quad (70)$$

Equation 70 is the ambiguity function of the waveform. The ambiguity function is the complex envelope of the matched filter response in delay and doppler (Ref9:112). The real response is calculated by taking the real part of $\chi(\tau, w_0) \exp(jw_0t)$ (Ref9:112). If $|\chi(\tau, w)|^2$ is calculated and plotted in the τ, w plane, a 3-dimensional diagram is generated. The ambiguity surface $[|\chi(\tau, w)|^2]$ visually depicts responses of the matched filter for various τ, w combinations. The central peak of the diagram ($\tau=0, w=0$) is the filter response for a perfect match, and all other response peaks are resultant from scatterers (or targets) which are non-matched. Thus, any waveform which generates sufficiently high subsidiary responses has potential targets at the corresponding τ, w values. In the case of a single target, more than one target might be incorrectly detected or in the case of several targets, only one might appear to dominate. The ideal ambiguity surface would be an impulse located at $\tau=w=0$ (Ref9:113-114). The objective would logically be to generate a waveform which has this characteristic. Unfortunately, specification of the ambiguity function does not uniquely define a waveform. The utility of the ambiguity diagram can be

further understood by developing several properties of the function.

In the frequency domain we have:

$$\chi(\tau, w) = \int M(f+w)M(f)\exp(-j2\pi ft) df \quad (71)$$

and we note that a maximum occurs at the origin

$$|\chi(\tau, w)| \leq \chi(0, 0) = 2E$$

Also, $|\chi^*(\tau, w)| = |\chi(\tau, w)|$ therefore $|\chi(-\tau, -w)| = |\chi(\tau, w)|$ and the function is symmetric about the origin (Ref9:118-126).

Next, we explore the volume under the function:

$$\text{volume} = \iint |\chi(\tau, w)|^2 d\tau dw$$

If we take the two-dimensional Fourier transform,

$$F_{\tau, w} [|\chi(\tau, w)|^2] = \iint |\chi(\tau, w)|^2 \exp(-j2\pi \tau u) \exp(-j2\pi w v) d\tau dw = |\chi(\tau, w)|^2 \quad (72)$$

We see that the ambiguity surface is its own two-dimensional transform and further by letting $u=w=0$ we have:

$$\iint |\chi(\tau, w)|^2 d\tau dw = |\chi(0, 0)|^2 = (2E)^2 \quad (73)$$

Equation 73 states that the area under the surface (and thus

the ambiguous responses) is constant and equal to 4 (assuming normalized signal energy, $E=1$) Thus, ambiguous returns may be shifted within the $\{,v$ plane but the sum total remains constant (Ref9:120-122). The objective is to design a waveform whose ambiguity diagram has the response peaks distributed to minimize the self-clutter. Targets at ranges and velocities such that $|\chi(\{,v)|$ is comparable to $|\chi(0,0)|$ are indistinguishable to the radar (Ref8:26). The width of the response peak about $|\chi(0,0)|$ defines the waveform resolution while the peaks located away from the origin are ambiguous (Ref8:26).

Sampled Signal Theory

In any digital computer simulation the radar signals must be sampled. This section derives the Fourier transform relationships of sampling in the time domain. Frequency domain sampling is derived in analogous manner.

Consider an arbitrary complex signal, $u(t)$, with Fourier transform $U(f)$ and energy E_c . Sampling $u(t)$ at discrete times $k\Delta t$ yields an approximation of $U(f)$:

$$U_s(f) = \Delta t \sum_{k=-\infty}^{+\infty} u(k\Delta t) \exp(-j2\pi f k\Delta t) \quad (74)$$

A function sampled in the time domain will be repetitive in the frequency domain (Ref4:85). Thus,

$$U_s(f+m/\Delta t) = \Delta t \sum_{k=-\infty}^{+\infty} u(k\Delta t) \exp(-j2\pi(fk\Delta t + mk)) \quad (75)$$

The product mk is an integer which leaves the phase unchanged and the mk term is omitted (Ref9:85). $U_s(f)$ is a periodic function with frequency $f_r = 1/\Delta t$. Replacing the Fourier transform for $u(k\Delta t)$ in equation 74 we find:

$$U_s(f) = \int_{-\infty}^{+\infty} U(f') [\Delta t \sum_{k=-\infty}^{+\infty} \exp(-j2\pi(f-f')k\Delta t)] df' \quad (76)$$

and noting that

$$\Delta t \sum_{k=-\infty}^{+\infty} \exp(-j2\pi f k \Delta t) = \sum_{m=-\infty}^{+\infty} \delta(f - mf_r)$$

we obtain

$$U_s(f) = \sum_{m=-\infty}^{+\infty} U(f - mf_r) \quad (77)$$

which states that the spectrum due to time sampling is the sum of the original continuous spectrum shifted at intervals equal to f_r . Figure 12 illustrates the phenomenon.

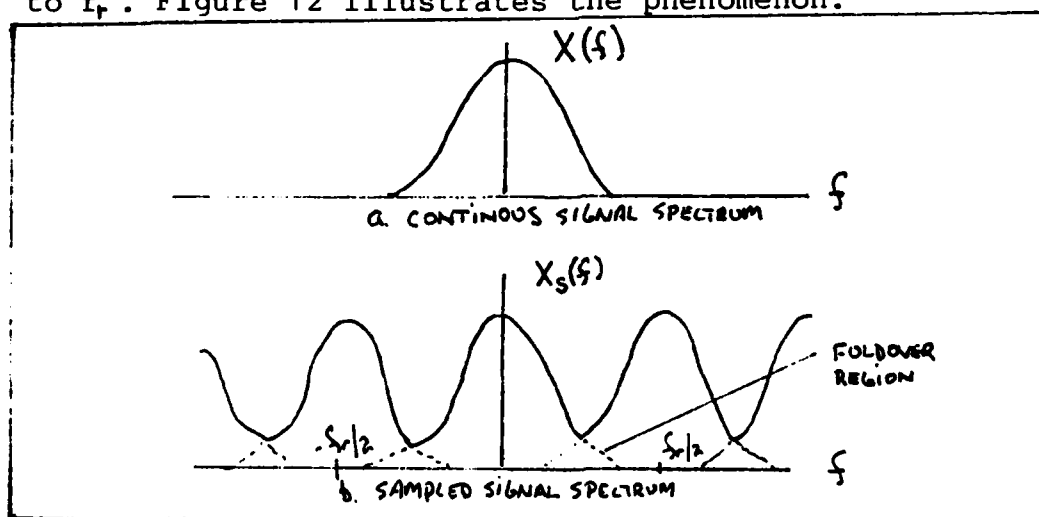


Figure 12. Spectra of Continuous and Sampled Signals (Ref4:86)

The two spectra are comparable for $f_r = 1/\Delta t$, and aliasing is minimized if $\Delta t < 1/\text{bandwidth}$. Since $U_s(f)$ is repetitive on

the interval f_r , it is useful to define the time function corresponding to only one period:

$$u'(T) = \int_0^{f_r} U_g(f) \exp j 2 \pi f t \, df \quad (77)$$

This leads to the relationship:

$$u(k \Delta t) = \int U_g(f) \exp j 2 \pi f k \Delta t \quad (78)$$

and

$$U_g(f) = \sum_{k=-\infty}^{+\infty} \Delta t u(k \Delta t) \exp -j 2 \pi f k \Delta t \quad (79)$$

For any finite duration sequence, the discrete Fourier transform, $X(K)$, of the sequence $x(n)$ is:

$$X(K) = \begin{cases} \sum_{n=0}^{N-1} x(n) \exp(-j 2 \pi k n / N), & 0 < k < N-1 \\ 0 & \text{e.w.} \end{cases} \quad (80)$$

N is the number of samples in the sequence. The inverse transform is:

$$x(n) = \begin{cases} 1/N \sum_{K=0}^{N-1} X(K) \exp(j 2 \pi k n / N), & 0 < n < N-1 \\ 0 & \text{e.w.} \end{cases} \quad (81)$$

Equations 81 and 82 can be implemented via computationally efficient algorithms such as Fast-Fourier Transforms (FFT). Also, discrete convolutions (ie $z(t) = y(t) * x(t)$) can be performed by computing the $Y(K)$ and $X(K)$ sequences, computing

$Z(K)=Y(K)X(K)$, and taking the inverse Fourier transform of $Z(K)$ to obtain $z(n)$ (Ref4:98).

IV Computer Simulation Development

Approach

The objectives of this study are to generate the following for each signal tested:

- (1) Ambiguity diagram plot
- (2) Signal spectrum plot
- (3) Received signal spectrum plot (due to 10 scatterer target)
- (4) Ideal matched filter output plot
- (5) Target filter spectral characteristics plot
- (6) Incoherent target filter output plot
- (7) Coherent target filter output plot

Objectives one through four are included to verify the work of Salzman (Ref11) and provide a complete description of the different signal processing and target modeling schemes simulated. Objectives six and seven are the main results which this paper requires. The data generated for these two plots will be compared at the appropriate sample time in order to determine which filter implementation provides superior signal-to-noise ratio.

In this section of the paper, the algorithms developed will be explained. Appendix A contains the system flowchart for the software and appendix B contains the program listing. The software is written in FORTRAN V.

Calculating the Magnitude of the Ambiguity Function

The ambiguity function (and diagram) is the correlation

of the complex envelope of the signal with a doppler-shifted, time-delayed version of itself; that is, the ambiguity function is the two-dimensional correlation function in delay and doppler. It is defined:

$$\chi(\tau, w) = \int_{-\infty}^{+\infty} u(t) u^*(t - \tau) \exp[j2\pi w t] dt \quad (83)$$

The ambiguity function can be expressed as a convolution of the following:

$$\chi(\tau, w) = u(\tau) \exp[j2\pi w \tau] * u^*(-\tau) \quad (84)$$

In this simulation we define the arguments of the convolution as finite sequences and calculate the ambiguity function via a linear convolution. Each argument is sampled to form an N-point sequence and then at least N-1 zeros are added. The N-1 zeros are necessary for the discrete convolution calculations to be correct (Ref4:85-88). The linear convolution is calculated by the indirect method which, given two time sequences x_k and y_k , consists of:

- 1) compute the sequences X_k and Y_k via the discrete Fourier transformation (FFT) of x_k and y_k respectively.
- 2) form $Z_k = X_k Y_k$ for $k=0, 1, 2, \dots, 2N-1$
- 3) compute the sequence z_k via the discrete Fourier transform (FFT) of Z_k (Ref4:98)

Sufficient sampling of the waveform requires knowledge

of the Nyquist rate. The time-bandwidth product (TB or signal duration multiplied by signal bandwidth) of the complex envelope provides the Nyquist rate (Ref6:254). If the signal is sampled at $1/TB$ or less, the N-point sequence is generated. The Fast Fourier Transform algorithm used in this simulation was available through the IMSL mathematical library (CDC Cyber computer system). Good resolution of the resultant convolution may require sampling rates which are higher than the Nyquist rate. The sequences generated by the software are limited to 1024 points. This constraint was primarily imposed by the 100,000 words of compilation memory available for interactive computations on the Cyber. This limitation will severely constrain both the number of pulses and subpulses which can be simulated. This in turn limits the length of coding (either FM or phase) possible and will be elaborated on when a simulation waveform is selected.

Sampling repeated and/or coded waveforms requires careful consideration. Each element of the code (ie subpulse interval) must be sampled equally in order to eliminate any bias and skewing of the plotted function. Consider a two pulse signal with each pulse 1 second in duration and duty factor of $1/3$. If we choose to make 16 samples of the waveform, each sample is separated by $3/8$ seconds. This results in two samples made of the first pulse and three samples made of the second pulse. This would of course result in an incorrect answer. The problem is avoided by weighting the samples in such a manner as to insure each elemental portion of the

waveform is sampled uniformly. We have specified the number of samples we wish to make, the signal duration, and pulse width. By forming the expression $\lfloor \text{number of samples} / \text{signal duration} \rfloor \times \text{pulse width}$ and truncating the result, we obtain the largest integer value for the number of samples per pulse which can be achieved and insure uniform sampling (Ref8:45).

As an example, assume we are simulating a phase coded waveform where the amplitude of the complex envelope is modulated. Given a single, 1 second pulse of unity amplitude, we choose to make 8 samples. Also, assuming a 5-element Barker code, the phase of each element would be $0, 0, 0, \pi, 0$. The sequence corresponding to $u(t)\exp[j\omega t]$ would be:

$$\begin{aligned} & \exp[j\omega(1/5)], \exp[j\omega(2/5)], \exp[j\omega(3/5)], -\exp[j\omega(4/5)] \\ & \exp[j\omega], 0, 0, 0, 0, 0, 0, 0, 0, 0, 0, 0. \end{aligned}$$

The sequence representing $u^*(-\mathfrak{J})$ is:

0,0,0,0,0,0,0,0,0,0,0,0,1,-1,1,1,1

Once the proper sequences are formed for $u(\tau)\exp[j\omega\tau]$ and $u(-\tau)$, the linear convolution must be performed. This is accomplished via the indirect method as previously stated. The simulation calculates the ambiguity diagram values as a function of delay given a particular doppler value. The result is a cross-sectional view of the diagram which is perpendicular to the doppler axis. Any value of doppler may be

selected, however, this study will always select the zero doppler cut since this corresponds to the output of a matched filter which is perfectly matched to the waveform. In this manner, we are only viewing a particular cross-sectional "slice" of the total ambiguity diagram. After calculating the values of the ambiguity function, their magnitude (or magnitude squared) is plotted. This plot represents the best possible range response of the radar waveform.

All of the ensuing sections of this chapter describe software which rely extensively on the algorithm just described. The same procedure for setting up the proper sampling and resultant sequences is fundamental to matched filter and target filter calculations as well. This will become apparent as the chapter develops.

Signal Spectrum Calculations

Two signal spectrum calculations (plots) are generated. The first is simply the signal spectrum of the original radar waveform, and the second is the spectral characteristics of the received signal. The first is generated by performing a discrete Fourier transform of the sequence corresponding to $u(\tau)$ and plotting the result. Generation of the received signal spectrum is not as straight forward and requires the following assumptions: 1) the target consists of ten independent scatterers which may or may not be fluctuating in amplitude, 2) the target acts as a filter and thus can be described via a range extended scatterering function, 3) the

range extended scatterering function can be modeled as a decaying exponential in the frequency domain (Ref5). The procedure is to specify (in frequency) the exponential as a Gaussian pulse centered at zero. From this model of the range extended scatterering function, a complex impulse response is developed. The original signal spectrum is multiplied by the complex range extended scatterering function, Fourier transformed, and plotted. The development of the range extended function starts with a real, bandpass Gaussian spectrum:

$$H(j\omega) = \frac{\exp[-\alpha(\omega - \omega_0)^2] + \exp[-\alpha(\omega + \omega_0)^2]}{2} \quad (85)$$

noting that,

$$H(j\omega) = \frac{\tilde{H}(\omega - \omega_0) + \tilde{H}^*(-\omega - \omega_0)}{2} \quad (86)$$

where $\tilde{H}(j\omega)$ is complex and

$$\begin{aligned} H(j\omega) &= \mathcal{F}[h(t)] = \text{Re}[\tilde{h}(t)\exp(j\omega_0 t)] \\ &= \frac{\tilde{h}(t)\exp(j\omega_0 t) + \tilde{h}^*(t)\exp(-j\omega_0 t)}{2} \end{aligned} \quad (87)$$

Equation 85 dictates the real impulse response:

$$h(t) = 1/2\sqrt{\pi\alpha} \exp[-t^2/4\alpha] \cos\omega_0 t$$

thus,

$$H(j\omega) = 1/2 \left\{ \begin{aligned} &1/2\sqrt{\pi\alpha} \exp[-t^2/4\alpha] \exp[j\omega_0 t] + \\ &1/2\sqrt{\pi\alpha} \exp[-t^2/4\alpha] \exp[-j\omega_0 t] \end{aligned} \right\} \quad (88)$$

and by comparing equations 88 and 87 we see that

$$\tilde{h}(t) = 1/2\sqrt{\pi\alpha} \exp[-t^2/4\alpha] \quad (89)$$

which implies that

$$\tilde{H}(j\omega) = \exp[-\alpha\omega^2] \quad (90)$$

Equation 89 requires the addition of a time shift, t_0 , which accounts for causality (Ref2:8c), and results in the final form of the complex range extended scatterering function:

$$\tilde{H}(j\omega) = \exp[-\alpha\omega^2] \exp[-j\omega t_0] \quad (91)$$

Equation 91 is simulated directly. $\tilde{H}(j\omega)$ is sampled according to the same criteria as the signal, multiplied sample by sample with the original signal frequency domain samples, and plotted as the received signal spectrum. The process is repeated for both fluctuating and non-fluctuating target cross-section.

Matched Filter and Target Filter Calculations

The procedure for calculating both the target and matched filter outputs is essentially the same. The only difference is that a unique filter impulse response is simulated for each.

The matched filter output is the discrete convolution of the received signal time samples with a conjugated, time inverted version of the original signal. The next section develops the governing equations.

The target filter output is the discrete convolution of the received signal with the Fourier transform of the conjugated range extended scatterer impulse response. The target filter impulse response parameter α , generally is not equal to the α which characterizes the received signal structure. Specifically, equation 89 or alternatively 91, is used to generate the received signal (ie model the target) and designate the target filter impulse response, but different values of α are used in each. A larger value of α will be used for the target filter impulse response, resulting in a narrowbanding of the return. This is a critical point in that narrowbanding the return may provide and is indeed necessary to yield a practical spread spectrum system (assuming current technology limitations as presented in chapter II).

As a last note, it is apparent that we have assumed a received signal which was generated via a known filtering process (ie the range extended scatterer function of equation 91), and further that we have set up a matched filter (the target filter) which compensates for the known target scatterer characteristics. This might appear to be a self-fulfilling prophecy or a circular argument. Two important points must be considered: first, the validity of the results rests partly on the validity of the assumption and approximation of the form of the target density function. For this assumption, the author has relied on the article "Effect of a Few Dominant Specular Reflectors Target

Model Upon Target Detection" (Ref5:670-671). Second, the value of α for the target filter is larger than the one used for generation of the received signal, thus constituting the ability or inability to successfully narrowband the return prior to range and doppler processing. With the above in mind, the next section will develop the equations which support this section and define the relationship between coherent and incoherent processing.

Coherent and Incoherent Target Filtering

This section will develop the equations for coherent and incoherent filtering of complex signal envelopes. It should be kept in mind that the target filter is actually a matched filter which is matched to the received signal.

On page 338 of DiFranco and Rubin (Ref3) we find: "Matched filter processing for a pulse train is sometimes called coherent processing or predetection integration". In other words, the matched filter is inherently a coherent device. The phase matching is based on the signal spectrum alone and results in a maximum peak response occurring at $t=T$, where T is the causality delay. The amplitude matching is dependent on both the signal and noise spectrum, resulting in the maximization of the signal-to-noise ratio (Ref2:On Understanding the Matched Filter in the Frequency Domain by Theodore G. Birdsall). The complex response function is

$$\rho(\gamma) = 1/2 \int_{-\infty}^{\infty} \psi(t) \psi^*(t-\gamma) dt \quad (92)$$

where $\Phi(t) = s(t) + j\hat{s}(t)$

and $s(t)$ is the real signal,

$\hat{s}(t)$ is the Hilbert transform of the real signal.

Further,

$$\text{Re}[\rho(\tau)] = 1/2 \int_{-\infty}^{+\infty} s(t)s(t-\tau) dt + 1/2 \int_{-\infty}^{+\infty} \hat{s}(t)\hat{s}(t-\tau) dt \quad (93)$$

In real notation, the real autocorrelation function (matched filter response) of $s(t)$ is

$$r(\tau) = \int s(t)s(t-\tau) dt = \int |S(f)|^2 \exp[j2\pi f\tau] df \quad (94)$$

$\hat{s}(t)$ has the same spectrum as $s(t)$, thus the integrals of equation 93 are equivalent (Ref9:32).

We note that

$$r(\tau) = \text{Re}[\rho(\tau)]$$

Also,

$$\Phi(t) = u(t)\exp[j2\pi f_0 t]$$

where f_0 is the center frequency and

$$\rho(\tau) = 1/2 \exp[j2\pi f_0 \tau] \int u(t)u^*(t-\tau) dt \quad (95)$$

Equation 95 is simulated directly (convolution process discussed previously) with $f_0 = 0$ by ignoring the insignificant conversion to video. The actual plotted response is calculated by taking the real part of equation 95.

The incoherent target filter is the combination of the matched filter followed by an envelope detector(Ref12:201). In other words, the phase information is destroyed and the samples are incoherently collapsed (added). Starting with equation 95, the envelope of the real target filter response (incoherent) is:

$$\begin{aligned} \text{Env}\{r(\tau)\} &= |\rho(\tau)| \\ &= 1/2 \left| \int u(t)u^*(t-\tau) dt \right| \quad (96) \end{aligned}$$

where again $\exp[j\omega_0 t]$ has been suppressed. Equation 96 is simulated via the techniques of the previous sections of this chapter.

In summary, both target filters are simulated by discrete convolutions according to equation 95 with $f_0=0$ and $u^*(t-\tau)$ replaced with the range extended scatterering function impulse response. The coherent target filter takes the real part of this result, where as the incoherent filter requires taking the magnitude of the integral. These two output are compared at the sample point corresponding to the $\tau=0$, $v=0$ point on the ambiguity surface. The larger value constitutes the greater signal-to-noise ratio at the output of the since $r(0)=\rho(0)=\text{energy}$ (Ref9:33). The next chapter presents the results of the processes presented above.

V. Software Application and Results

Simulaton Test Waveform

Due to computer memory limitations and thus array size constraints, the maximum number of data points is fixed to 1024. With this in mind, a four pulse, rectangular pulse train of $1/4$ duty factor was selected as the base signal. The signal is then coded in phase or frequency as will be discussed. The above selection results in a maximum of 512 samples (after weighting) of the signal and up to 32 allowable subpulses or elements.

The key to the simulation process is the ambiguity calculations and resultant plot. All other matched filter, signal spectrum, and target filter plots follow the same basic software manipulations. A single run through the algorithm produces one of the following:

- 1) Ambiguity plot and signal spectrum plot.
- 2) Received signal plot and matched filter plot.
- 3) Target filter(coherent or incoherent) spectrum plot and target filter ouput plot.

In order to test the software, a 13-element Barker code was injected into the simulation. The verification signal contained 13 pulses, phase-coded, with $1/2$ duty ratio. The resultant spectrum and ambiguity cut (doppler=0) are shown in figures 13 and 14 respectively. Both plots are verified in the literature, in particular by Salzman(Ref11) and Rihaczek(Ref9:215-216).

Phase Coded Signal

The basic test waveform of the previous section was intrapulse phase coded ($0, \pi$) and simulated. Each of the four pulses contain 25 elements generated from a pseudo-random code of length 63. A 50 element section of the code is repeated throughout the signal. Figure 15 is the signal spectrum and figure 16 is the zero-doppler cut of the phase coded signal. The central peak of figure 16 designates the sample point of the matched filter and is located at 15.96 on the time units scale. Note the level of the two ambiguous peaks on either side of the main response peak. This provides a clear area of approximately 14 time units (from 9.0 to 23.0). The clear area is that delay span in which signals can be searched and separated in range (ie area of sufficiently low ambiguous peaks). The central peak is at 40dB, with the next highest response level within the clear area at approximately 21dB. This is clearly a thumbtack-type ambiguity function as would be expected from a coded or noise-type radar waveform (Ref10). Figures 17 and 18 show the received signal spectrum and matched filter output for non-fluctuating target cross-section. The sample point has a magnitude of 15.59dB. Figures 19 and 20 show the target filter spectral characteristics and coherent target filter outputs respectively. The coherent target filter has been modeled with the same value of d as the received signal spectrum. The magnitude at the sample point (15.96 time units) is 7.58dB. The corresponding value for the incoherent target filter was 9.34dB. Thus, the incoherent

filter shows a 1.76dB improvement in output signal-to-noise ratio for the non-fluctuating case.

The following series of plots are for the coherent filter(s). The incoherent filter output is identical except for a slight widening of the main lobe. Figures 21 and 22 depict the received signal spectrum and matched filter output for scan-to-scan fluctuating RCS target (Swerling I). The effect appears to be slight and further RCS fluctuations will be pulses-to-pulse or Swerling II modeled. Figures 23-26 show the same series of events but α has been reduced from 0.1 to 0.01. The coherent target filter does appear to widen the main lobe response slightly. The next sequence of plots, figures 27-30, are for a target of different Swerling II statistics. The results are similar to the previous plots. In figures 31-34, the value of α used to generate the received signal spectrum is 0.01, whereas the value for the target filter spectrum equals 0.01. The result of narrowbanding the return by 60% is the smooth response shown in figure 34. The incoherent target filter performs similarly with a sampled value 7.62dB higher. Figures 35-38 are the same sequence of events once again with α (received signal spectrum) = 0.001 and α (coherent target filter) = 0.2. The results for these plots (including data for the incoherent filter) and an additional 20 runs are tabulated in table II.

It is clear from table II that the coherent target filter produces too narrow a main peak and thus an unacceptable sampled output signal power for values of α 0.1.

Further, in each of the simulation runs the incoherent realization provided the best output signal-to-noise ratio.

Interpulse Frequency Hopping Waveform

A four pulse, 20% duty cycle signal was simulated over 10 runs with Swerling II RCS fluctuations. The results are tabulated in table III. Again, the coherent target filter proved slightly superior. The ratio of incoherent to coherent signal output power remained within 0.01dB for the 10 run data set.

Interpulse Frequency Hopping with Subpulse Chirp

The same basic waveform was again simulated with intrapulse chirp (25 separate, linear frequency slopes) added. The incoherent target filter once again shows a slight advantage in output signal power. Table IV shows the results for 5 separate runs with Raleigh (Swerling II) RCS fluctuations. The non-fluctuating scenario is also included. The constant average advantage of the incoherent filter varies only a few tenths of a decibel.

Summary

It appears that for all three waveforms, and under Swerling II-type RCS fluctuations, the incoherent target filter is superior in terms of greater output signal power. This will yield a higher output signal-to-noise ratio. The advantage of the incoherent filter is generally on the order

Target Filter Sampled Value(dB)

Coherent	Incoherent	*	RCS fluctuation	α (filter)
7.58	9.34	1.76	non-fluctuating	-
-60.00	-0.32	59.70	Swerling II	0.01
-60.00	0.44	60.40	Swerling II	0.01
-7.87	-0.25	7.40	Swerling II	0.10
-2.92	1.00	3.90	Swerling II	0.20
-2.84	-1.32	1.50	Swerling II	0.20
-1.83	-0.47	1.30	Swerling II	0.20
-1.85	0.09	1.90	Swerling II	0.20
-3.75	-1.95	1.80	Swerling II	0.20
-3.52	0.24	3.80	Swerling II	0.20
0.27	1.15	0.90	Swerling II	0.30
-5.36	-3.63	1.70	Swerling II	0.30
0.67	0.97	0.30	Swerling II	0.40
-3.92	-2.39	1.50	Swerling II	0.40
-2.18	-1.66	0.50	Swerling II	0.40
-2.42	-1.45	0.90	Swerling II	0.40
-0.79	-0.24	0.50	Swerling II	0.40
-1.62	-0.98	0.60	Swerling II	0.40
-0.57	-0.18	0.40	Swerling II	0.40
-0.58	-0.12	0.50	Swerling II	0.40
-2.61	-2.00	0.60	Swerling II	0.40
-0.22	0.43	0.70	Swerling II	0.40
-1.46	-1.00	0.50	Swerling II	0.40
-3.25	-2.37	0.90	Swerling II	0.40
-5.35	-4.49	0.90	Swerling II	0.40

* - the ratio of incoherent/coherent target filter output signal power in dB.

Table II. Coherent vs. Incoherent Target Filter Output Signal Power for a Phase Coded Waveform

Target Filter Sampled Value (dB)

Coherent	Incoherent	*	RCS Fluctuation	α (filter)
-7.38	-6.64	0.74	non-fluctuating	-
-6.15	-5.40	0.75	Swerling II	0.40
-7.35	-6.60	0.75	Swerling II	0.40
-5.98	-5.24	0.74	Swerling II	0.40
-4.41	-3.67	0.74	Swerling II	0.40
-9.78	-9.06	0.72	Swerling II	0.40
-11.49	-10.76	0.73	Swerling II	0.40
-5.60	-4.85	0.75	Swerling II	0.40
-5.03	-4.28	0.75	Swerling II	0.40
-10.20	-9.45	0.75	Swerling II	0.40

* - the ratio of incoherent/coherent target filter output signal power in dB.

Table III. Coherent vs. Incoherent Target Output Signal Power for Interpulse FM Waveform

Target Filter Sampled Value (dB)

Coherent	Incoherent	*	RCS Fluctuation	α (filter)
19.24	19.42	0.18	non-fluctuating	-
14.62	14.18	0.44	Swerling II	0.40
16.52	16.70	0.18	Swerling II	0.40
14.45	14.63	0.18	Swerling II	0.40
15.97	16.15	0.18	Swerling II	0.40
15.83	16.02	0.18	Swerling II	0.40

* - the ratio of incoherent/coherent target filter output signal power in dB

Table IV. Coherent vs. Incoherent Target Filter Output Signal Power for Interpulse w/subpulse Chirp

of 1-3 dB for the phase coded waveform and less than 1 dB for the frequency coded waveforms.

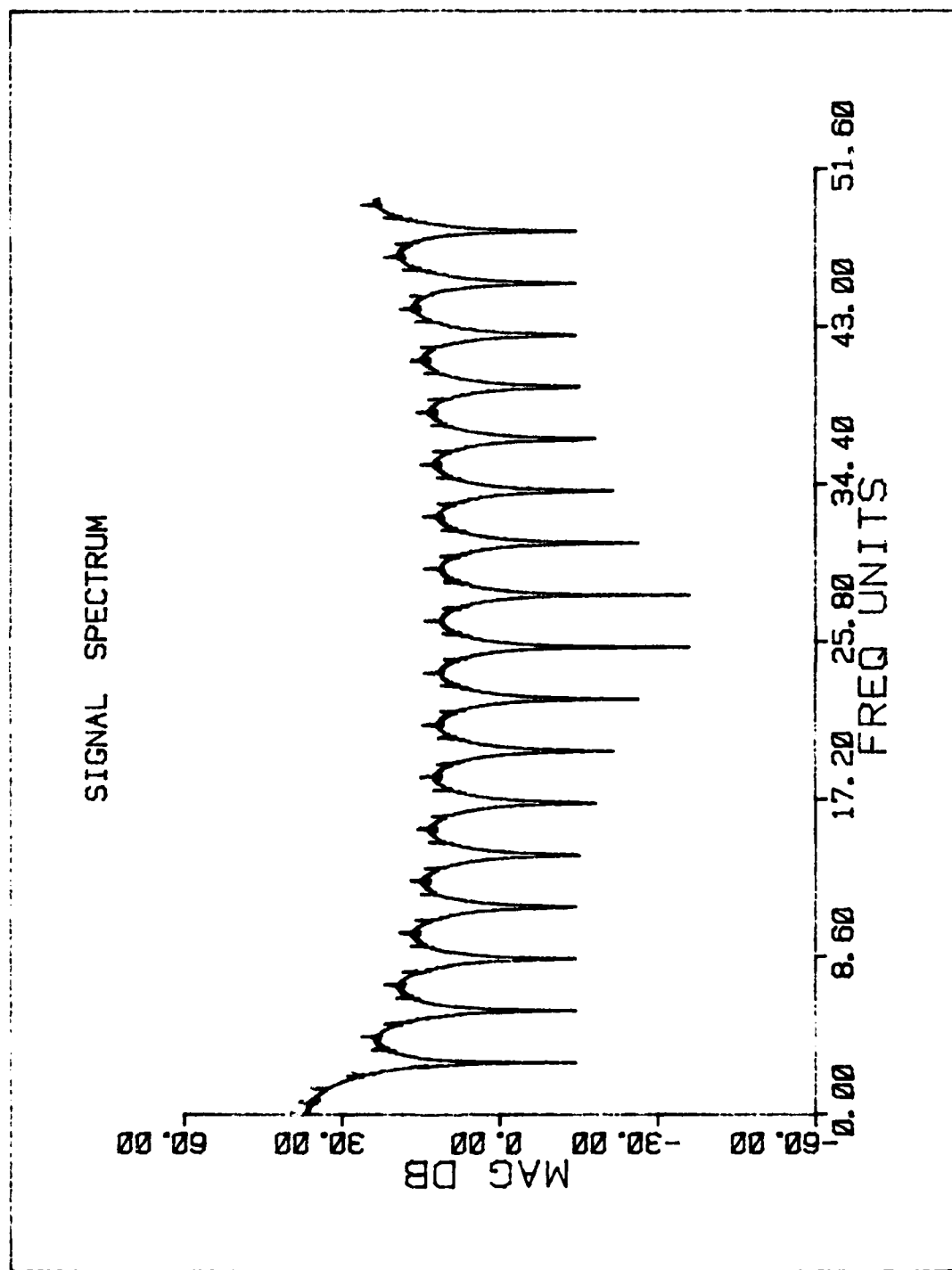


Figure 17. Signal Spectrum for P-Higher Order Code

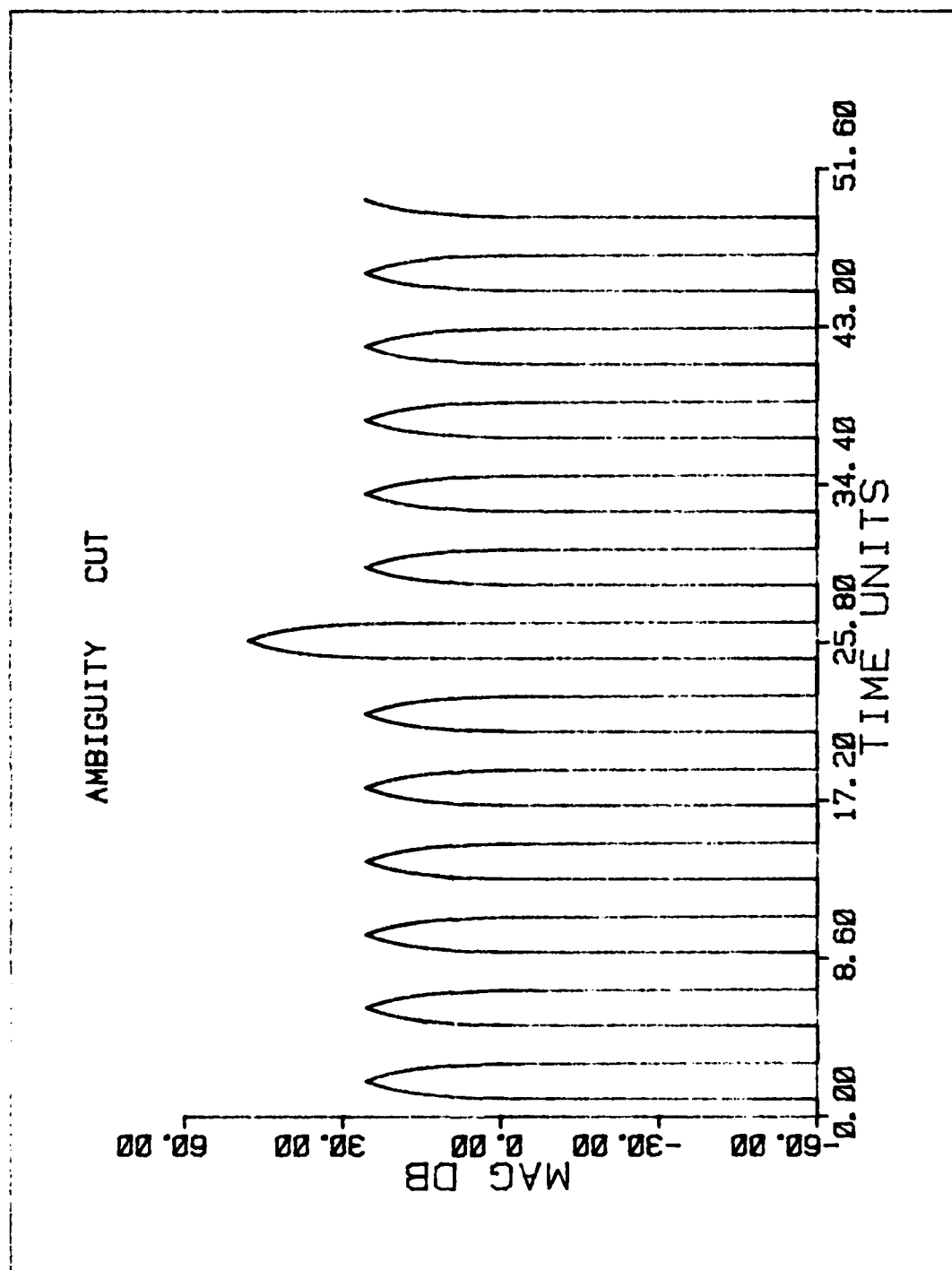


Figure 14. Ambiguity Cut for 10 Element Barker Code

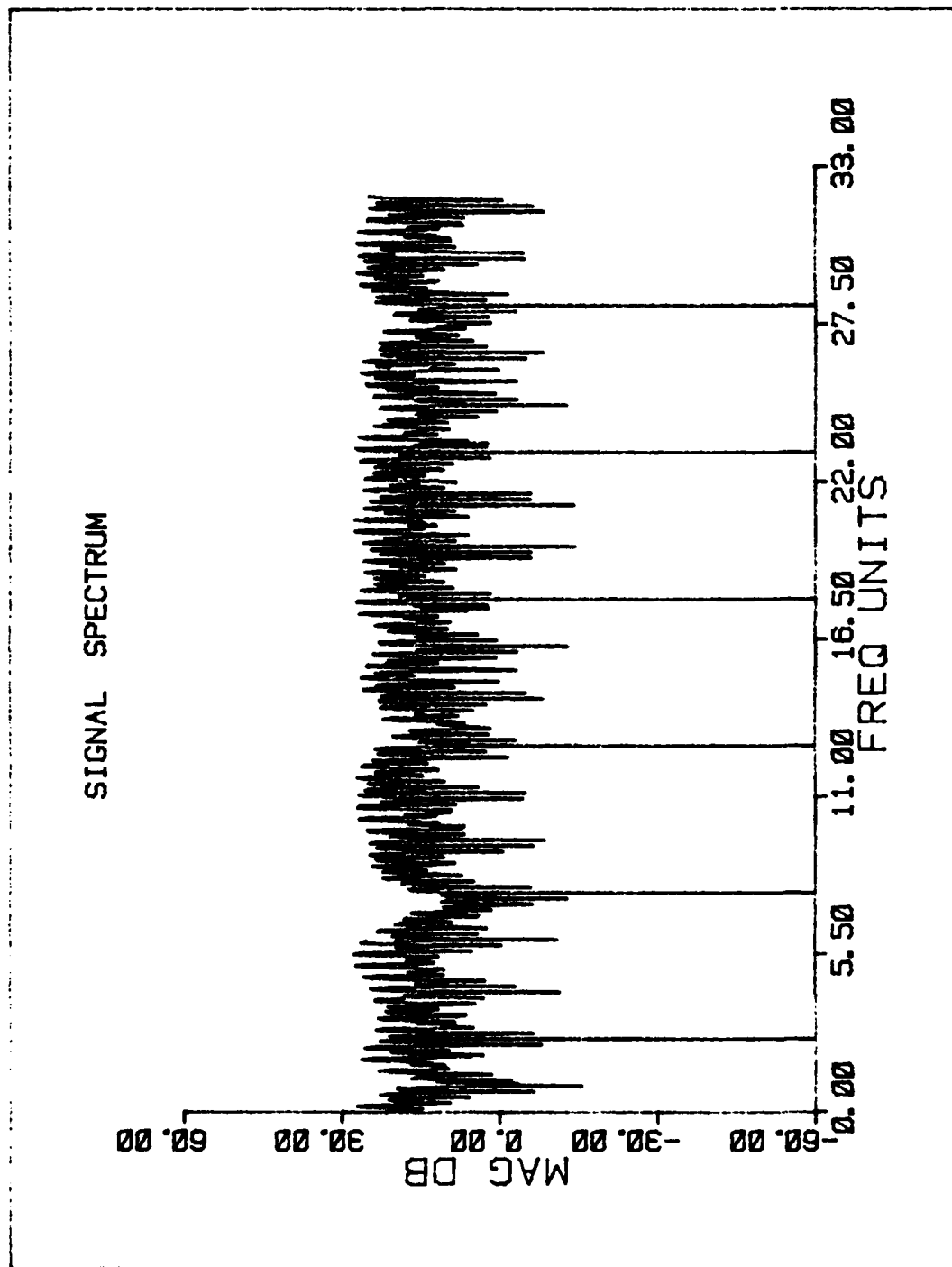


Figure 17. Signal Spectrum (Continued)

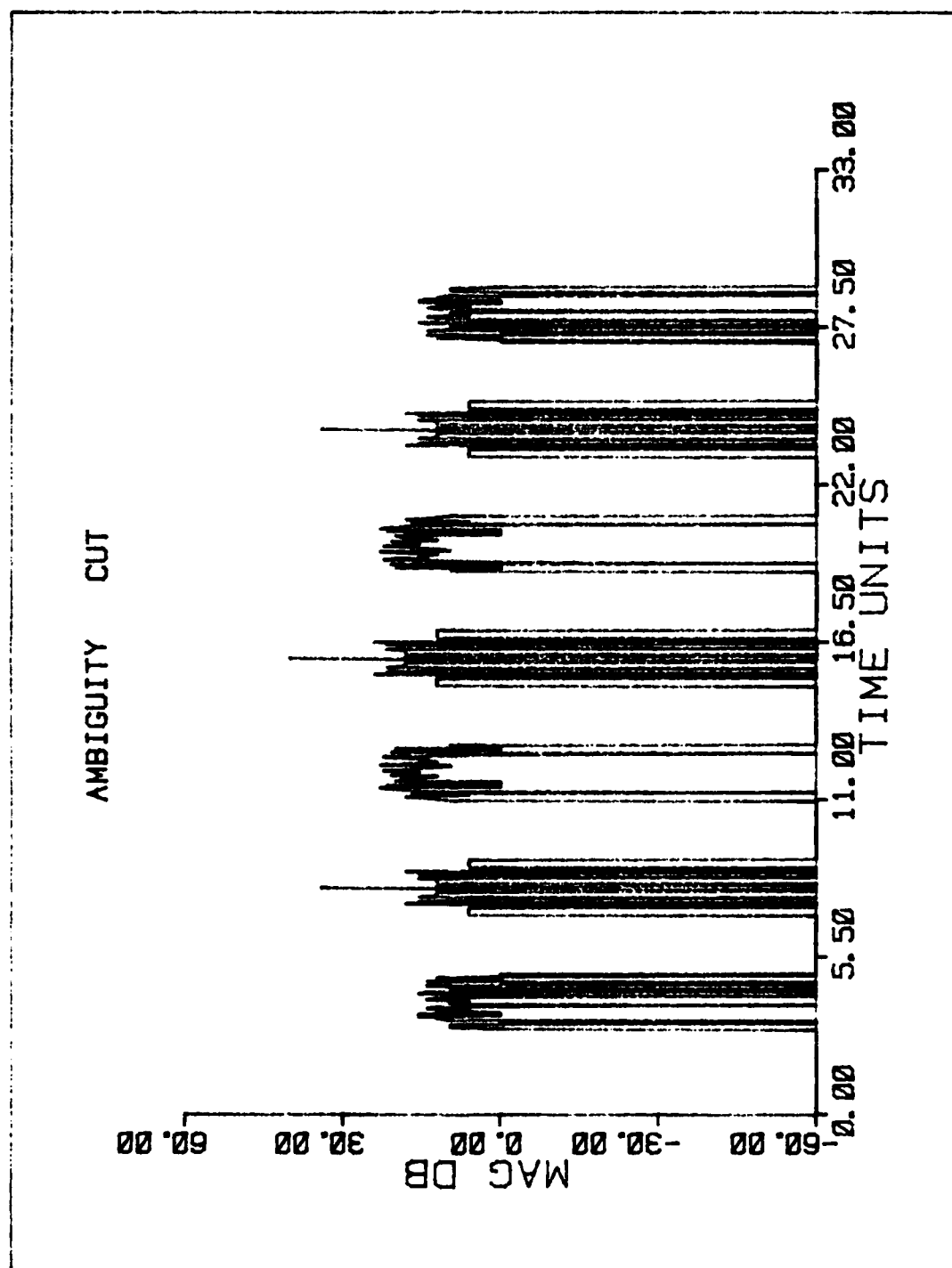


Figure 15. Ambiguity Cut, Phase Coded Signal

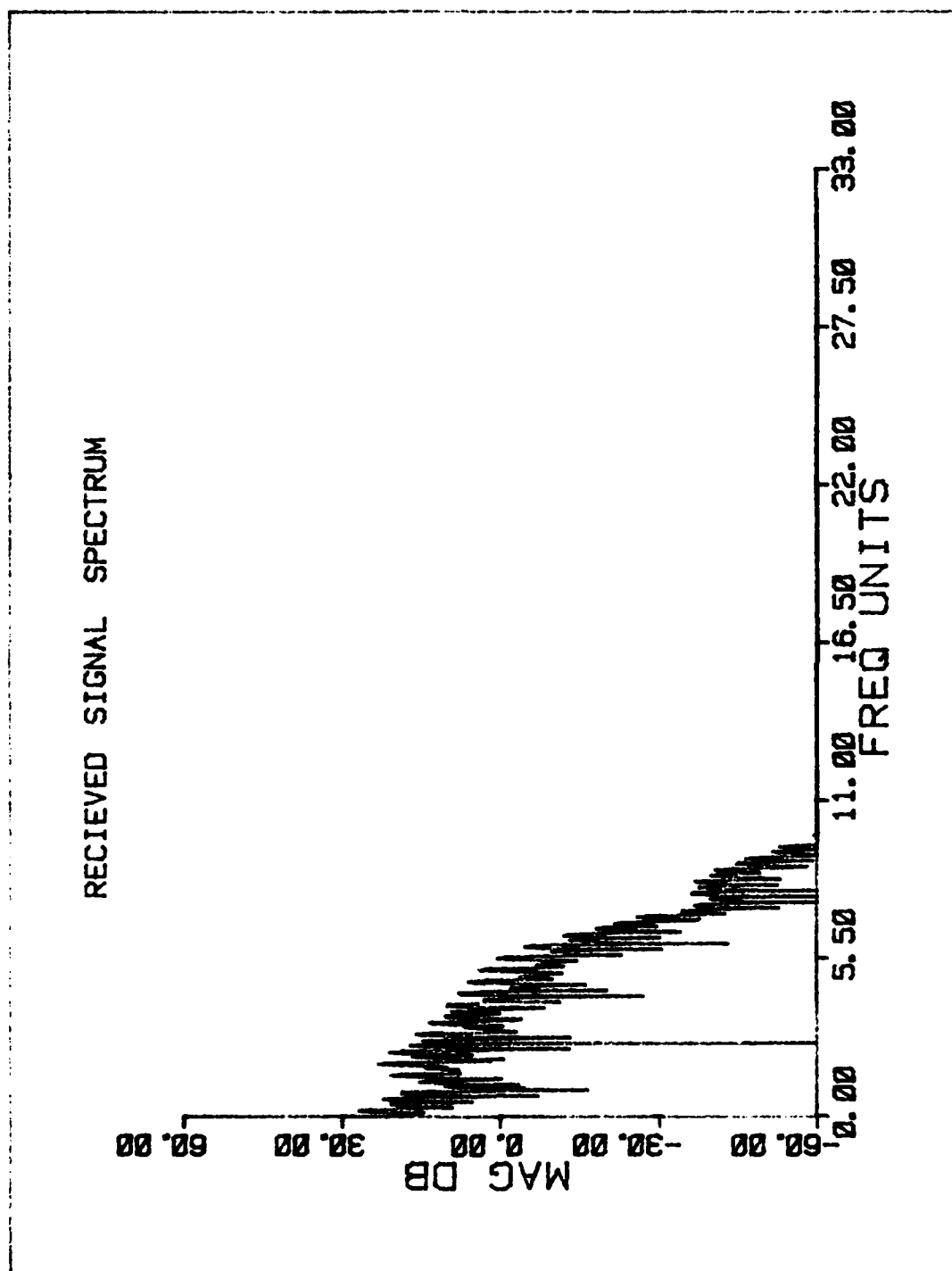


Figure 10. Received signal trace, Non-Fluctuating Case

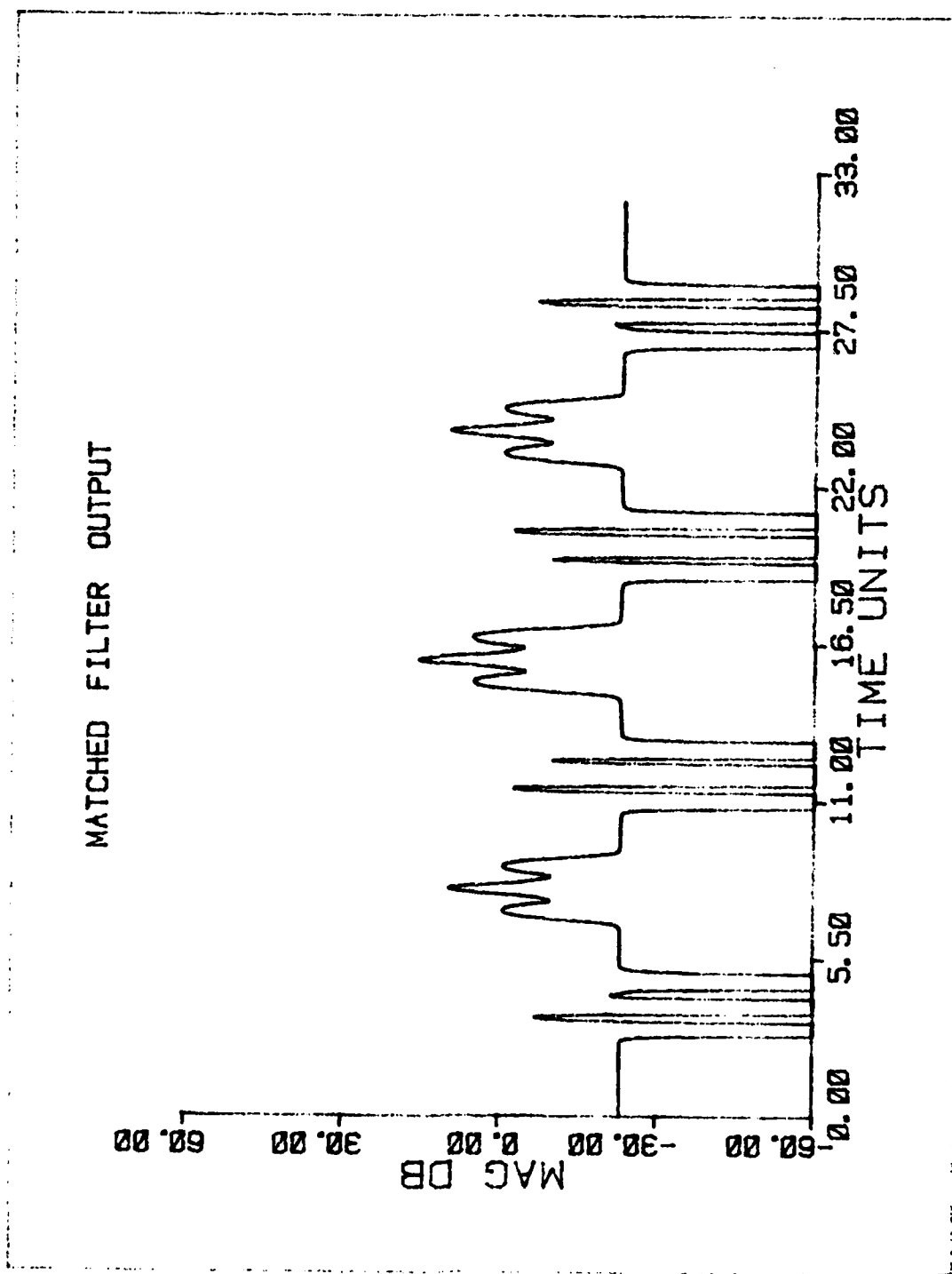


Figure 10. Matched Filter Output vs. Time (Units)

TARGET FILTER SPECTRUM

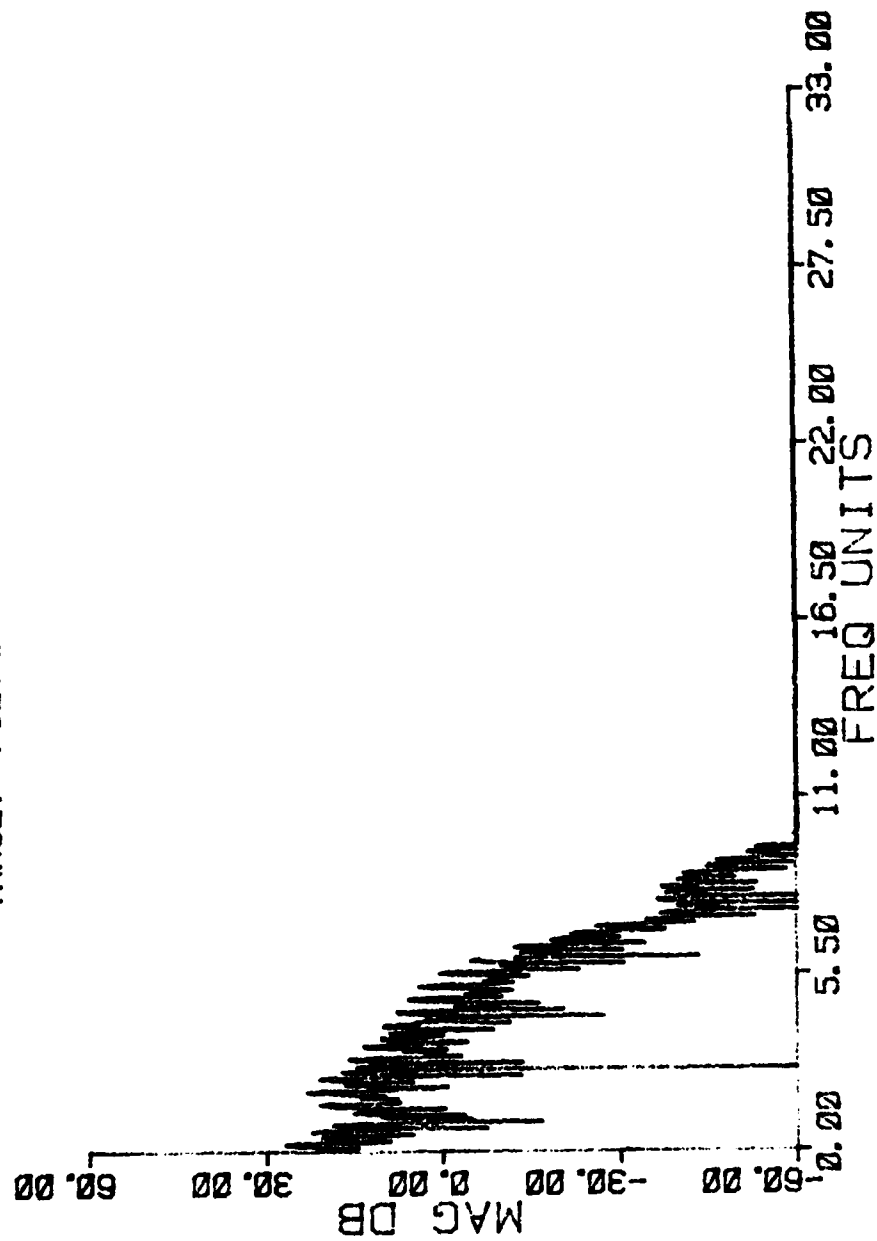


Figure 1. Target Filter, Alpha=0.1

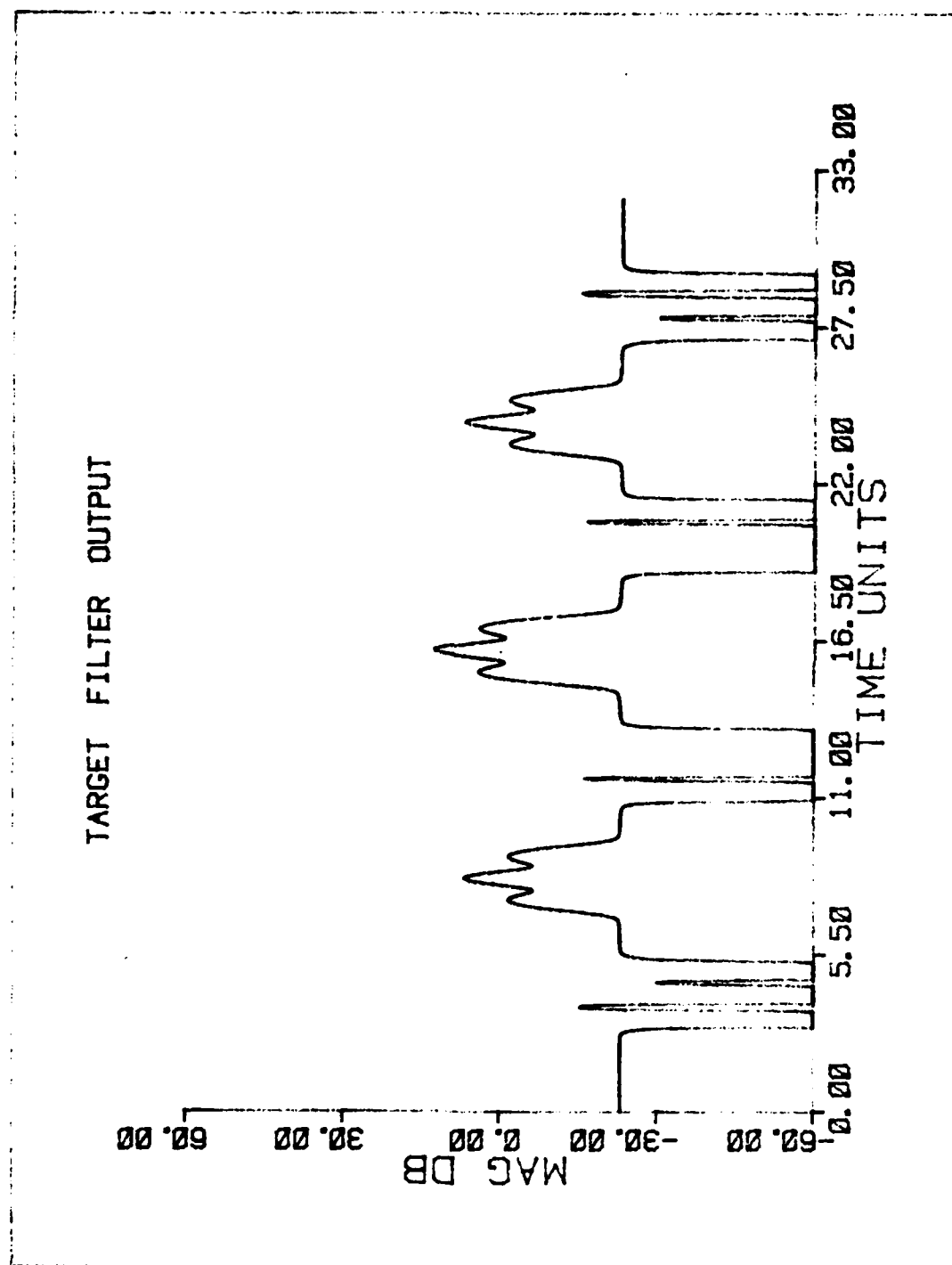


Figure 2. Target Filter Output

RECIEVED SIGNAL SPECTRUM

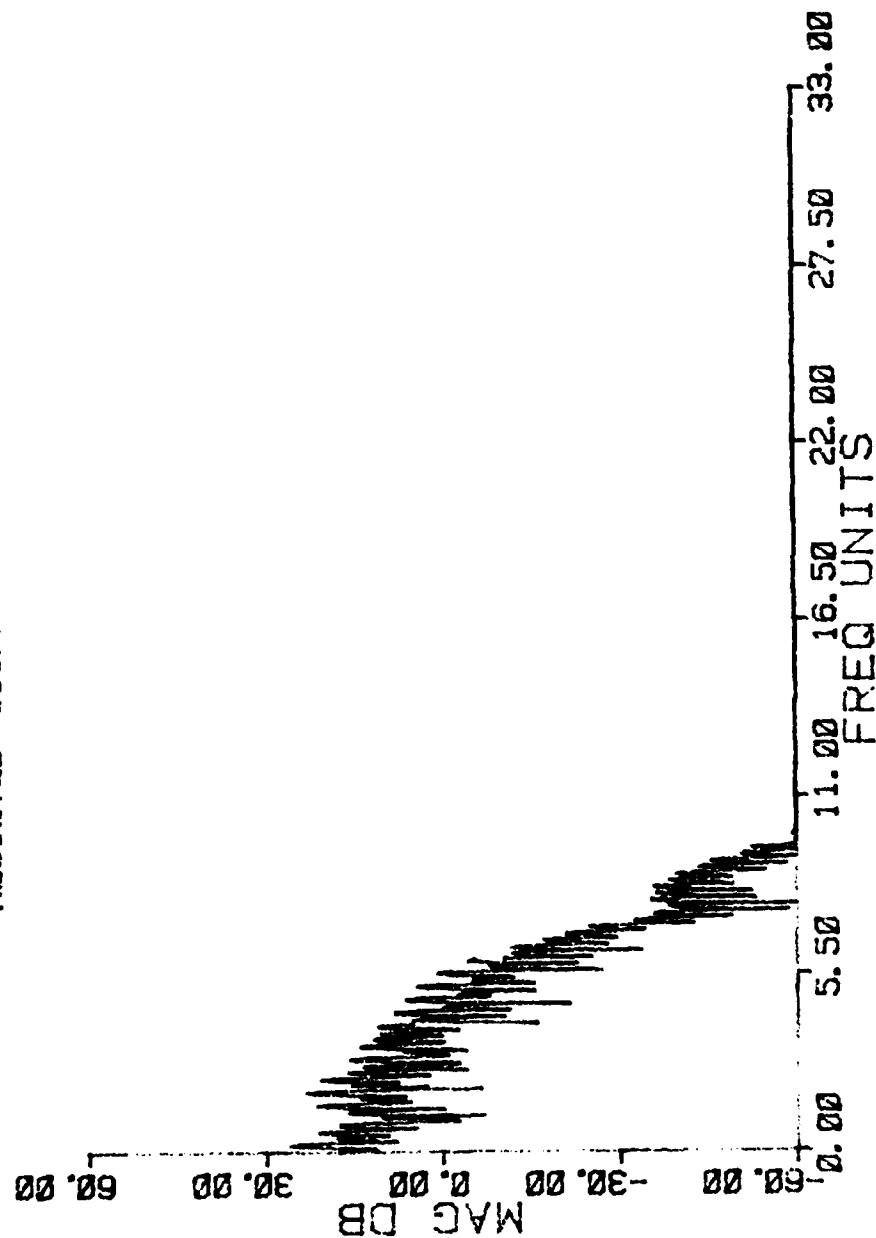


FIGURE 1. Received Signal Spectrum, Sounding

MATCHED FILTER OUTPUT

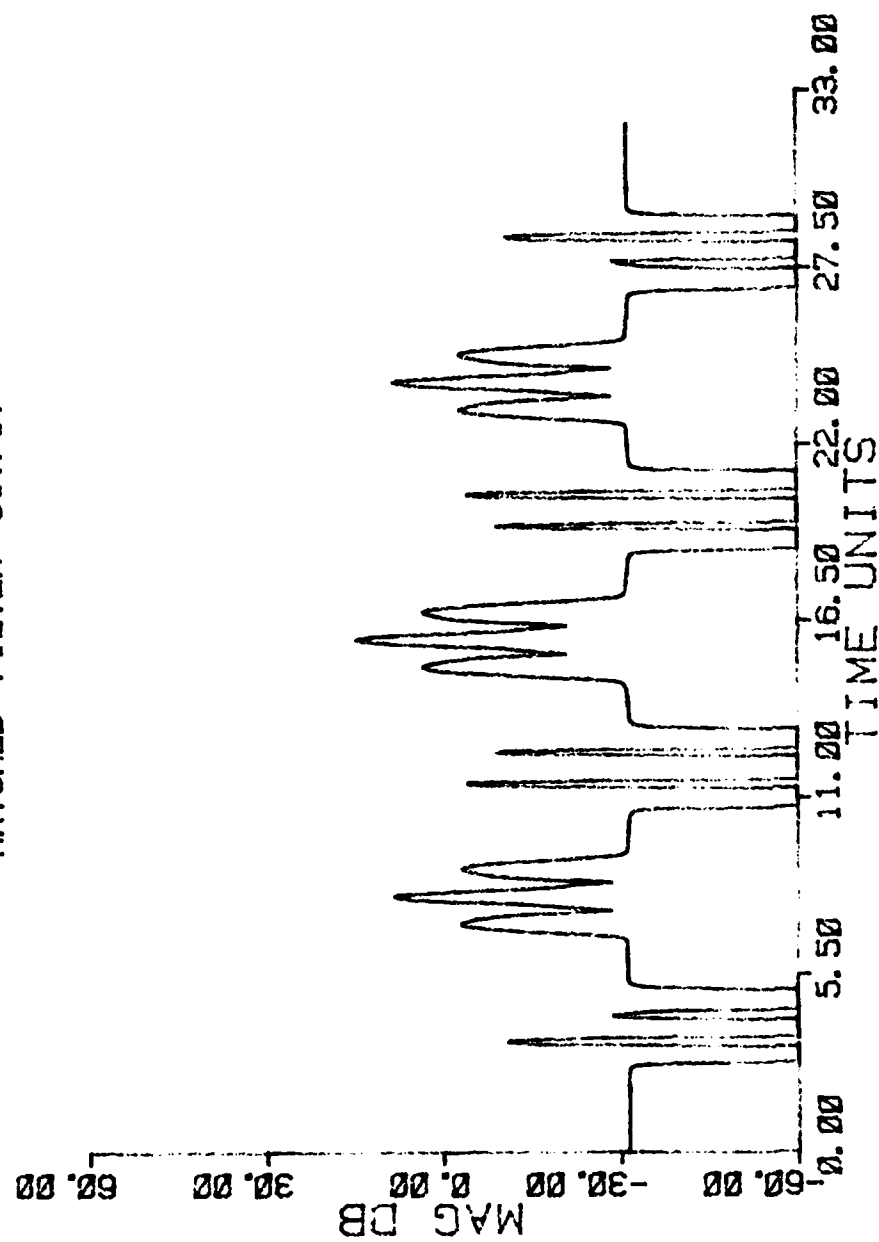


Figure 1. Matched filter output, averaged.

RECEIVED SIGNAL SPECTRUM

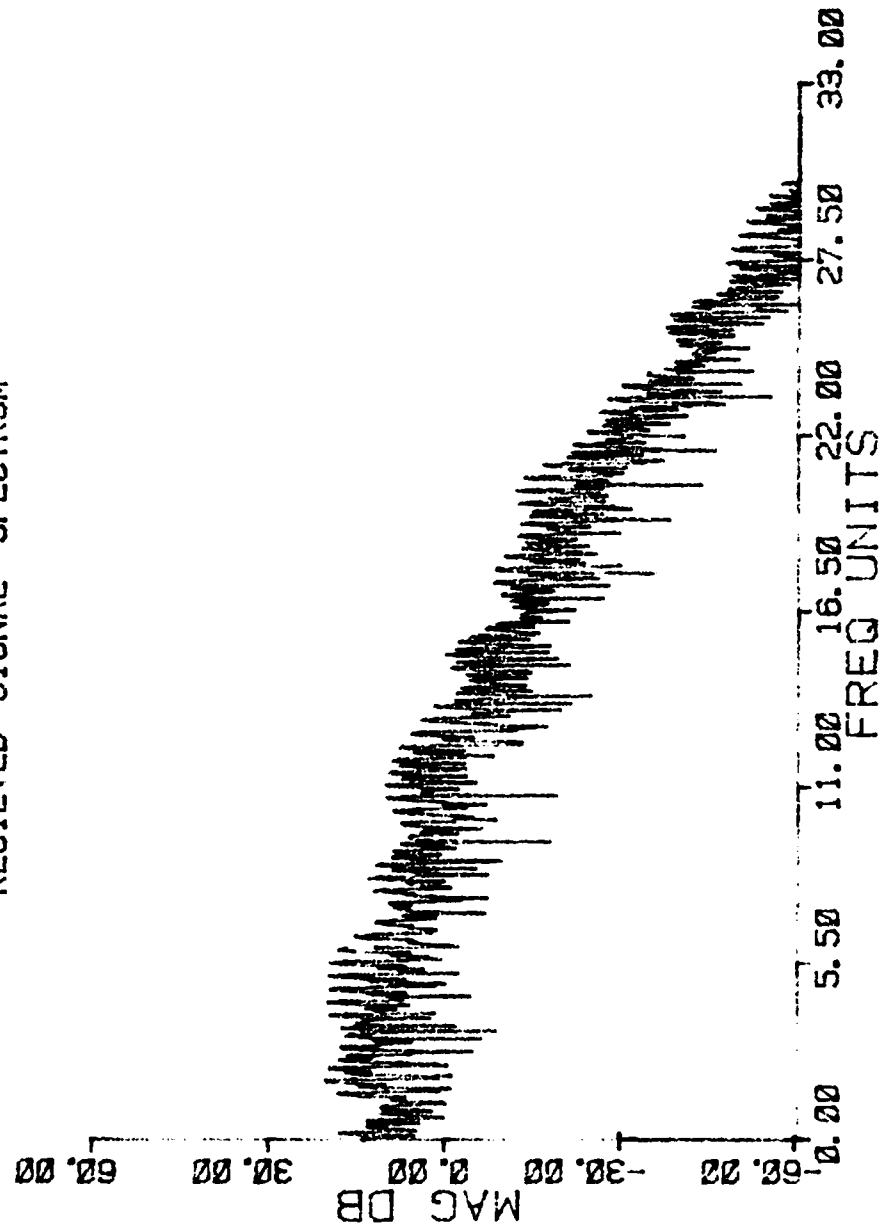


Figure 1. Received signal spectrum, 200 Hz, 11, 16, 22, 27, 33 units.

AD-A138 545	TARGET SUPER-RESOLUTION AIRBORNE RADAR UTILIZIN. (U) AIR FORCE INST OF TECH	2/2
UNCLASSIFIED	WRIGHT-PATTERSON AFB OH SCHOOL OF ENGI. K W ALBERT DEC 83 AFIT/GE/EE/83D-5 F/G 17/9	NL

TARGET SUPER-RESOLUTION COMPENSATION FOR COHERENT
AIRBORNE RADAR UTILIZING. (U) AIR FORCE INST OF TECH
WRIGHT-PATTERSON AFB OH SCHOOL OF ENGI. K W ALBERT
DEC 83 AFIT/GE/EE/83D-5 F/G 12/9

2/2

UNCLASSIFIED

F/G 17/9

NI

[illegible]



MICROCOPY RESOLUTION TEST CHART
NATIONAL BUREAU OF STANDARDS-1963-A

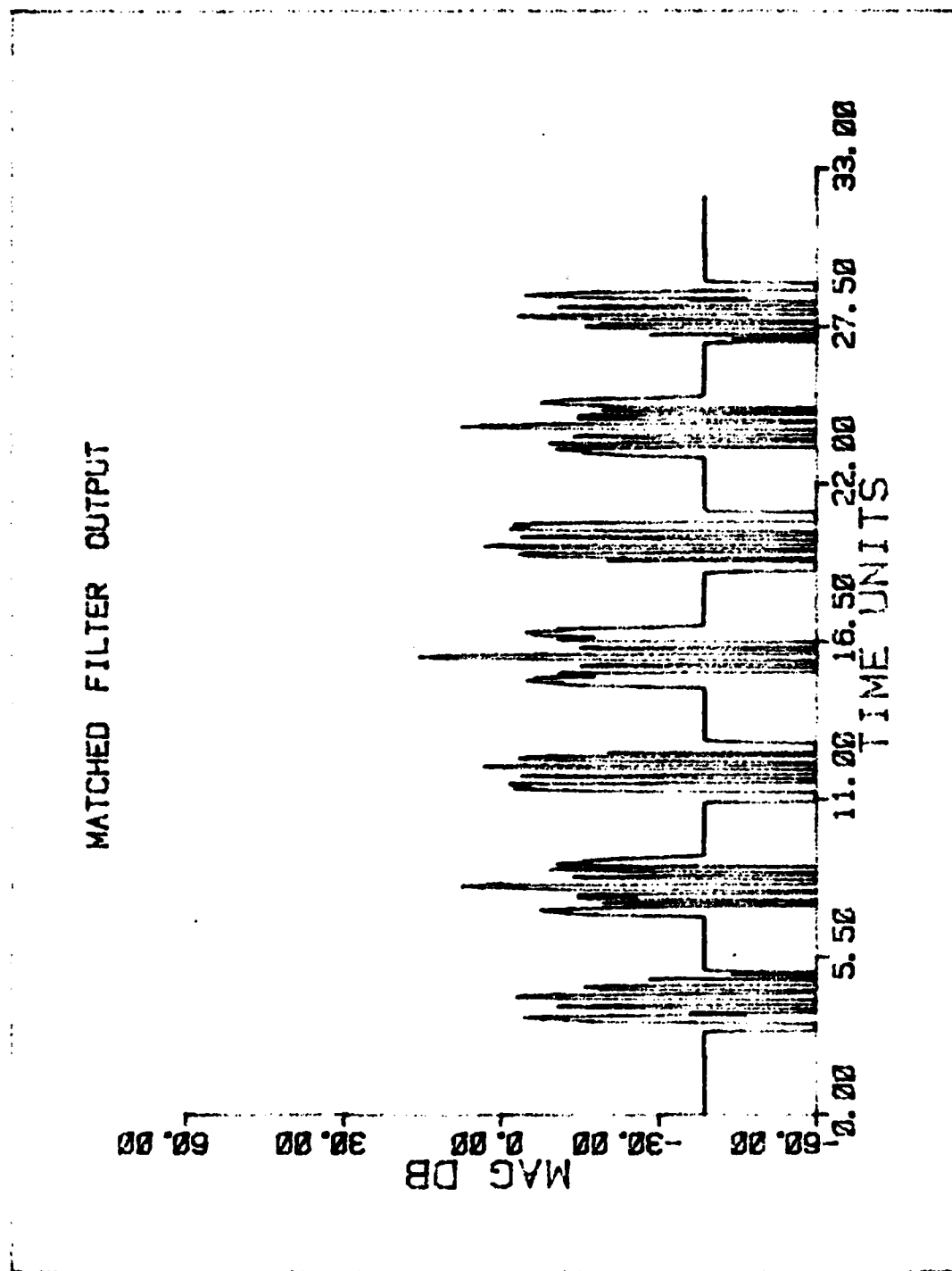


Figure 2a. Matched Filter Output, Averaging II,
 32,000,01

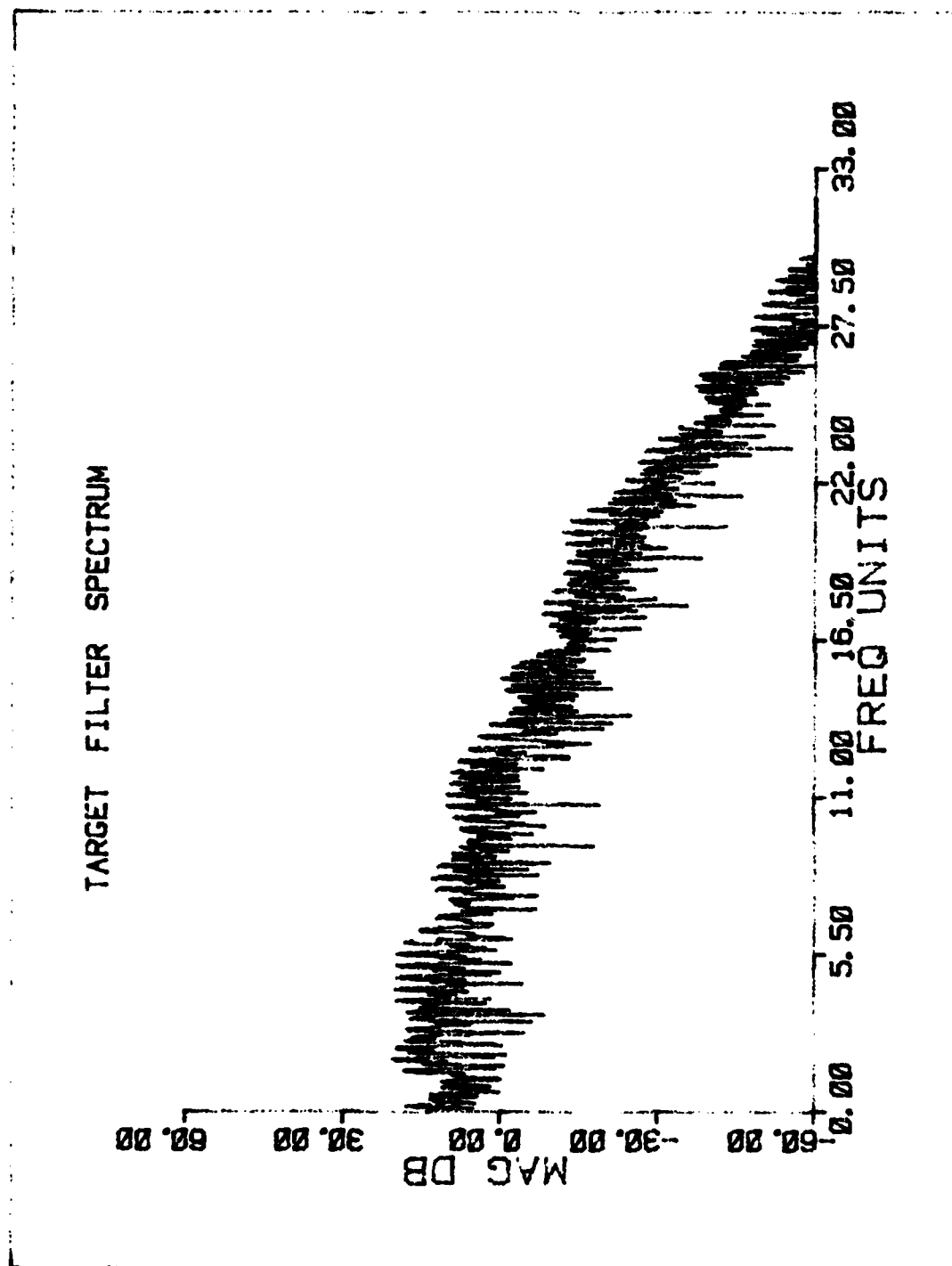


Figure 15. Target Filter, Overlaid II, Alpha=0.71

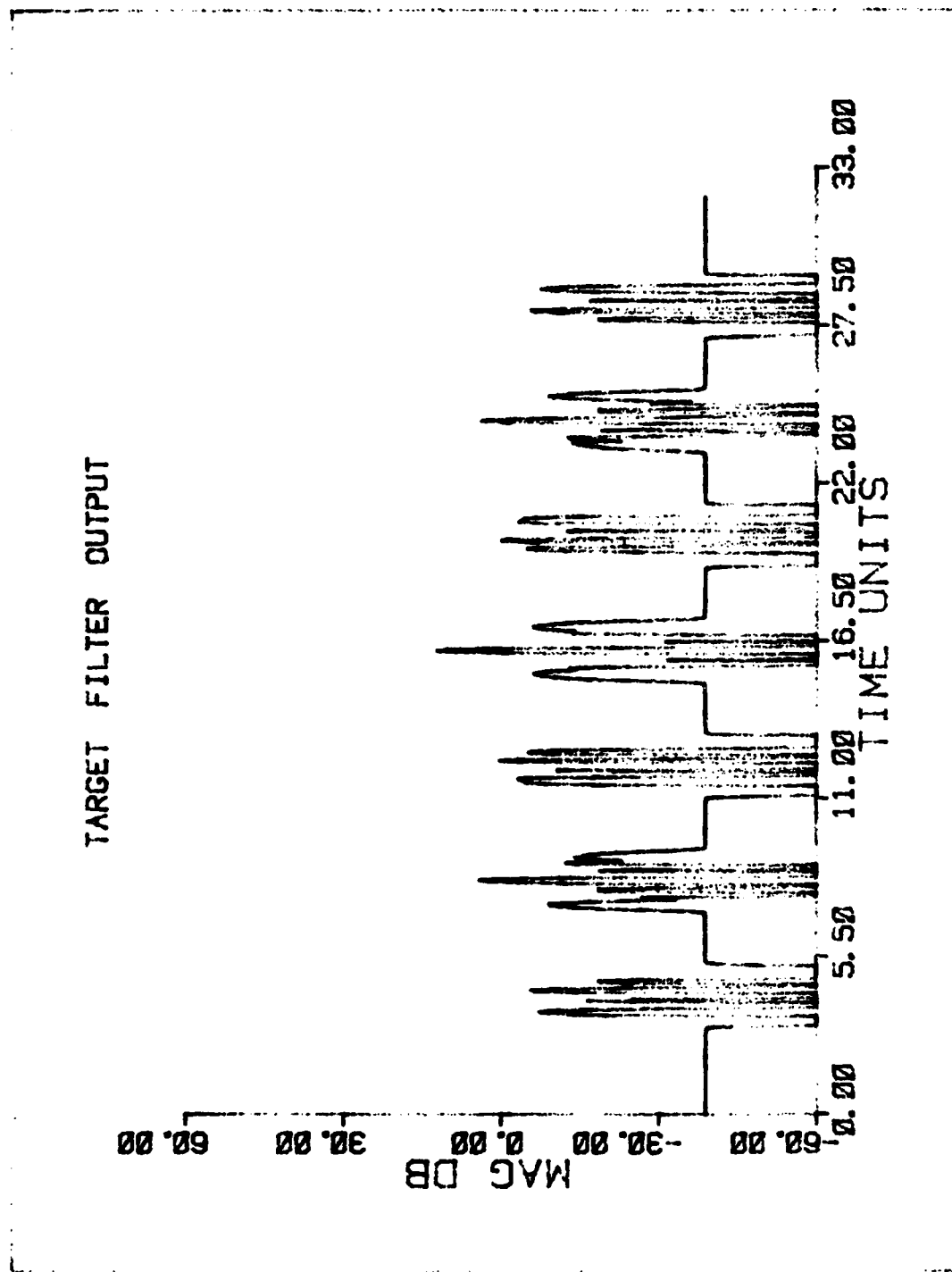


Figure 6. Target Filter Output, Correlation II,
Alpha 0.01

RECIEVED SIGNAL SPECTRUM

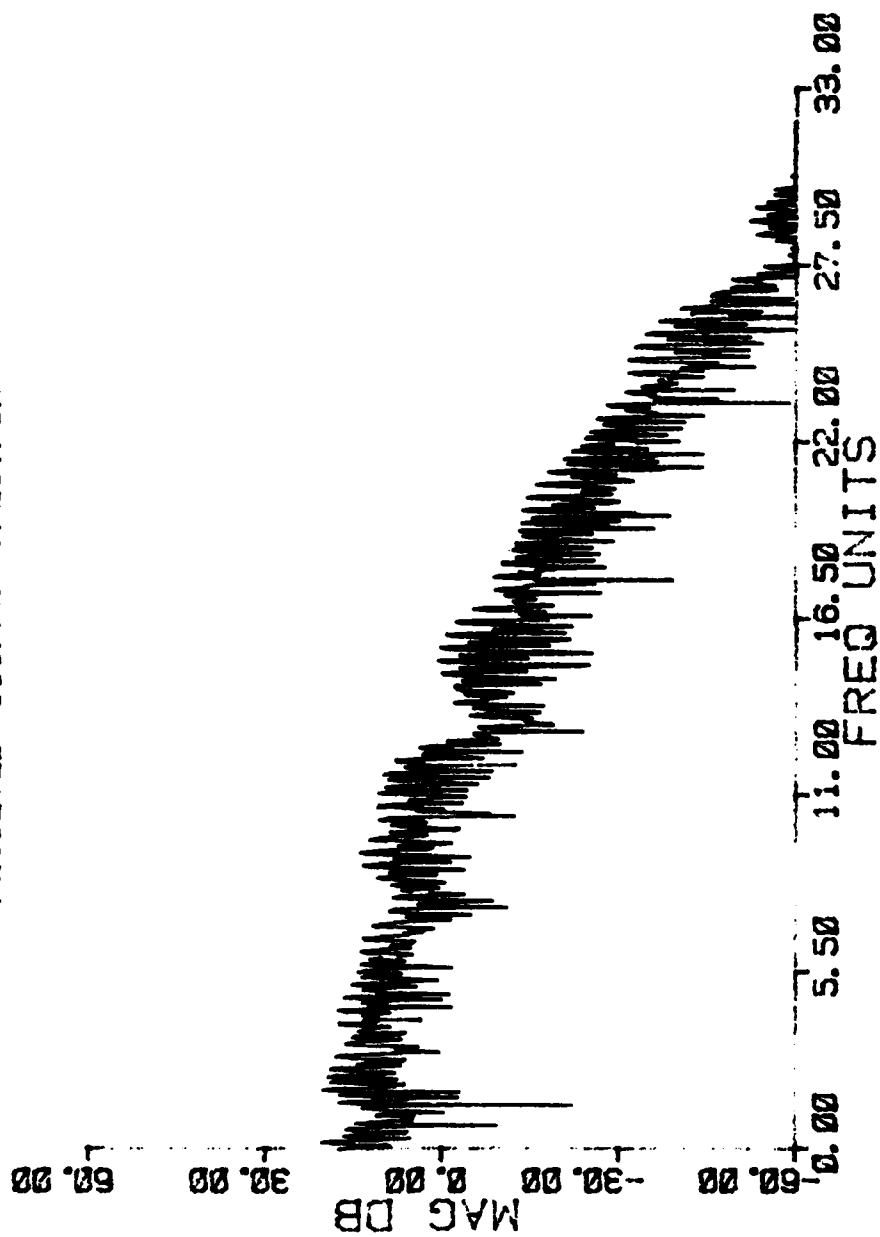


Figure 12. Received Signal Spectrum, Swerling II,
Alpha=0.01

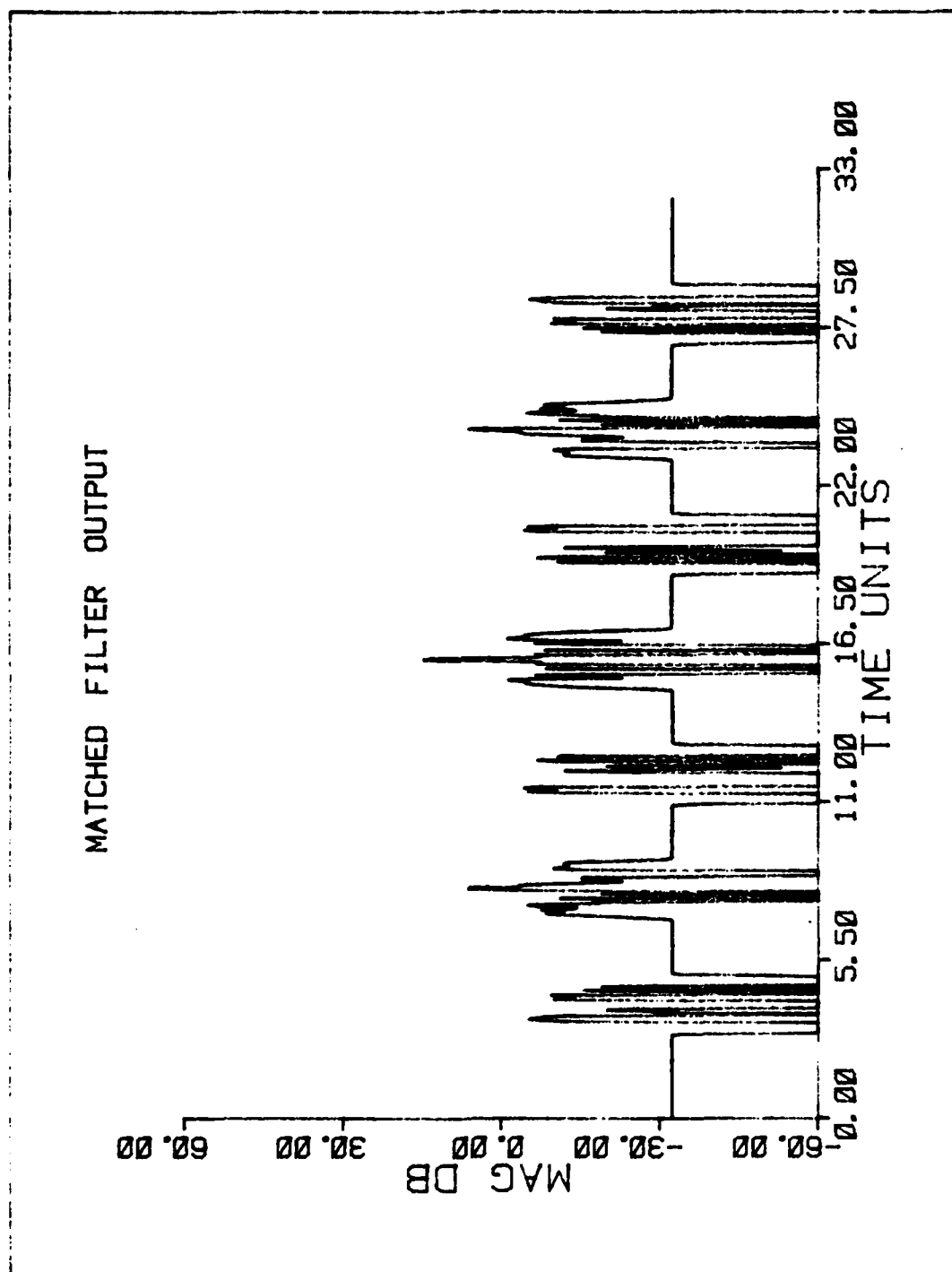


Figure 10. Matched Filter Output, Starting II,
 $\alpha_p = 0.7$

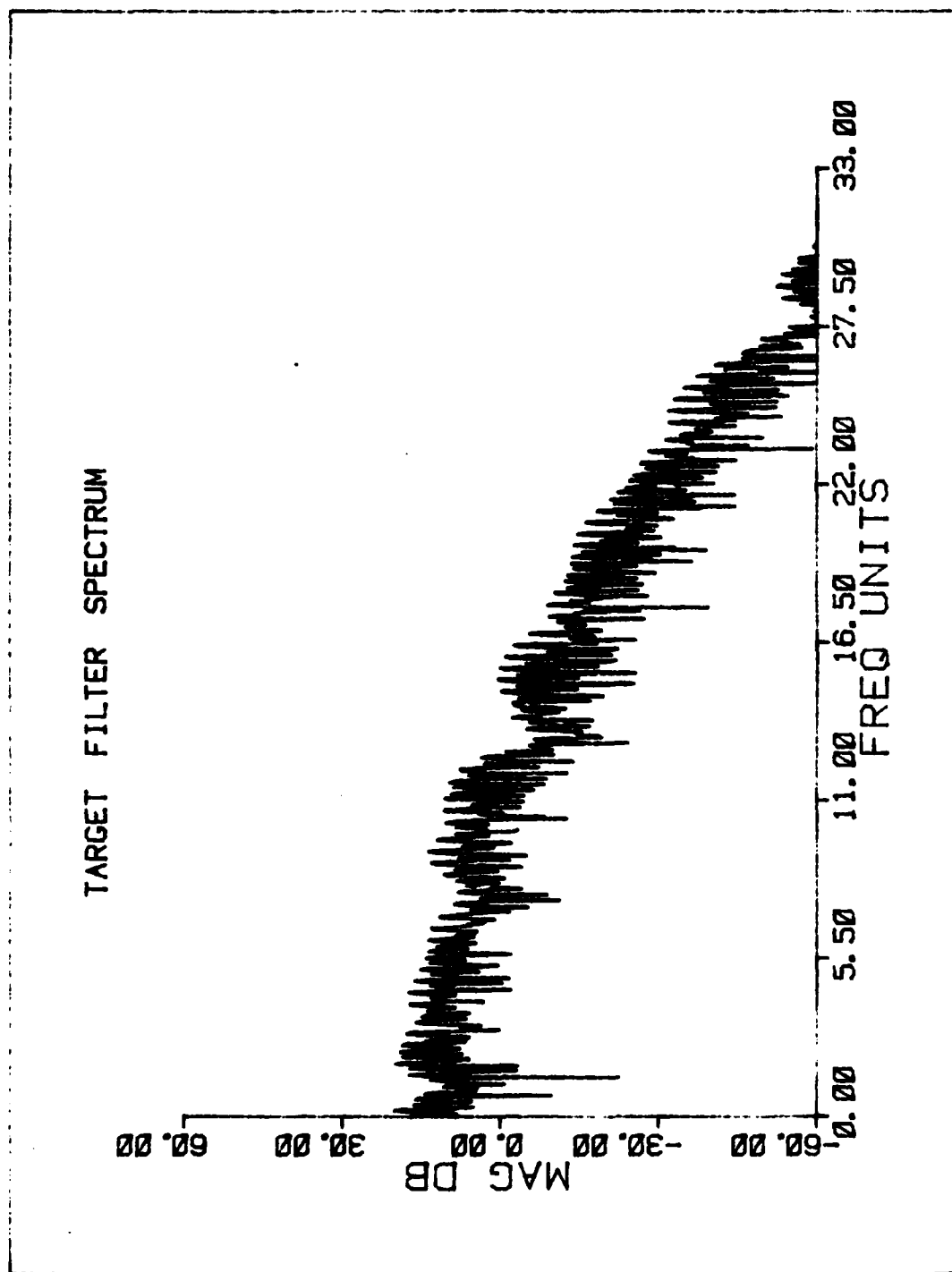


Figure 20. Target Filter, Overlaid, Alpha=0.01

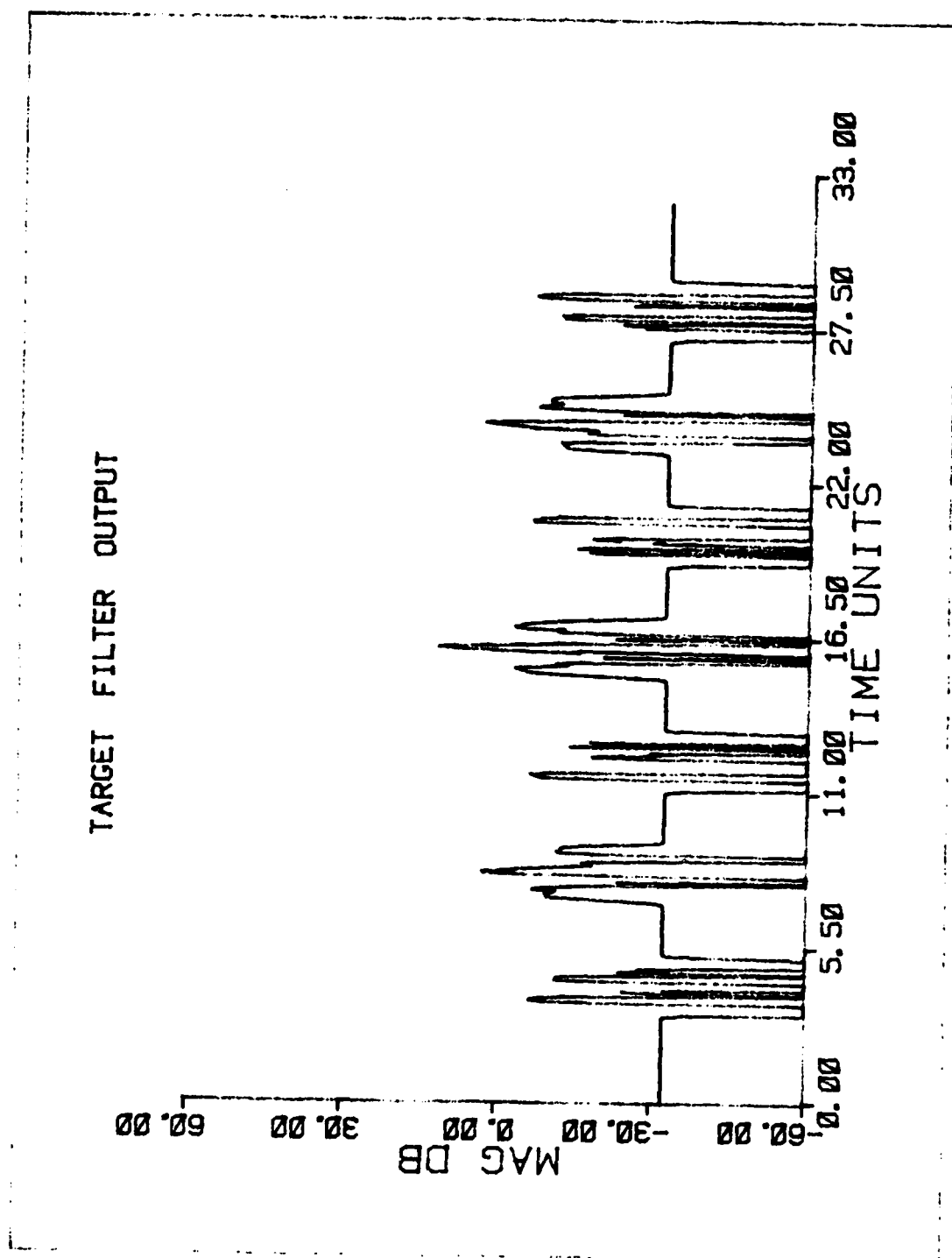


Figure 2. Target Filter Output, Sampling, 10, 1/10th, 0.01

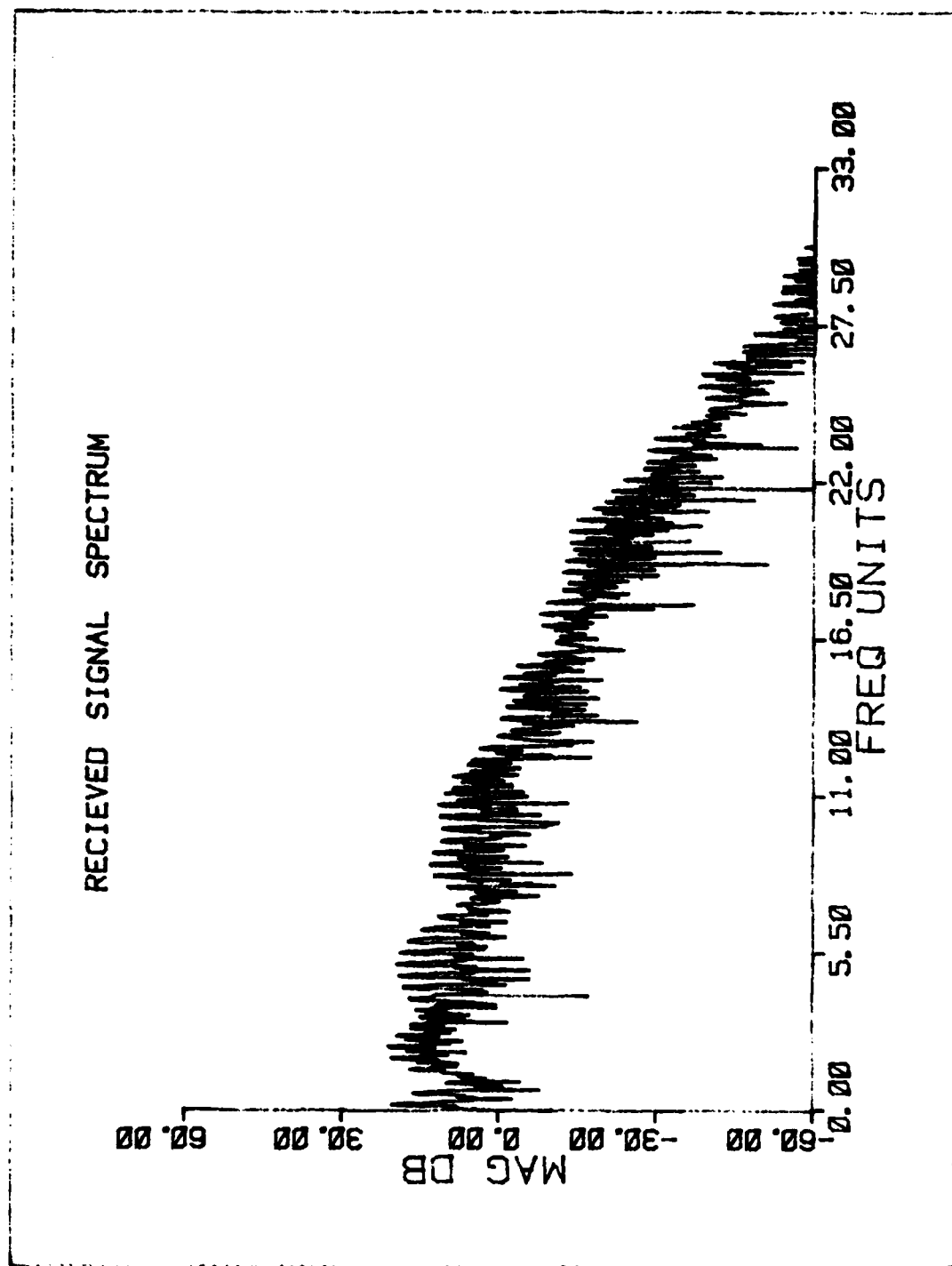


Figure 1. Received Signal Spectrum, Recording 17,
 $\text{Alpha} = 0.01$

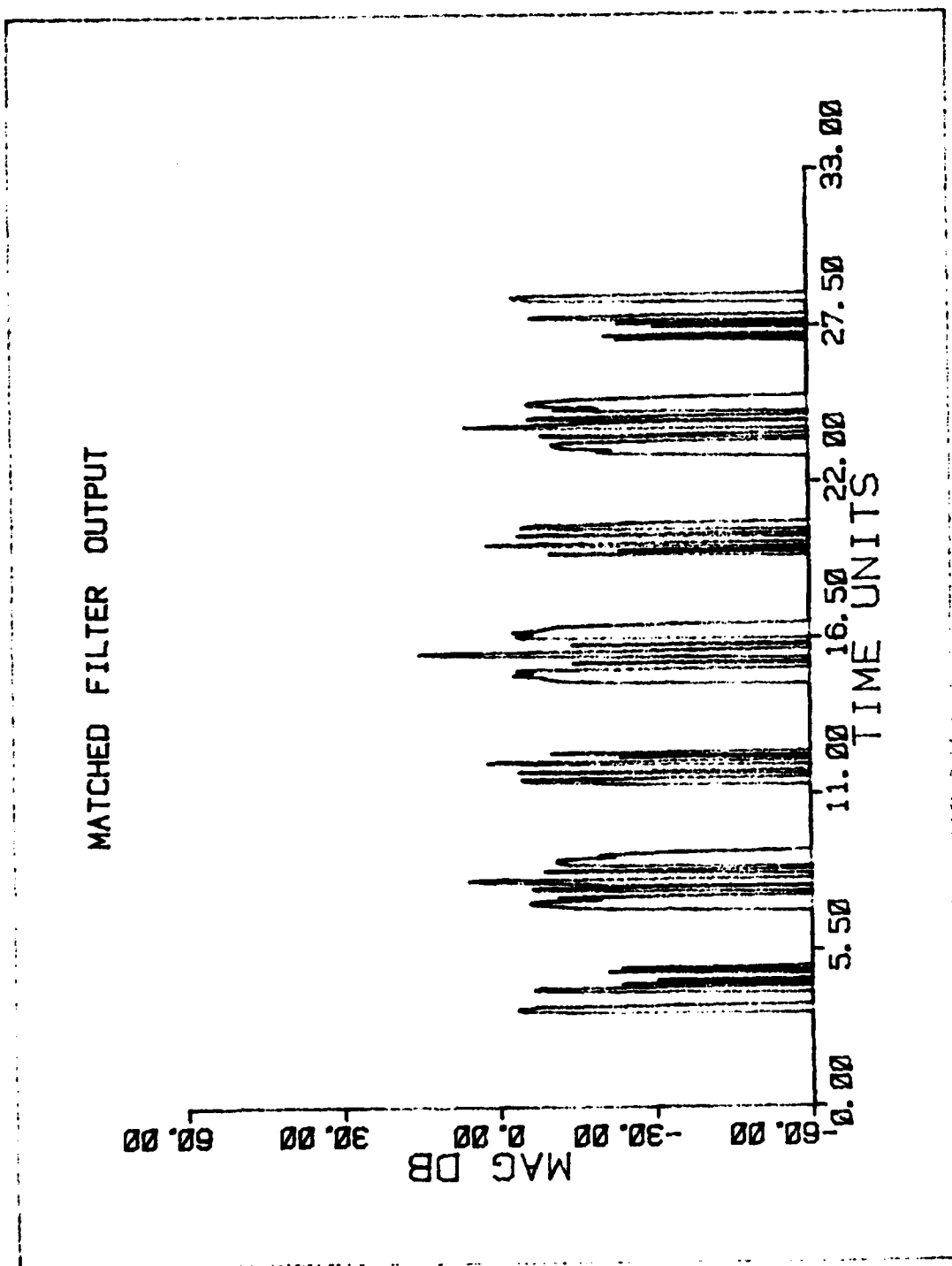


Figure 2.1. Matched Filter Output, Sweeping 11,
 $\Delta f_{\text{max}} = 0.01$

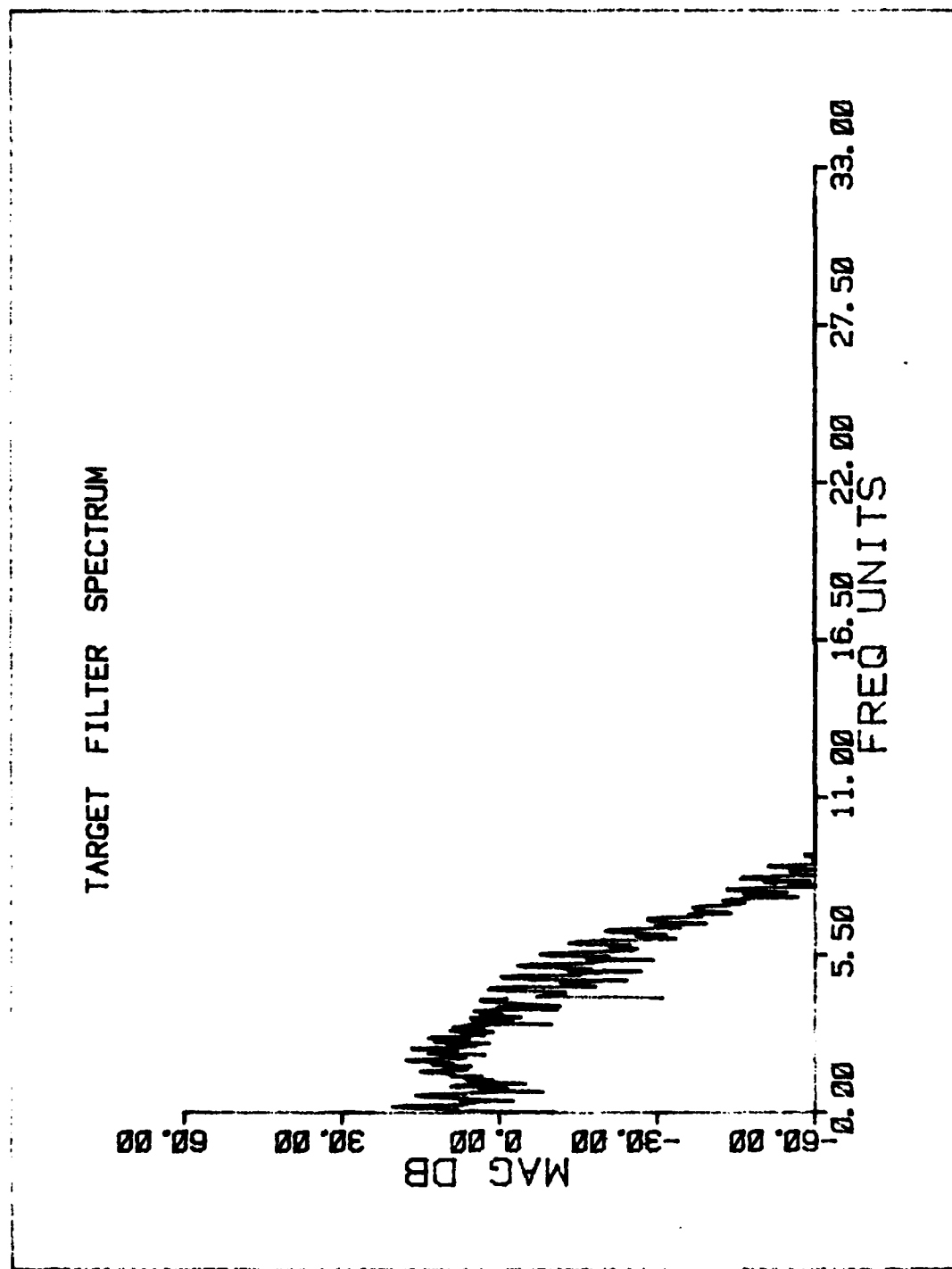


Figure 1. Target Filter Spectrum, $\alpha = 0.1$

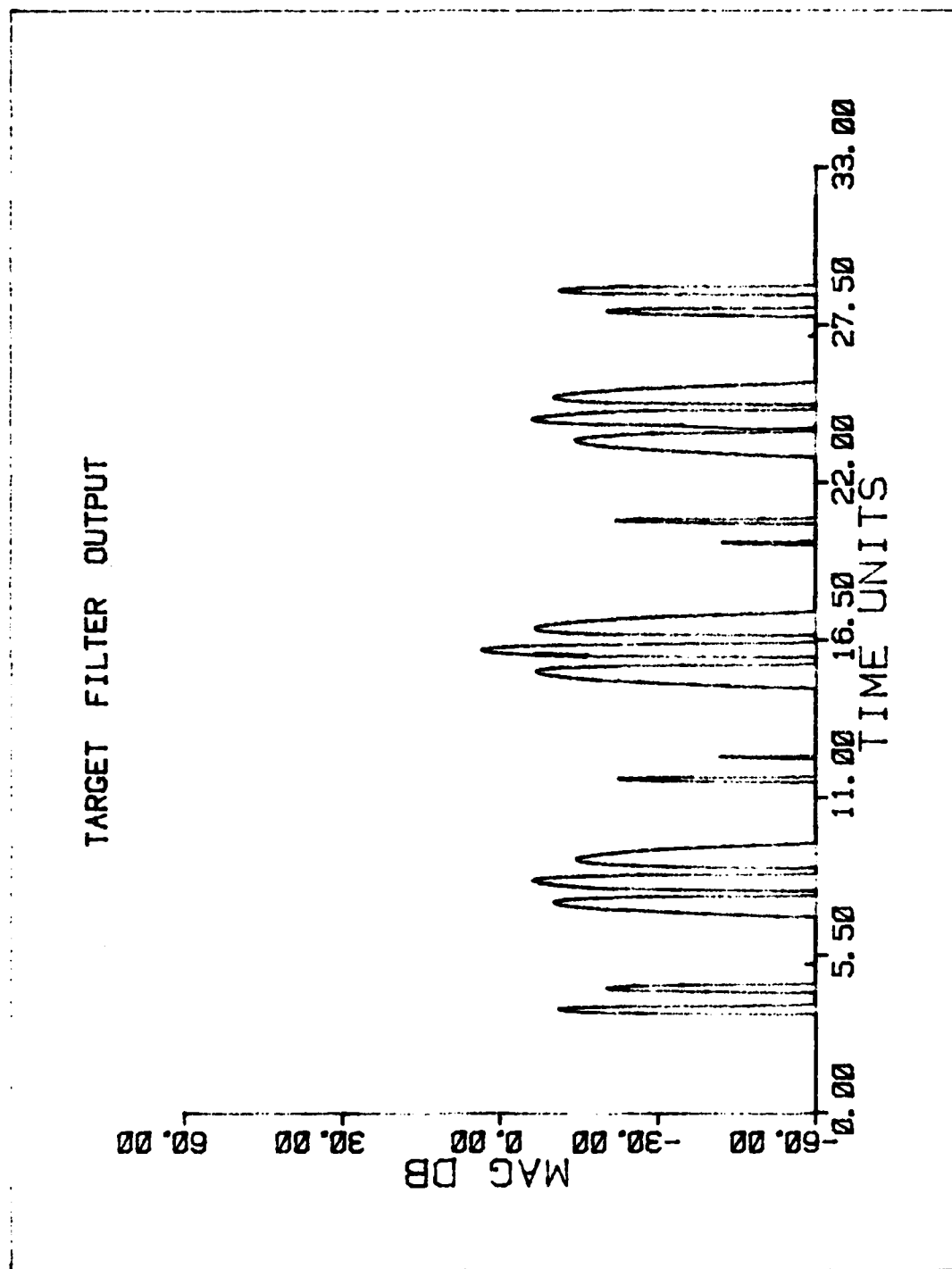


Figure 11. Target Filter Output, Swirling II, Alpha=0.1

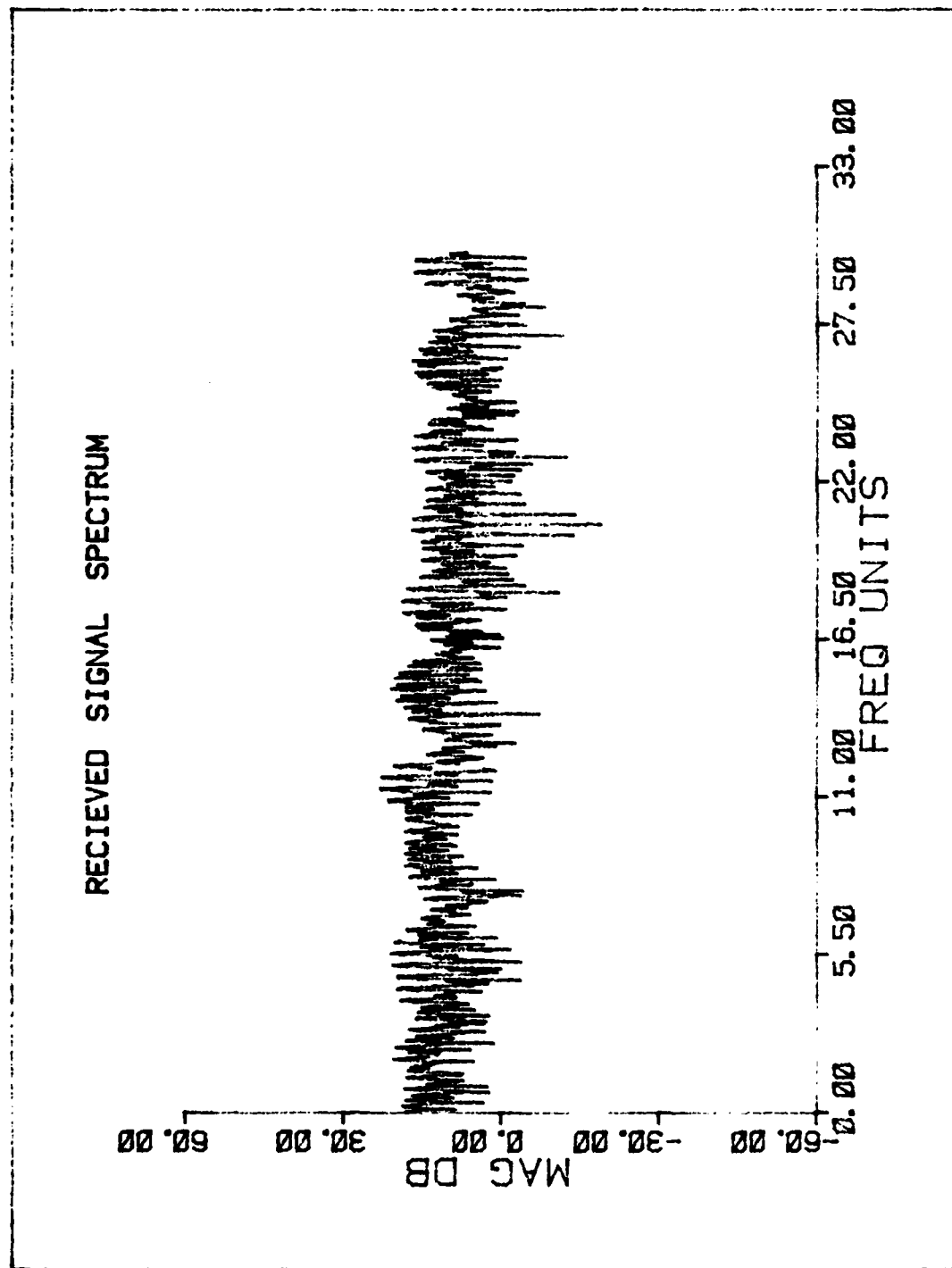


Figure 25. Received signal spectrum, Working II,
At $f = 0.001$

MATCHED FILTER OUTPUT

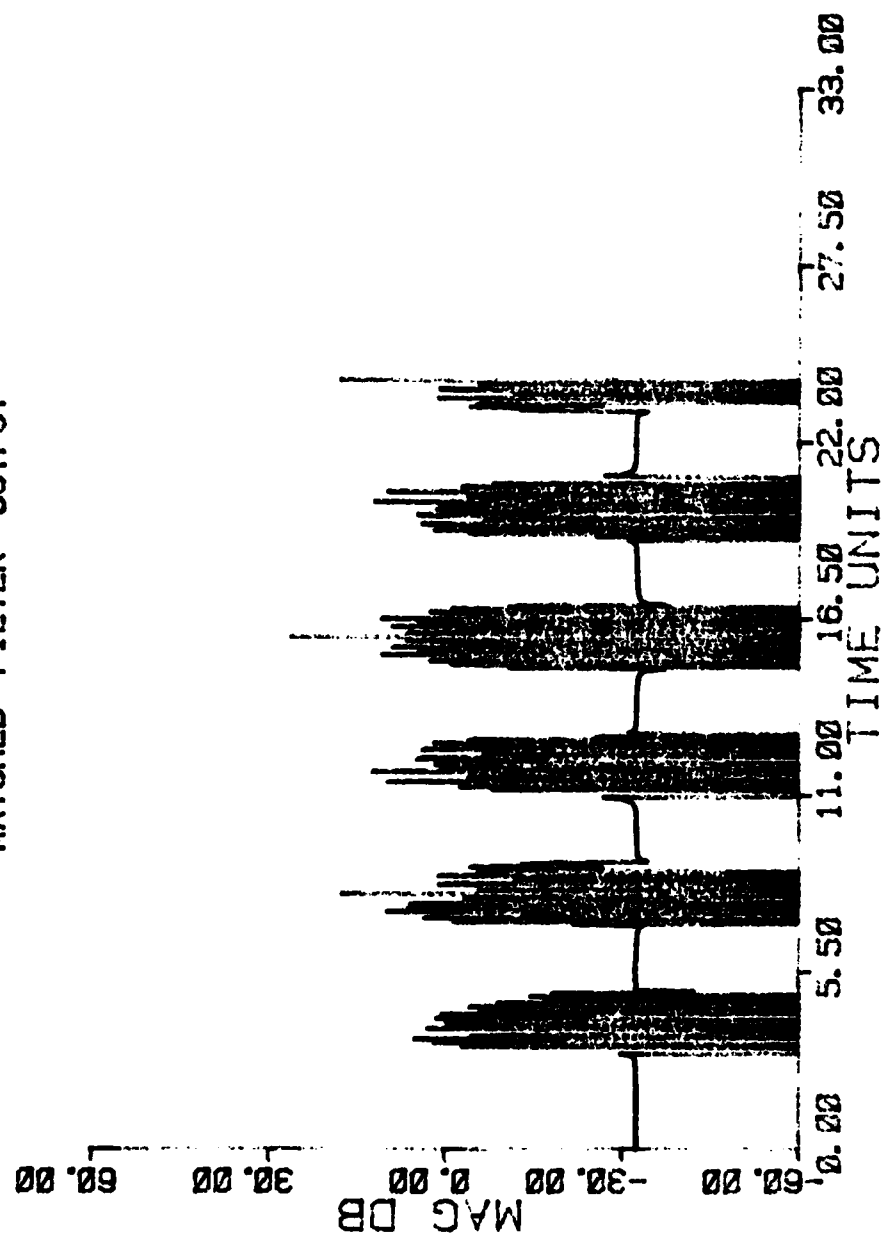


Figure 14. Matched Filter Output, Sterling II,
 1000 Hz, 0.001

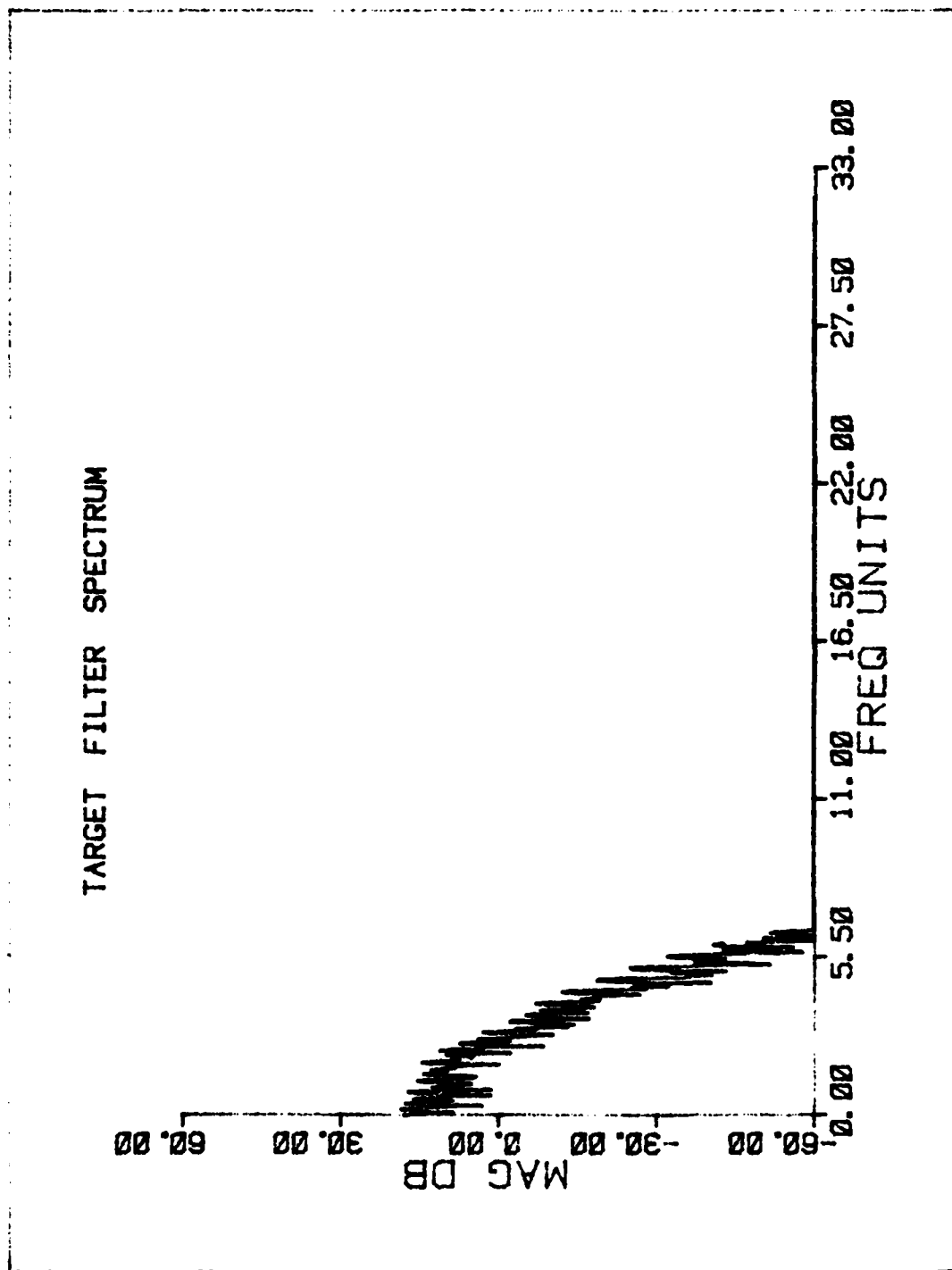


Figure 27. Target Filter, Stepping II, $\Delta f_{\text{band}}=0.2$

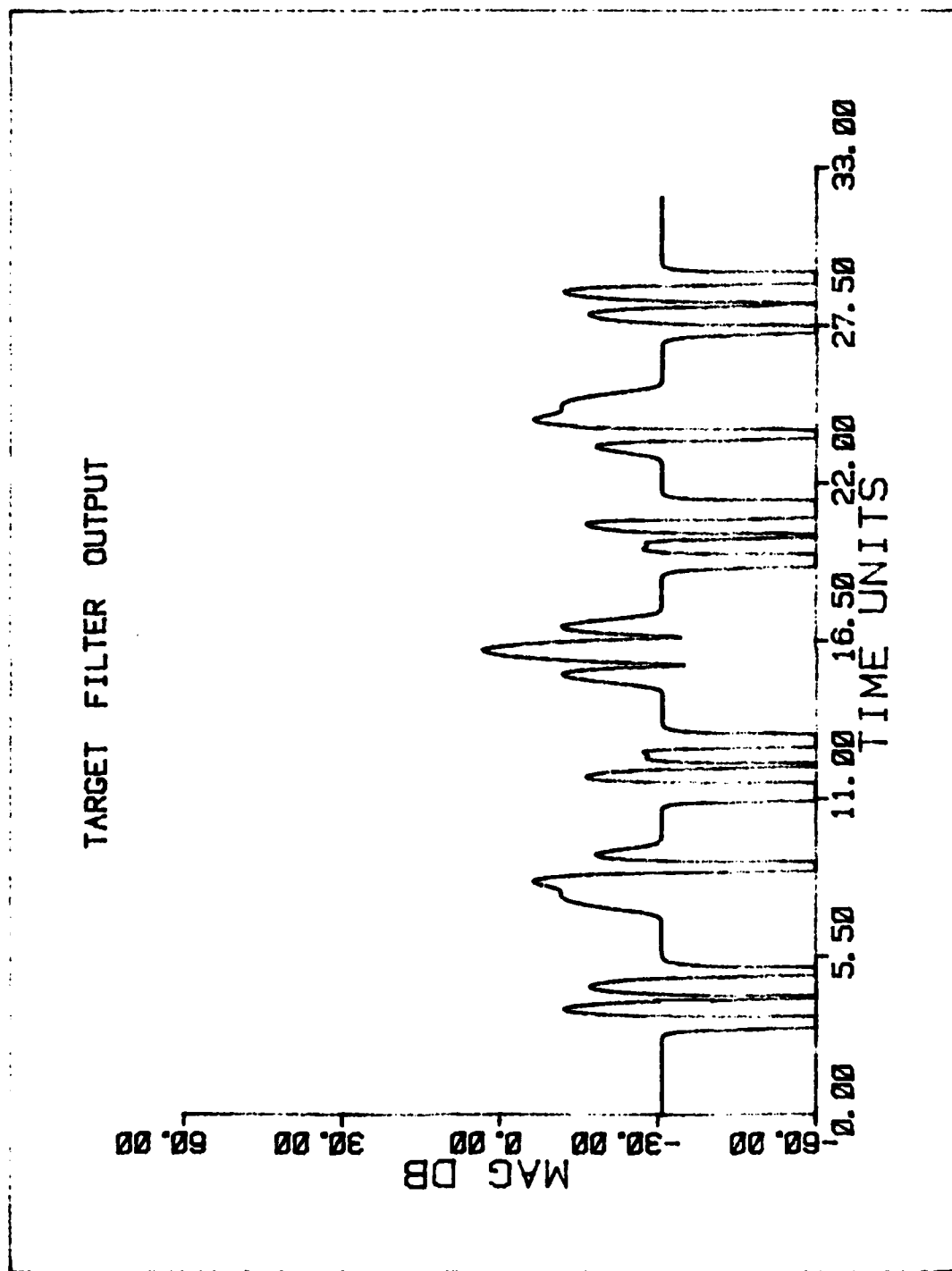


Figure 34. Target Filter Output, Sweeping II,
Alpha=0.2

VI Conclusions and Recommendations

Conclusions

The objective of this study was to determine whether a coherent or incoherent target filter provided greater output signal-to-noise ratio. The signals under test were all coded, spread spectrum waveforms designed for use in a coherent airborne radar system. It was noted that the computer simulation was dependent on the characterization of the range extended scattering function. Knowing the scattering characteristics and the accuracy of their approximations (ie decaying exponential, Gaussian pulse) is paramount to the type of analysis performed.

The 25 element, pseudo-random phase coded signal analysis showed two main features. First, values of α less than 0.1 yielded 50-60 dB higher output signal power for incoherent processing. Values of α at or above 0.1 allowed a smoother, wider peak around the 15.96 time unit sample point. Higher values of α correspond to a narrower filter bandwidth. The consistent performance edge (1-3 dB) of the incoherent target filter found by this study agrees with the findings of Salzman (Ref11:69-70). Second, the incoherent target filter provides improved signal-to-noise ratio due to its broader main peak. This produces a higher sampled value away from the output centroid (located at 15.96 time units) as compared with the coherent filter.

The interpulse frequency hopping and frequency hopping

with subpulse chirp show similar results. In both cases, the incoherent filter is superior. The performance difference for these two waveforms is much more consistent as compared to the phase coded signal. Interpulse coding yields a steady 0.72-0.75 dB incoherent filter advantage, whereas interpulse FH with subpulse chirp holds around 0.4-0.7 dB improvement margin.

It appears that with assumptions made concerning RCS fluctuations, target scatterering characteristics, and radar waveform, that the incoherent target filter is superior to the coherent target filter on the basis of output SNR.

Recommendations

In addition to the signals tested, the simulation software is capable of testing linear frequency modulated, variable frequency modulated, intrapulse frequency hopping, and intrapulse FH with subpulse chirp waveforms. The software is also capable of simulating Gaussian as well as rectangular pulse trains. Further, different types of RCS fluctuations and target scatterering characteristics can be easily accommodated. Due to time constraints involved in producing this paper, these possibilities were not explored. Whether or not they provide further insight into the applicability of the target filter is left for further research. However, based on the data presented, an incoherent target filter would be advantageous when SNR is a factor and ease of implementation important.

Future studies might consider testing those waveforms not tested in this study with and without different range extended scatterering functions. Alternatively, the concept of non-cooperative target recognition (NCTR) might be addressed by extending the software. NCTR is an attempt to exploit the range super-resolution phenomenon (rather than compensate for it) in order to provide a type of target signature. In this manner, the target could be detected, identified, and classed. The software used in this study might be extended to investigate target super-resolved range signatures.

Bibliography

1. Brookner, Eli, ed. Radar Technology, "Waveform Selection and Processing" by A.I. Sinsky. Dedham MA: Artech House Inc., 1977.
2. Carpinella, Lt Col Ronald J. Class notes for EE6.68 offered summer 1982, School of Engineering, Air Force Institute of Technology (AU), Wright-Patterson AFB OH.
3. DiFranco, J.V. and W.L. Rubin. Radar Detection. Dedham MA: Artech House Inc., 1980.
4. Mitchell, Richard L. Radar Signal Simulation. Dedham MA: Artech House, Inc., 1976.
5. Nitzberg, Ramon. "Effect of a Few Dominant Specular Reflectors Target Model Upon Detection", IEEE Transactions on Aerospace and Electronic Systems, AES-14 (4): 670-673 (July, 1978).
6. Oppenheim, Alan V. Applications of Digital Signal Processing. Englewood Cliffs NJ: Prentice Hall, Inc., 1978.
7. Oppenheim, Alan V. Digital Signal Processing. Englewood Cliffs NJ: Prentice Hall, Inc., 1975.
8. Reed, Capt John D. Radar Waveform Selection Based on the Calculation and Application of Radar Ambiguity Functions MS thesis GE/EE/82J-11, School of Engineering, Air Force Institute of Technology (AU), Wright-Patterson AFB OH, June 1982.
9. Rihaczek, August W. Principles of High Resolution Radar. New York: McGraw-Hill Book Company, 1969.
10. Rihaczek, August W. "Radar Waveform Selection - A Simplified Approach", IEEE Transactions on Aerospace and Electronic Systems, AES-7(6): 1078-1086 (November 1971).
11. Salzman, Joesph. pread Spectrum Applications to Coherent Airborne Radar Systems. AFWAL-TR-81-1249, Technology Service Corporation, Santa Monica, CA, 1982.
12. Whalen, Anthony D. Detection of Signals in Noise. New York, New York: Academic Press, 1971.

Appendix A: Simulation Flow Chart.

Flowchart for Simulation of Radar Waveform,
Spectrum Analysis, Matched Filter, and Target
Filter Processing

RUN Program 'MAIN'

call 'Input' to define
pulse parameters

call 'Code' to set
up pseudo-code values

is
pulse phase
shift coded

yes

call 'Phase' to set
frequency and amplitude
for waveform samples

no

call 'FM' to get frequency
modulation of waveform

call 'Recpl' to get
amplitude of waveform
samples

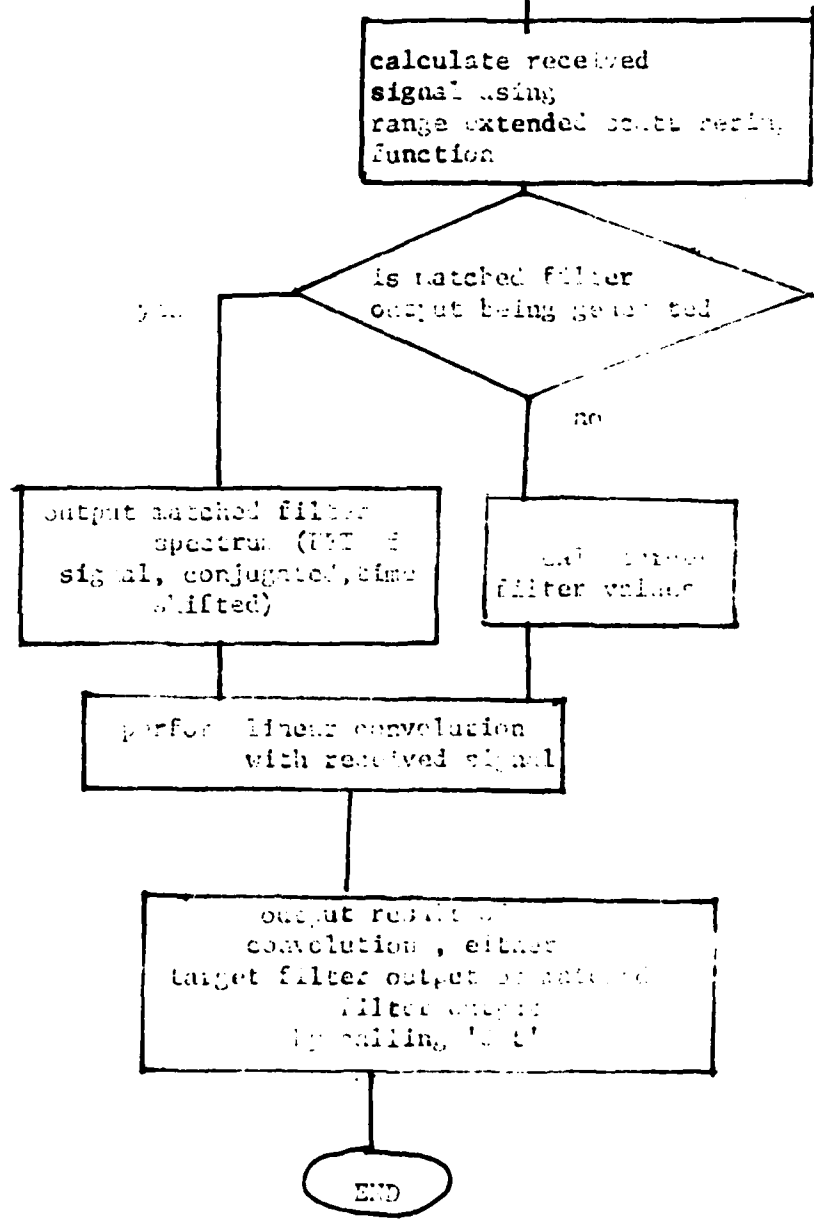
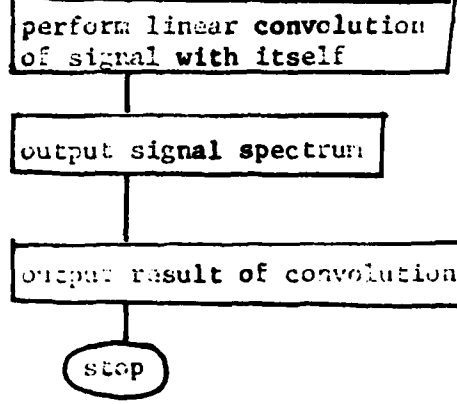
call 'Setup' to put
sequences in proper format
for linear convolutions

is
ambiguity not being
generated

Copy available to DTIC does not
permit fully legible reproduction.

yes

no



Appendix E: Program Listings

```

100=      PROGRAM MAIN
110=
120=
130=C      PROGRAM MAIN
140=C      WRITTEN BY KENNETH W. ALBERT/(REF:REED)
150=C      17 OCT 83
160=
170=
180=      COMPLEX XVALS(1024),YVALS(1024),Z(1024),VALUE,DELAY
190=      INTEGER SAMPLE,PERIOD(1024),D,C(64)
200=      REAL MAG(1024),FREQ(1024),FILTER(1024),MMAG(1024),PRT(50)
210=      OPEN(10,FILE='DATA')
220=      OPEN(12,FILE='RESUL2')
230=      OPEN(15,FILE='RESUL1')
240=      OPEN(11,FILE='RESUL3')
250=      REWIND 10
260=      REWIND 11
270=      REWIND 12
280=      REWIND 15
290=
300=
310=      CALL INPUT(PERIOD,PRT,PW,NPRT,TOTAL,SAMPLE,NUM,M,N)
320=      CALL CODE(C)
330=      READ(10,*)J
340=      IF (J.EQ.1) GO TO 5
350=      CALL PHASE(FREQ,PRT,PERIOD,7,M,N,NPRT,GFACT,
360=      PW,SAMPLE,TOTAL,C)
370=      GO TO 20
380=5      WRITE(*,*)'PULSE(S) IS FREQUENCY CODED'
390=      CALL FM(FREQ,PERIOD,NPRT,PW,N,C,M,TOTAL,PRT)
400=      CALL RECP1(PERIOD,7,GFACT,NPRT,N)
410=20     SCALE=GFACT/(N*NPRT)
420=      WRITE(12,*)M
430=      WRITE(15,*)M
440=      WRITE(11,*)M
450=      READ(10,*)W
460=25     VALUE=CMPLX(0.0,W)
470=      WRITE(*,300)W
480=      READ(10,*)D
490=      WRITE(*,*)'THE VALUE OF D IS',D
500=      IWK=6*SAMPLE+150
510=      WK=6*SAMPLE+150
520=      CALL SETUP(D,Z,FREQ,XVALS,YVALS,VALUE,TOTAL,SAMPLE,M)
530=      @IWK,WK,PW,N)
540=      CALL FFTCC(YVALS,SAMPLE,IWK,WK)
550=      IF(D.EQ.0)THEN
560=      WRITE(*,301)
570=      ELSE
580=      IF(D.EQ.1) THEN
590=      WRITE(*,307)
600=      ELSE
610=      WRITE(*,315)

```

Following

Reproduced from
best available copy.

PAGE 5

```

620=      END IF
630=      END IF
640=      DO 30 I=1,2*M
650=          TIME=(TOTAL/M)*(I-1)
660=          X=CABS(YVALS(I))
670=          IF(X.LT.0.001) THEN
680=              X=0.001
690=          END IF
700=          MMAG(I)=10*ALOG10(X*X)
710=          IF(D.EQ.0) THEN
730=              WRITE(15,305) TIME,MMAG(I)
740=          END IF
750=          IF(D.EQ.1) THEN
770=              WRITE(15,310) TIME,MMAG(I)
780=          END IF
790=30      CONTINUE
810=      IF(D.EQ.3) THEN
815=          READ(10,*) ALPHA2
820=      DO 42 I=1,SAMPLE
830=          TIME=(PW/N)*(I-1)
840=          DELAY=CMPLX(0.0,62.)
850=          FILTER(I)=EXP(-ALPHA2*TIME*TIME)
860=          Z(I)=FILTER(I)*YVALS(I)
870=          XVALS(I)=CONJG(Z(I))*CFXF(DELAY*TIME)
880=          X=CABS(XVALS(I))
890=          IF(X.LT.0.001) THEN
900=              X=0.001
910=          END IF
915=          MMAG(I)=10*ALOG10(X*X)
916=          WRITE(11,320) TIME,MMAG(I)
920=42      CONTINUE
930=      ELSE
940=          CALL FFTCC(XVALS,SAMPLE,IWK,WK)
950=      END IF
960=      DO 50 I=1,SAMPLE
970=          XVALS(I)=XVALS(I)*YVALS(I)
980=50      CONTINUE
990=      DO 51 I=1,SAMPLE
1000=          XVALS(I)=CONJG(XVALS(I))
1010=51      CONTINUE
1020=          CALL FFTCC(XVALS,SAMPLE,IWK,WK)
1030=      DO 52 I=1,SAMPLE
1040=          XVALS(I)=CONJG(XVALS(I))/SAMPLE
1050=52      CONTINUE
1060=      IF(D.EQ.0) THEN
1070=          DO 55 I=1,SAMPLE
1080=              ZDUM=CABS(XVALS(I))
1090=              IF(ZDUM.LT.0.001) THEN
1100=                  ZDUM=0.001
1110=              END IF
1120=              MAG(I)=10*ALOG10(ZDUM*ZDUM)
1130=55      CONTINUE
1140=      ELSE
1150=          DO 65 I=1,SAMPLE

```

```

1150=      Y=REAL(XVALS(I))
1170=      IF(Y.LT.0.001)THEN
1180=      Y=0.001
1190=      END IF
1200=      MAG(I)=10*ALOG10(Y)
1210=65    CONTINUE
1220=      END IF
1230=      CALL OUT(MAG,NUM,PW,TOTAL,M,D)
1240=      READ(10,*)W
1250=      IF(W.EQ.999) GO TO 500
1260=      GO TO 25
1270=300    FORMAT(1X,'W=',F12.2)
1280=301    FORMAT(5X,'TIME DELAY',5X,'SIGNAL SPECTRUM')
1290=305    FORMAT(5X,F10.4,5X,F10.4)
1300=307    FORMAT(5X,'TIME DELAY',5X,'RECEIVED SIGNAL SPECTRUM')
1310=310    FORMAT(5X,F10.4,5X,F10.4)
1320=315    FORMAT(5X,'VALUE OF I',5X,'TARGET FILTER SPECTRUM')
1330=320    FORMAT(5X,F10.4,5X,F10.4)
1340=500    END
1350=*****
1360=*****
1370=*      SUBROUTINE INPUT
1380=*      WRITTEN BY KENNETH W. ALBERT/(REF:REED)
1390=*      17 OCT 83
1400=*****
1410=*****
1420=      SUBROUTINE INPUT(PERIOD,PRT,PW,NPRT,TOTAL,SAMPLE,NUM,M,N)
1430=
1440=      INTEGER SAMPLE,PERIOD(1024)
1450=      REAL PRT(50),CPRT(50)
1460=
1470=      READ(10,*)PW
1480=      READ(10,*)I
1490=      IF(I.EQ.0) GO TO 25
1500=      WRITE(*,*)'WAVEFORM HAS REPEATED PULSES'
1510=      READ(10,*)J
1520=      IF(J.EQ.0) GO TO 10
1530=      READ(10,*)SAME
1540=      READ(10,*)NPRT
1550=      DO 5 I=1,NPRT
1560=      PRT(I)=SAME
1570=5      CONTINUE
1580=      WRITE(*,300)SAME,NPRT
1590=      TOTAL=SAME*NPRT
1600=      GO TO 30
1610=10     WRITE(*,*)'STAGGERED PRTS TO BE USED'
1620=      READ(10,*)NPRT
1630=      READ(10,*)PRT(1)
1640=      DO 15 I=2,NPRT
1650=      READ(10,*)PRT(I)
1660=15     CONTINUE
1670=      TOTAL=0.0
1680=      DO 20 I=1,NPRT
1690=      TOTAL=TOTAL+PRT(I)

```

```

1700=      WRITE(*,305)I,PRT(I)
1710=20    CONTINUE
1720=      GO TO 30
1730=25    WRITE(*,*)'WAVEFORM HAS ONLY ONE PULSE'
1740=      TOTAL=PW
1750=      NPRT=1
1760=      PRT(I)=PW
1770=      READ(10,*)NUM
1780=      SAMPLE=2*NUM
1790=      PERIOD(1)=NUM
1800=      M=NUM
1810=      N=NUM
1820=      WRITE(*,*)'N=',N,'M=',M,'      PERIOD(1)=',PERIOD(1)
1830=      GO TO 36
1840=30    READ(10,*)NUM
1850=      SAMPLE=NUM*2
1860=      IF(PW.EQ.1.E-11)GO TO 32
1870=      CPW=PW*1.E10
1880=      CTOTAL=TOTAL*1.E10
1890=      N=NUM/CTOTAL*CPW
1900=      M=N*CTOTAL/CPW
1910=      WRITE(*,*)'N=',N,'      M=',M
1920=      DO 31 I=1,NPRT
1930=      CPRT(I)=PRT(I)*1.E10
1940=      PERIOD(I)=N*CPRT(I)/CPW
1950=      WRITE(*,*)'I=',I,'      PERIOD(I)=',PERIOD(I)
1960=31    CONTINUE
1970=      GO TO 36
1980=32    IF(PW.EQ.0.0001) GO TO 34
1990=      CPW=PW*10000.0
2000=      CTOTAL=TOTAL*10000.0
2010=      N=NUM/CTOTAL*CPW
2020=      M=N*CTOTAL/CPW
2030=      WRITE(*,*)'N=',N,'      M=',M
2040=      DO 33 I=1,NPRT
2050=      CPRT(I)=PRT(I)*10000.0
2060=      PERIOD(I)=N*CPRT(I)/CPW
2070=      WRITE(*,*)'I=',I,'      PERIOD(I)=',PERIOD(I)
2080=33    CONTINUE
2090=      GO TO 36
2100=34    N=NUM/TOTAL*PW
2110=      M=N*TOTAL/PW
2120=      WRITE(*,*)'M=',M
2130=      WRITE(*,*)'N=',N
2140=      DO 35 I=1,NPRT
2150=      PERIOD(I)=N*PRT(I)/PW
2160=      WRITE(*,*)'I=',I,'      PERIOD(I)=',PERIOD(I)
2170=35    CONTINUE
2180=36    RETURN
2190=300    FORMAT(1X,'PKTS ARE THE SAME...PRT=',F12.10,
2200=      @5X,'# OF REPETITIONS=',I3)
2210=305    FORMAT(1X,'FOR I=',I3,5X,'PRT=',F12.10)
2220=      END
2230=*****

```

```

2240=*****
2250=**** SUBROUTINE CODE
2260=**** WRITTEN BY KENNETH W. ALBERT
2270=**** 17 OCT 83
2280=*****
2290=*****
2300= SUBROUTINE CODE(C)
2310=
2320= INTEGER X(6),C(64)
2330=
2340= X(1)=1
2350= DO 5 K=2,6
2360= X(K)=0
2370=5 CONTINUE
2380= DO 10 J=1,64
2390= C(J)=X(1)+X(6)
2400= IF(C(J).EQ.2)C(J)=0
2410= X(6)=X(5)
2420= X(5)=X(4)
2430= X(4)=X(3)
2440= X(3)=X(2)
2450= X(2)=X(1)
2460= X(1)=C(J)
2470=10 CONTINUE
2480= WRITE(*,300)
2490= WRITE(*,305)(C(J),J=1,64)
2500= RETURN
2510=300 FORMAT(2X,'THE BINARY PSEUDORANDOM CODE - LENGTH
2520= @ 63 =')
2530=305 FORMAT(2X,64I1)
2540= END
2550=*****
2560=*****
2570=**** SUBROUTINE PHASE
2580=**** WRITTEN BY KENNETH W. ALBERT/(REF:REED)
2590=**** 17 OCT 83
2600=*****
2610=*****
2620= SUBROUTINE PHASE(FREQ,PRT,PERIOD,Z,M,N,NPRT,GFACT,
2630= @PW,SAMPLE,TOTAL,C)
2640=
2650=
2660= COMPLEX Z(1024),AMT2
2670= INTEGER PERIOD(1024),COUNT,SUM,TALLY,SAMPLE,START,F
2680= @,C(64),RATIO(50)
2690= REAL PRT(50),FREQ(1024),MEAN,R(1024),CPRT(50)
2700= DOUBLE PRECISION DSEED
2710=
2720= WRITE(*,*)'PULSES ARE PHASE-SHIFT CODED'
2730= READ(10,*)NELEM
2740= ITIME=N/NELEM
2750=*****
2760=** ADDITION OF FLUCTUATION COEF. MATRIX:R
2770=*****

```



```

2780=      READ(10,*)F
2790=      IF(F.EQ.1) GO TO 4
2800=      WRITE(*,*)'RAYLEIGH AMPLITUDE FLUCTUATIONS'
2810=      DSEED=31313131.D0
2820=      DO 1 J=1,SAMPLE
2830=      A=GGUBFS(DSEED)
2840=      B=-ALOG(A)
2850=      R(J)=SQRT(B)/2.0
2860=1     CONTINUE
2870=      GO TO 6
2880=4     WRITE(*,*)'NON-FLUCTUATING CASE'
2890=      DO 5 I=1,SAMPLE
2900=      R(I)=1.0
2910=5     CONTINUE
2920=6     CONTINUE
2930=      SUM=ITIME*NELEM
2940=      WRITE(*,*)'SUM=',SUM
2950=      IF(NPRT.NE.1)GO TO 7
2960=      PERIOD(1)=SUM
2970=      WRITE(*,*)'PERIOD(1)=',PERIOD(1)
2980=      GO TO 30
2990=7     IF(PW.EQ.1.E-11)GO TO 10
3000=      DO 8 I=1,NPRT
3010=      CPRT(I)=PRT(I)*1.E10
3020=      CPW=PW*1.E10
3030=      PERIOD(I)=SUM*CPRT(I)/CPW
3040=      WRITE(*,*)'I=',I,'      PERIOD(I)=',PERIOD(I)
3050=8     CONTINUE
3060=      GO TO 30
3070=10    IF(PW.GT.0.0001) GO TO 20
3080=      DO 15 I=1,NPRT
3090=      CPRT(I)=PRT(I)*10000.0
3100=      CPW=PW*10000.0
3110=      PERIOD(I)=SUM*CPRT(I)/CPW
3120=      WRITE(*,*)'I=',I,'      PERIOD(I)=',PERIOD(I)
3130=15    CONTINUE
3140=      GO TO 30
3150=20    DO 25 I=1,NPRT
3160=      PERIOD(I)=SUM*PRT(I)/PW
3170=      WRITE(*,*)'I=',I,'      PERIOD(I)=',PERIOD(I)
3180=25    CONTINUE
3190=30    READ(10,*)START
3200=      DO 35 I=1,50
3210=      RATIO(I)=C(START)
3220=      START=START+1
3230=35    CONTINUE
3240=      READ(10,*)I
3250=      IF(J.EQ.0)GO TO 60
3260=      WRITE(*,*)'ELEMENTS OF PHASE CODE ARE GAUSSIAN SHAPED'
3270=      MEAN=PW/(2*NELEM)
3280=      STDEV=MEAN/3.0
3290=      VAR=STDEV*STDEV
3300=      GAUSS=1.0/SQRT(2.0*VAR*3.1416)
3310=      GFACT=0.5923581*(PW/NELEM)*(PW/NELEM)
3320=

```

```

3330=      WRITE(*,305)MEAN,STDEV,VAR,GFACT
3340=      TALLY=0
3350=      DO 55 IA=1,NPRT
3360=      COUNT=TALLY+1
3370=      DO 45 I=1,NELEM
3380=      DO 40 J=COUNT,COUNT+ITIME-1
3390=      TIME=(PW/ITIME)*(J-COUNT+1)/NELEM
3400=      POWER=TIME-MEAN
3410=      WT=GAUSS*EXP(-POWER*POWER/(2.0*VAR))
3420=      AMT2=CMPLX(0.0,RATIO(I)*3.1416)
3430=      Z(J)=WT*CEXP(AMT2)
3440=40    CONTINUE
3450=      COUNT=COUNT+ITIME
3460=45    CONTINUE
3470=      DO 50 J=COUNT,COUNT+PERIOD(IA)-SUM-1
3480=      Z(J)=(0.0,0.0)
3490=50    CONTINUE
3500=      TALLY=TALLY+PERIOD(IA)
3510=55    CONTINUE
3520=      GO TO 100
3530=60    WRITE(*,*)'ELEMENTS OF PHASE CODE ARE RECTANGULAR
3540=      'SHAPED'
3550=      GFACT=1.0
3560=      TALLY=0
3570=      KSTART=1
3580=      KEND=NELEM
3590=      DO 80 IA=1,NPRT
3600=      COUNT=TALLY+1
3610=      DO 70 I=KSTART,KEND
3620=      DO 65 J=COUNT,COUNT+ITIME-1
3630=      AMT2=CMPLX(0.0,RATIO(I)*3.1416)
3640=      Z(J)=R(J)*CEXP(AMT2)
3650=65    CONTINUE
3660=      COUNT=COUNT+ITIME
3670=70    CONTINUE
3680=      DO 75 J=COUNT,COUNT+PERIOD(IA)-SUM-1
3690=      Z(J)=(0.0,0.0)
3700=75    CONTINUE
3710=      KSTART=KEND+1
3720=      KEND=KEND+NELEM
3730=      IF(KEND.GT.50)THEN
3740=      KSTART=1
3750=      KEND=NELEM
3760=      END IF
3770=      TALLY=TALLY+PERIOD(IA)
3780=80    CONTINUE
3790=      DO 85 I=1,SAMPLE
3800=      FREQ(I)=0.0
3810=85    CONTINUE
3820=      N=SUM*TOTAL/PW
3830=      N=SUM
3840=100    RETURN
3850=300    FORMAT(1X,'FOR I=',I3,5X,'PHASE=',I2,'*PI')
3860=305    FORMAT(1X,'M=',F12.10,3X,'ST=',F12.10,

```

```

3870=      @3X, 'VAL', F12.10, 3X, 'GFAC=', F12.10,
3880=      END
3890=
3900=*****
3910=*****
3920=****      SUBROUTINE FM
3930=****      WRITTEN BY KENNETH W. ALBERT/(REF:REF)
3940=****      18 OCT 83
3950=*****
3960=*****
3970=      SUBROUTINE FM(FREQ,PERIOD,NPRT,PW,N,C,M,TOTAL,PRT)
3980=
3990=      INTEGER PERIOD(1024),SUM,COUNT,REMAIN,
4000=      @X1,X2,X3,X4,X5,X6,FCODE(58),C(64)
4010=      REAL FREQ(1024),TXFREQ,PRT(50)
4020=
4030=
4040=      DO 1 JJ=1,1024
4050=      FREQ(JJ)=0.0
4060=1      CONTINUE
4070=      DF=7.8125
4080=      DO 10 I=1,58
4090=      X1=C(I)
4100=      X2=C(I+1)
4110=      X3=C(I+2)
4120=      X4=C(I+3)
4130=      X5=C(I+4)
4140=      X6=C(I+5)
4150=      IF(X2.EQ.1)X2=2
4160=      IF(X3.EQ.1)X3=4
4170=      IF(X4.EQ.1)X4=8
4180=      IF(X5.EQ.1)X5=16
4190=      IF(X6.EQ.1)X6=32
4200=      IF((X1+X2+X3+X4+X5+X6).EQ.0)THEN
4210=      WRITE(*,*)'ALL ZERO CODEWORD FOUND IN SUBROUTINE
4220=      @ FM,FCODE(*) SET EQUAL TO 64'
4230=      FCODE(I)=64
4240=      END IF
4250=      FCODE(I)=X1+X2+X3+X4+X5+X6
4260=10      CONTINUE
4270=      WRITE(*,*)'FCODE (I) VALUES'
4280=      DO 7 KK=1,58
4290=      WRITE(*,*) FCODE(KK)
4300=7      CONTINUE
4310=      READ (10,*)ISUBEL
4320=      ITIME=N/ISUBEL
4330=      N=ITIME*ISUBEL
4340=      DO 5 J=1,NPRT
4350=      PERIOD(J)=N*PRT(J)/PW
4360=      WRITE(*,*)'I=',J,          PERIOD(I)=' ,PERIOD(I)
4370=5      CONTINUE
4380=      M=N*TOTAL/PW
4390=      BAND=500
4400=      WRITE(*,*)'BANDWIDTH SWEEP =',BAND,'HZ

```

```

4410= READ(10,*)K
4420= IF(K.EQ.1) GO TO 25
4430= IF(K.EQ.2) GO TO 45
4440= IF(K.EQ.3) GO TO 60
4450= IF(K.EQ.4) GO TO 75
4460= IF(K.EQ.5) GO TO 90
4470= WRITE(*,*)'LFM IMPLEMENTED'
4480= SUM=0
4490= DO 20 I=1,NPRT
4500= COUNT=SUM+1
4510= REMAIN=COUNT+N-1
4520= DO 15 J=COUNT,REMAIN
4530= TIME=(PW/N)*(J-SUM-1)
4540= FREQ(J)=BAND*TIME*TIME*3.1416/PW
4550=15 CONTINUE
4560= SUM=SUM+PERIOD(I)
4570=20 CONTINUE
4580= GO TO 200
4590=25 WRITE(*,*)'VFM IMPLEMENTED'
4600= SUM=0
4610= DO 40 I=1,NPRT
4620= COUNT=SUM+1
4630= REMAIN=COUNT+N-1
4640= DO 30 J=COUNT,REMAIN/2
4650= TIME=PW/N*(N-J*2-SUM)
4660= FREQ(J)=0.5*BAND*TIME*TIME*3.1416/PW
4670=30 CONTINUE
4680= DO 35 J=REMAIN/2+1,REMAIN
4690= TIME=PW/N*(J*2-N-SUM-1)
4700= FREQ(J)=0.5*BAND*TIME*TIME*3.1416/PW
4710=35 CONTINUE
4720= SUM=SUM+PERIOD(I)
4730=40 CONTINUE
4740= GO TO 200
4750=45 WRITE(*,*)'INTERPULSE FM IMPLEMENTED'
4760= SUM=0
4770= DO 55 I=1,NPRT
4780= COUNT=SUM+1
4790= REMAIN=COUNT+N-1
4800= DO 50 J=COUNT,REMAIN
4810= TIME=(PW/N)*(J-1)
4820= FREQ(J)=FCODE(I)*I*TIME/(2*3.1416)
4830=50 CONTINUE
4840= SUM=SUM+PERIOD(I)
4850=55 CONTINUE
4860= GO TO 200
4870=60 WRITE(*,*)'INTRAPULSE FM IMPLEMENTED'
4880= SUM=0
4890= DO 70 I=1,NPRT
4900= COUNT=SUM+1
4910= REMAIN=COUNT+N-1
4920= KSET=1
4930= ISET=0
4940= DO 65 J=COUNT,REMAIN

```

```

4950=      TIME=(PW/N)*(J-1)
4960=      IF(ISET.EQ.ITIME)THEN
4970=      KSET=KSET+1
4980=      ISET=0
4990=      END IF
5000=      ISET=ISET+1
5010=      FREQ(J)=FCODE(KSET)*DF*TIME/(2*3.1416)
5020=65    CONTINUE
5030=      SUM=SUM+PERIOD(I)
5040=70    CONTINUE
5050=      GO TO 200
5060=75    WRITE(*,*)'INTERPULSE FH WITH INTRAPULSE CHIRP'
5070=      SUM=0
5080=      DO 85 I=1,NPRT
5090=      COUNT=SUM+1
5100=      REMAIN=COUNT+N-1
5110=      DO 80 J=COUNT,REMAIN
5120=      TIME=(PW/N)*(J-SUM-1)
5130=      FREQ(J)=(FCODE(I)/64)*BAND*TIME*TIME*3.1416/PW
5140=80    CONTINUE
5150=      SUM=SUM+PERIOD(I)
5160=85    CONTINUE
5170=      GO TO 200
5180=90    WRITE(*,*)'INTRAPULSE FH W/SUBPULSE CHIRP'
5190=      SUM=0
5200=      DO 100 I=1,NPRT
5210=      COUNT=SUM+1
5220=      REMAIN=COUNT+N-1
5230=      KSET=1
5240=      IC=0
5250=      ISET=0
5260=      DO 95 J=COUNT,REMAIN
5270=      TIME=(PW/N)*(J-SUM-IC-1)
5280=      IF((J-SUM-IC).EQ.ITIME)IC=IC+ITIME
5290=      IF(ISET.EQ.ITIME)THEN
5300=      KSET=KSET+1
5310=      ISET=0
5320=      END IF
5330=      ISET=ISET+1
5340=      FREQ(J)=(FCODE(KSET)/64)*BAND*TIME*TIME*3.1416/PW
5350=95    CONTINUE
5360=      SUM=SUM+PERIOD(I)
5370=100   CONTINUE
5380=200   RETURN
5390=      END
5400=*****
5410=*****
5420=***    SUBROUTINE RECPL
5430=***    WRITTEN BY KENNETH W. ALBERT/(REF:REED)
5440=***    18 OCT 83
5450=*****
5460=*****
5470=      SUBROUTINE RECPL(PERIOD,Z,GFACT,NPRT,N)
5480=

```

```

5490=      COMPLEX Z(1024)
5500=      INTEGER SUM,COUNT,REMAIN,PERIOD(1024),F
5510=      DOUBLE PRECISION DSEED
5520=
5530=      SUM=0
5540=      GFACT=1.0
5550=      WRITE(*,*)'PULSE(S) IS RECTANGULAR SHAPED'
5560=      READ(10,*)F
5570=      IF(F.EQ.0) GO TO 20
5580=      WRITE(*,*)'NON-FLUCTUATING TARGET'
5590=      DO 15 I=1,NPRT
5600=      COUNT=SUM+1
5610=      REMAIN=COUNT+N-1
5620=      DO 5 J=COUNT,REMAIN
5630=      Z(J)=(1.0,1.0)
5640=5      CONTINUE
5650=      DO 10 J=REMAIN+1,SUM+PERIOD(1)
5660=      Z(J)=(0.0,0.0)
5670=10     CONTINUE
5680=      SUM=SUM+PERIOD(1)
5690=15     CONTINUE
5700=      GO TO 40
5710=20     WRITE(*,*)'RAYLEIGH AMPLITUDE FLUCTUATIONS'
5715=      DSEED=69.00
5720=      DO 35 I=1,NPRT
5770=      COUNT=SUM+1
5780=      REMAIN=COUNT+N-1
5790=      DO 25 J=COUNT,REMAIN
5792=      A=GOUMPS(DSEED)
5794=      R=-ALOG(A)
5796=      COE=SQRT(B)
5800=      Z(J)=COE
5810=25     CONTINUE
5820=      DO 30 J=REMAIN+1,SUM+PERIOD(1)
5830=      Z(J)=(0.0,0.0)
5840=30     CONTINUE
5850=      SUM=SUM+PERIOD(1)
5860=35     CONTINUE
5870=40     RETURN
5880=      END
5890=*****
5900=*****
5910=*****      SUBROUTINE SETUP
5920=*****      WRITTEN BY KENNETH W. ALBERT/(REF:REED)
5930=*****      18 OCT 83
5940=*****
5950=*****
5960=      SUBROUTINE SETUP(D,Z,FREQ,XVALS,YVALS,VALUE,TOTAL,SAMPLE,M,
5970=      @IWK,WK,PW,N)
5980=
5990=      COMPLEX XVALS(1024),YVALS(1024),Z(1024),VALUE,AMT1,AMT2,
6000=      @CTIME,AMT3,FILTER(1024),AMT4
6010=      INTEGER SAMPLE,NSCAT,I
6020=      REAL FREQ(1024)

```

```

6030=
6040=      DO 5 I=M+1,SAMPLE
6050=      YVALS(I)=CMPLX(0.0,0.0)
6060=5      CONTINUE
6070=      DO 10 I=M+1,SAMPLE
6080=      XVALS(I)=CMPLX(0.0,0.0)
6090=10     CONTINUE
6100=      DO 15 I=1,M
6110=      AMT2=CMPLX(0.0,FREQ(I))
6120=      TIME=TOTAL/M*(I-1)
6130=      CTIME=CMPLX(TIME,0.0)
6140=      AMT3=VALUE*CTIME+AMT2
6150=      YVALS(I)=Z(I)*CEXP(AMT3)
6160=15     CONTINUE
6170=      DO 20 I=1,M
6180=      AMT1=Z(1+(M-I))
6190=      AMT2=CMPLX(0.0,-FREQ(1+(M-I)))
6200=      XVALS(I)=AMT1*CEXP(AMT2)
6210=20     CONTINUE
6220=      IF(D.EQ.0) GO TO 200
6230=      READ(10,*)ALPHA
6240=      DO 40 J=1,SAMPLE
6250=      TIME=(PW/N)*(J-1)
6260=      AMT4=CMPLX(-ALPHA*TIME*TIME,0.0)
6270=      FILTER(J)=CEXP(AMT4)
6280=40     CONTINUE
6290=      CALL FFTCC(YVALS,SAMPLE,IWK,WK)
6300=      DO 50 I=1,SAMPLE
6310=      YVALS(I)=YVALS(I)*FILTER(I)
6320=50     CONTINUE
6330=      DO 51 I=1,SAMPLE
6340=      YVALS(I)=CONJG(YVALS(I))
6350=51     CONTINUE
6360=      CALL FFTCC(YVALS,SAMPLE,IWK,WK)
6370=      DO 52 I=1,SAMPLE
6380=      YVALS(I)=CONJG(YVALS(I))/SAMPLE
6390=52     CONTINUE
6400=200    RETURN
6410=      END
6420=*****
6430=*****
6440=***      SUBROUTINE OUT
6450=***      WRITTEN BY KENNETH W. ALBERT/(REF:REED)
6460=***      18 OCT 83
6470=*****
6480=*****
6490=      SUBROUTINE OUT(MAG,NUM,PW,TOTAL,M,D)
6500=
6510=      REAL MAG(1024)
6520=      INTEGER D
6530=
6540=      WRITE(*,300)PW,NUM
6550=      IF(D.EQ.0)THEN
6560=      WRITE(*,305)

```

```

6570=      ELSE
6580=      IF(D.EQ.1)THEN
6590=      WRITE(*,310)
6600=      ELSE
6610=      WRITE(*,315)
6620=      END IF
6630=      END IF
6640=      DO 5 I=1,M*2
6650=      TIME=TOTAL/M*(I-1)
6670=      WRITE(12,320)TIME,MAG(I)
6680=5     CONTINUE
6690=      RETURN
6700=300   FORMAT(1X,'PW=',F12.10,5X,'# OF SAMPLES MADE OF
6710=      @ WAVEFORM=',I5)
6720=305   FORMAT(1X,'TIME DELAY',5X,'MAGNETUDE OF AMBIGUITY
6730=      @ FUNCTION')
6740=310   FORMAT(1X,'TIME DELAY',5X,'MAGNETUDE OF MATCHED
6750=      @ FILTER OUTPUT')
6760=315   FORMAT(1X,'TIME DELAY',5X,'MAGNETUDE OF TARGET
6770=      @ FILTER OUTPUT')
6780=320   FORMAT(1X,F10.4,7X,F10.4)
6790=      END
6791=*EOR

```


VITA

Kenneth W. Albert was born on November 21, 1959 in Tucson, Arizona. He graduated Rome Free Academy High School in Rome, New York in June, 1977. He recieved his B.S.E.E. degree from the Pennsylvania State University and a commission in the United States Air Force in May, 1982. In June, 1982, he was assigned to the School of Engineering, Air Force Institute of Technology, to pursue a M.S.E.E. with emphasis in communications and radar systems. The author's permanent address is:

6341 Milles Drive
Rome, New York, 13440

UNCLASSIFIED

SECURITY CLASSIFICATION OF THIS PAGE

REPORT DOCUMENTATION PAGE

1. REPORT SECURITY CLASSIFICATION UNCLASSIFIED		1b. RESTRICTIVE MARKINGS	
2a. SECURITY CLASSIFICATION AUTHORITY		3. DISTRIBUTION/AVAILABILITY OF REPORT Approved for Public Release; distribution unlimited	
2b. DECLASSIFICATION/DOWNGRADING SCHEDULE		5. MONITORING ORGANIZATION REPORT NUMBER(S)	
4. PERFORMING ORGANIZATION REPORT NUMBER(S)		7a. NAME OF MONITORING ORGANIZATION	
6a. NAME OF PERFORMING ORGANIZATION Electrical Engr. Dept	6b. OFFICE SYMBOL (If applicable) AFIT/EN	7b. ADDRESS (City, State and ZIP Code)	
6c. ADDRESS (City, State and ZIP Code) Air Force Institute of Technology Wright-Patterson AFB OH 45433		9. PROCUREMENT INSTRUMENT IDENTIFICATION NUMBER	
8a. NAME OF FUNDING/SPONSORING ORGANIZATION	8b. OFFICE SYMBOL (If applicable)	10. SOURCE OF FUNDING NOS.	
8c. ADDRESS (City, State and ZIP Code)		PROGRAM ELEMENT NO.	TASK NO.
11. TITLE (Include Security Classification) Target Super-Resolution Compensation for Coherent Airborne Radar utilizing Spread Spectrum Waveforms (U)		PROJECT NO.	WORK UNIT NO.
12. PERSONAL AUTHOR(S) Kenneth W. Albert, 2Lt, USAF			
13a. TYPE OF REPORT MS Thesis	13b. TIME COVERED FROM _____ TO _____	14. DATE OF REPORT (Yr., Mo., Day) December 1983	15. PAGE COUNT 132
16. SUPPLEMENTARY NOTATION AFIT/GE/EE/83D-5			
17. COSATI CODES		18. SUBJECT TERMS (Continue on reverse if necessary and identify by block number)	
FIELD	GROUP	18. SUBJECT TERMS (Continue on reverse if necessary and identify by block number) Approved for public release: IAW AFR 190-17 LYNN E. WOLVER 7 Feb 84 Wright-Patterson AFB OH 45433	
19. ABSTRACT (Continue on reverse if necessary and identify by block number) Both a coherent and incoherent target filter are compared on an output signal-to-noise power ratio basis. Three spread spectrum waveforms are tested: intrapulse biphasic coded, interpulse frequency hopped, and interpulse frequency hopped with subpulse chirp. In all three cases, the incoherent target filter provided superior output power. Typical incoherent/coherent signal power ratios were 1-3 dB, 0.75 dB, and 0.18 dB for the phase coded, FM, and FM with subpulse chirp respectively.			
20. DISTRIBUTION/AVAILABILITY OF ABSTRACT UNCLASSIFIED/UNLIMITED <input checked="" type="checkbox"/> SAME AS RPT. <input type="checkbox"/> DTIC USERS <input type="checkbox"/>		21. ABSTRACT SECURITY CLASSIFICATION UNCLASSIFIED	
22a. NAME OF RESPONSIBLE INDIVIDUAL Kenneth W. Albert, 2Lt, USAF		22b. TELEPHONE NUMBER (Include Area Code) 513-255-5533	22c. OFFICE SYMBOL AFIT/EN

END

FILMED

4-84

DTIC